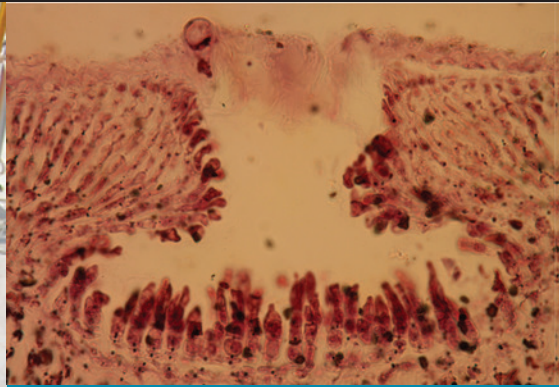
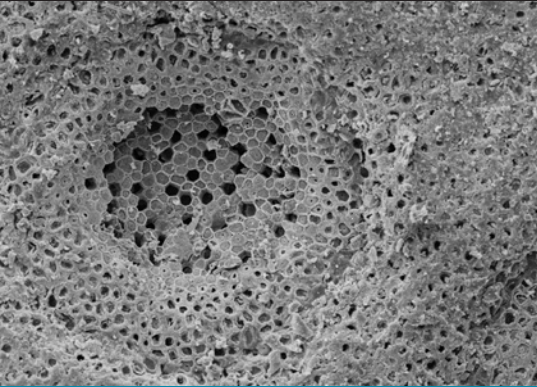




Smithsonian Institution
Scholarly Press

SMITHSONIAN CONTRIBUTIONS TO THE MARINE SCIENCES • NUMBER 41



Phymatolithon
(Melobesioideae, Hapalidiales)
in the Boreal–Subarctic
Transition Zone of the
North Atlantic

A Correlation of Plastid DNA Markers with
Morpho-Anatomy, Ecology, and Biogeography

*Walter H. Adey, Jazmin J. Hernandez-Kantun,
Paul W. Gabrielson, Merinda C. Nash,
and Lee-Ann C. Hayek*

SERIES PUBLICATIONS OF THE SMITHSONIAN INSTITUTION

Emphasis upon publication as a means of “diffusing knowledge” was expressed by the first Secretary of the Smithsonian. In his formal plan for the Institution, Joseph Henry outlined a program that included the following statement: “It is proposed to publish a series of reports, giving an account of the new discoveries in science, and of the changes made from year to year in all branches of knowledge.” This theme of basic research has been adhered to through the years in thousands of titles issued in series publications under the Smithsonian imprint, commencing with Smithsonian Contributions to Knowledge in 1848 and continuing with the following active series:

Smithsonian Contributions to Anthropology
Smithsonian Contributions to Botany
Smithsonian Contributions to History and Technology
Smithsonian Contributions to the Marine Sciences
Smithsonian Contributions to Museum Conservation
Smithsonian Contributions to Paleobiology
Smithsonian Contributions to Zoology

In these series, the Smithsonian Institution Scholarly Press (SISP) publishes small papers and full-scale monographs that report on research and collections of the Institution’s museums and research centers. The Smithsonian Contributions Series are distributed via exchange mailing lists to libraries, universities, and similar institutions throughout the world.

Manuscripts intended for publication in the Contributions Series undergo substantive peer review and evaluation by SISP’s Editorial Board, as well as evaluation by SISP for compliance with manuscript preparation guidelines (available at <https://scholarlypress.si.edu>). For fully searchable PDFs of all open access series and publications of the Smithsonian Institution Scholarly Press, visit Open SI at <http://opensi.si.edu>.

Phymatolithon
(Melobesioideae, Hapalidiales)
in the Boreal–Subarctic
Transition Zone of the
North Atlantic

A Correlation of Plastid DNA Markers with
Morpho-Anatomy, Ecology, and Biogeography

*Walter H. Adey, Jazmin J. Hernandez-Kantun,
Paul W. Gabrielson, Merinda C. Nash,
and Lee-Ann C. Hayek*



Smithsonian Institution
Scholarly Press

WASHINGTON D.C.

2018

ABSTRACT

Adey, Walter H., Jazmin J. Hernandez-Kantun, Paul W. Gabrielson, Merinda C. Nash, and Lee-Ann C. Hayek. *Phymatolithon* (Melobesiaceae, Hapalidiales) in the Boreal–Subarctic Transition Zone of the North Atlantic: A Correlation of Plastid DNA Markers with Morpho-Anatomy, Ecology, and Biogeography. *Smithsonian Contributions to the Marine Sciences*, number 41, viii + 90 pages, 21 figures, 11 plates, 5 tables, 1 appendix, 2018.—Species of the coralline algal genus *Phymatolithon* are the dominant algal calcifiers in the rocky intertidal and shallow photic sublittoral zone of the Boreal–Subarctic transition zone that stretches across the North Atlantic from the Gulf of Maine and the southern Canadian Maritimes to southwestern Iceland and the Norwegian outer coast. In this paper, we use extensive field and laboratory data on the biology, physiology, and ecology of *Phymatolithon* species, supported by statistical analysis and DNA sequence data, to develop a multiscale view of this key genus of the ecosystems of this region. We demonstrate that species of *Phymatolithon* that occur in the Boreal–Subarctic transition zone in the North Atlantic can be segregated systematically by a statistical/developmental analysis of their morpho-anatomical characters. We show these results to be congruent with DNA sequence-based methods. Six species are recognized: *Phymatolithon laevigatum*, *P. rugulosum* (*P. lamii*), *P. squamulosum* (*P. lenormandii*), *P. investiens*, *P. borealis* sp. nov. (*P. polymorphum*), and *P. nantuckensis* sp. nov.). Based on paraffin section, compound microscope, and EDS-SEM analysis, we show that coralline anatomy comprises a diversity of both tissue types and high magnesium carbonate wall structure. Variations in vegetative tissue morphology, particularly with respect to cell division and elongation patterns, as well as variation in conceptacle (reproductive structure) location and development, are the result of a complex of genetic and environmental factors. Some of these factors can be linked to adaptation to environmental and biogeographical niches, providing a basis for experimental analysis of the mechanisms of adaptation. We have analyzed conceptacle development in *Phymatolithon* and demonstrated the linkage between genetic control and concurrent vegetative growth; these parameters interact to produce considerable variation in some characters of final gross morphology but not in others. These results strongly demonstrate that morpho-anatomical research in the broader Corallinophycidae requires greater biological sophistication, with utilization of quantitative population-level data, if success in correlating it with DNA sequence data is to be generally achieved.

Cover images: Left, Maine coast *Phymatolithon rugulosum* specimen with bi-tetrasporangial conceptacle seen from the surface; SEM by W. H. Adey. Center, dive crew preparing for a coralline station in northern Newfoundland: (left to right) Alok Mallick, Walter Adey, and Alex Miller; photo by Karen Loveland Adey. Right, northern Norwegian *Phymatolithon investiens* young female conceptacle seen in stained microtome section; compound light microscope image by W. H. Adey.

Published by SMITHSONIAN INSTITUTION SCHOLARLY PRESS
P.O. Box 37012, MRC 957, Washington, D.C. 20013-7012
<https://scholarlypress.si.edu>

Compilation copyright © 2018 Smithsonian Institution

The rights to all text and images in this publication, including cover and interior designs, are owned either by the Smithsonian Institution, by contributing authors, or by third parties. Fair use of materials is permitted for personal, educational, or noncommercial purposes. Users must cite author and source of content, must not alter or modify copyrighted content, and must comply with all other terms or restrictions that may be applicable. Users are responsible for securing permission from a rights holder for any other use.

Library of Congress Cataloging-in-Publication Data

Names: Adey, Walter H., author. | Smithsonian Institution Scholarly Press, publisher.

Title: *Phymatolithon* (Melobesiaceae, Hapalidiales) in the Boreal–Subarctic Transition Zone of the North Atlantic : a correlation of plastid DNA markers with morpho-anatomy, ecology, and biogeography / W. H. Adey [and four others].

Other titles: Correlation of plastid DNA markers with morpho-anatomy, ecology, and biogeography | Smithsonian contributions to the marine sciences ; no. 41

Description: Washington, D.C. : Smithsonian Institution Scholarly Press, 2018. | Series: Smithsonian contributions to the marine sciences ; number 41 | Includes bibliographical references.

Identifiers: LCCN 2017059107

Subjects: LCSH: *Phymatolithon*—North Atlantic Ocean | Coralline algae—North Atlantic Ocean.

Classification: LCC QK569.C8 A34 2018 | DDC 571.592989—dc23 | SUDOC SI 1.41:41

LC record available at <https://lccn.loc.gov/2017059107>

ISSNs: 1943-667X (online); 0196-0768 (print)

Publication date (online): 6 April 2018

© The paper used in this publication meets the minimum requirements of the American National Standard for Permanence of Paper for Printed Library Materials Z39.48–1992.

Contents

LIST OF FIGURES	v
LIST OF TABLES	vii
INTRODUCTION	1
MATERIALS AND METHODS	2
RESULTS	18
DISCUSSION	43
CONCLUSIONS	50
PLATES 1–11	51
APPENDIX: SUPPLEMENTARY MATERIALS	75
REFERENCES	85
INDEX	89

Figures

1. Phylograms inferred from maximum likelihood (ML) analyses of <i>psbA</i> and <i>rbcL</i> plastid markers for selected species of <i>Phymatolithon</i>	19
2. Mean hypothallial cell shape (length/diameter) as a function of hypothallial thickness	20
3. Change in mean cell length (pit to pit) of perithallial cells as a function of cell position	22
4. The coefficient of variation of cell length as a function of cell position	23
5. Change in cell diameter (width mid-cell lumen) as a function of cell position and positive slope of deeper cell diameter	24
6. Cell diameter coefficient of variation as a function of cell position	25
7. Ratio of cell length to cell diameter as a function of cell position	26
8. Percent of cells with fusions as a function of cell position and mean cell length at each cell position	27
9. Mean staining body diameter as a function of cell position	28
10. Bi-tetrasporangial conceptacle height to crust surface (pore plate surface height above or below crust surface) as a function of conceptacle cavity diameter	30
11. Conceptacle dimensions as a function of conceptacle pore plate diameter for <i>Phymatolithon laevigatum</i>	31
12. Development of female carpogonium from formation to carpospores after fertilization	34
13. Distribution of <i>Phymatolithon laevigatum</i> in Boreal–Subarctic Atlantic	35
14. Distribution of <i>Phymatolithon rugulosum</i> in Boreal–Subarctic Atlantic	36
15. Distribution of <i>Phymatolithon squamulosum</i> in Boreal–Subarctic Atlantic	37
16. Distribution of <i>Phymatolithon borealis</i> in Boreal–Subarctic Atlantic	38
17. Distribution of <i>Phymatolithon investiens</i> and <i>P. nantuckensis</i> in Boreal–Subarctic Atlantic	39
<i>Appendix Figures</i>	
A1. <i>Phymatolithon</i> tree of all utilized samples	76
A2a. Station locality information for <i>Phymatolithon laevigatum</i>	77
A2b. Station locality information for <i>Phymatolithon rugulosum</i> , <i>P. squamulosum</i> , and <i>P. nantuckensis</i>	78
A2c. Station locality information for <i>Phymatolithon borealis</i> and <i>P. investiens</i>	79

Tables

1. <i>Phymatolithon</i> stations in the Boreal–Subarctic transition zone of the North Atlantic	4
2. Dimensions of asexual conceptacles of <i>Phymatolithon</i>	29
3. Dimensions of female conceptacles of <i>Phymatolithon</i>	32
4. Dimensions of cystocarpic conceptacles of <i>Phymatolithon</i>	33
<i>Appendix Table</i>	
A1. DNA specimen information, station locality data, and museum/herbarium acquisition codes	80

Phymatolithon (Melobesioideae, Hapalidiales) in the Boreal–Subarctic Transition Zone of the North Atlantic

A Correlation of Plastid DNA Markers with Morpho-Anatomy, Ecology, and Biogeography

Walter H. Adey,^{1*} Jazmin J. Hernandez-Kantun,¹

Paul W. Gabrielson,² Merinda C. Nash,¹ and Lee-Ann C. Hayek³

INTRODUCTION

Since the last decade of the nineteenth century, when a basic knowledge of coralline biology and subsequently classical taxonomy fully developed (e.g., Foslie, 1895; Heydrich, 1897a,b), it was assumed that features of surface morphology were sufficient to define species. Even though Darwin's (1859) *Origin of Species* had been published nearly four decades earlier, there was still little understanding of the role of natural selection. Because there was virtually no direct access to the subtidal environment, coralline ecology and the potential factors driving natural selection were rarely even contemplated. One result, among many, was that numerous branching species of *Lithothamnion* Heydrich were described for the Norwegian coast of the North Atlantic Ocean based solely on the gross morphology of the branches (Foslie, 1895). Later, based on a realization that the apparent “branching characters” of these species graded into each other, many of the names became disused. Nevertheless, new species, which did not appear to match earlier proposed species, continued to be described on the basis of a broader, biosystematic understanding (Adey, 1970a).

Similarly, new genera were proposed based on features that could easily be observed, primarily focused on surface morphology, especially of reproductive structures. Thus, *Phymatolithon* Foslie was separated from *Lithothamnion* on the basis of the presence of sunken conceptacles. *Clathromorphum* Foslie also had sunken conceptacles, but differed from *Phymatolithon* in early development by having “slightly convex light dots” over the conceptacles. Subsequent authors, recognizing that the depth of conceptacles graded widely between genera and that the “white spots” also appeared in *Phymatolithon*, either rejected both genera (for *Lithothamnion*) or used one or the other, depending on the author (see Adey, 1964). Beginning 70 years later, for all three genera, complex,

¹ Department of Botany, National Museum of Natural History, Smithsonian Institution, Washington, DC, 20013-7012, USA.

² Department of Biology and Herbarium, University of North Carolina, Chapel Hill, North Carolina, USA.

³ Statistics and Mathematics, National Museum of Natural History, Smithsonian Institution, Washington, DC, 20013-7012, USA.

* Correspondence: adeyw@si.edu

Manuscript received 23 January 2017; accepted 5 October 2017.

quantifiable, and statistically significant patterns of anatomy were identified; included was a newly described intercalary meristem (an uncommon feature in red algae) underlying the superficial morphology (Adey, 1964, 1965; Adey et al., 2001, 2005, 2013, 2015a,b). The evolution of the diverse anatomy in these genera was hypothesized, in large measure, to be a defense against mollusk grazing (Steneck, 1982, 1992); different genera and species showed a wide variety of anatomical strategies to counter that grazing. Furthermore, with the advent of scuba, the ecological and biogeographical distributions of these Northern Hemisphere species and genera studied by Adey (1964, 1965, 1966a,b, 1968, 1971) provided quantitatively recognizable patterns.

In the several decades before the application of DNA sequencing to corallines, their taxonomy became a shifting arena of personal opinion as to what characters were or were not taxonomically informative and at what ranks they should be applied (Woelkerling, 1988; Irvine and Chamberlain, 1994). These opinions were not based on a broader use of statistically characterized morpho-anatomical characters in the framework of ecological and biogeographical knowledge, with some exceptions (Lebednik, 1977; Steneck, 1982). With the advent of DNA sequencing, genera and species of the more intensively studied non-geniculate corallines, especially in Subarctic and Boreal waters in the North Atlantic, have been supported by DNA sequencing and phylogenetic reconstructions (Adey et al., 2015). This support has not proved true for many coralline genera and species in the rest of the world, where DNA sequencing is revealing a multitude of undescribed taxa (e.g., Basso et al., 2015; Hind et al., 2015, 2016; Hernandez-Kantun et al., 2016; Peña et al., 2015a,b; Rosler et al., 2016).

The region treated herein that we call the Boreal–Subarctic transition zone is that part of the coastal North Atlantic that has shallow, warmer-water Boreal species underlain by deeper, colder-water Subarctic species. Adey and Hayek (2011) showed that this distribution is characteristic for the entire macroalgal flora of this zone, a feature revealed only by depth-calibrated collections. Adey and Steneck (2001) treated this as a well-defined transition (unnamed zone) between the Subarctic and the Boreal (Celtic). It is notable that the transition becomes more geographically distributed than depth distributed in Norway (Adey, 1971), where the inner fjords are Subarctic and the outer coast, with only a weak thermocline, is mostly Boreal in coralline composition. Based on the rocky bottom area covered, Boreal and Subarctic non-geniculate coralline species together provide roughly 80% of the coralline flora in the Boreal–Subarctic transition zone that we cover in this paper (Table 1; Adey and Steneck, 2001); *Phymatolithon* species are about half of that value (Adey, 1964, 1968, 1971). The Boreal species *Lithophyllum orbiculatum* (Foslie) Foslie in shallow water and *Lithothamnion sonderi* Hauck in deep water make up the remaining 20%. In shallow to midphotoc depths (intertidal to ~20 m; to depth ~30 m on the outer Norwegian coast), *Phymatolithon* species are the dominant crustose elements of the rocky bottom flora. We present an extensive set of DNA analyses applied to a very large ecologically

based sampling of more than 12,000 specimens, including six *Phymatolithon* species from more than 300 stations, across this entire region in the North Atlantic Ocean. In addition, we introduce carbonate cell wall ultrastructure and chemistry to the morpho-anatomical characterization of these species.

MATERIALS AND METHODS

COLLECTIONS AND PREPARATION

Specimens were sampled from 278 stations with collections from 125 intertidal sites, 728 dive zones of 3–6 m range (to depth 35 m), and 44 dredge sites at depths greater than the 35 m dive limit employed (Table 1). The collecting effort, primarily by scuba, required approximately 25 summer months and 50 winter days. Four research vessels (R/V *Pelion* and R/V *Bjorneng* of author W.H.A., the chartered vessel R/V *Akpatok*, and Tromsø Marinbiologisk Station R/V *Asterias*) were employed. Approximately 40 of the stations (18 in Iceland) were worked from shore with a Boston Whaler independent of a larger research vessel.

Most specimens were taken by scuba as representative samples of station substrate and consisted of rocks, pebbles, or shells encrusted with species mosaics of corallines. More than 12,000 specimens were collected and more than 40,000 species area measurements (in cm², reported as % of total coralline cover) were taken, mostly while on station (see detailed description in Adey and Steneck, 2001). Most samples were tentatively identified while alive and fresh in research vessels or at local shore-based laboratories. Subsamples were taken for preservation in paraffin and subsequent microtome sectioning, and coralline surface areas were measured with clear plastic grids for biogeographical and ecological analysis. A number of specimen fragments were preserved and sectioned by microtome for stained slide viewing within several days of collecting. Based on these sections, a relatively small proportion of the identifications (10%–20%) were corrected while still in the field. Later, mostly during the following winter season, collections were reviewed again and “final” identifications applied. This procedure as confirmed by DNA analysis was more than 95% successful.

Collections are permanently stored in the Coralline Collection of the U.S. National Herbarium (US). During the past two decades, many specimens from the extensive dried collections, as well as specimens on loan from other herbaria, have been mounted for scanning electron microscopy (SEM) and examined using a Leica 440. All numerical data were collected manually, either directly with a compound microscope or from SEM images. More than 200 paraffin blocks of preserved specimens produced over 1,000 slides from which measurements and more than 200 micro-images were obtained; 30 SEM mounts were made that produced more than 250 images. For cell dimensions and other characters, the numbers of stations/plants/filaments measured (i.e., for each data point) are as follows: *Phymatolithon rugulosum*, 25/41/52; *P. laevigatum*, 33/44/47;

P. squamulosum, 22/27/33; *P. nantuckensis*, 1/2/10; *P. borealis*, 18/28/31; and *P. investiens*, 17/29/31. The numerical data for bi-tetrasporangial conceptacles were taken from stations/plants/conceptacles (i.e., for each data point from a single conceptacle) as follows: *P. rugulosum*, 11/13/53; *P. laevigatum*, 14/16/43; *P. squamulosum*, 14/16/35; *P. nantuckensis*, 1/2/10; *P. borealis*, 5/5/20; and *P. investiens*, 1/1/6. These data, on 25 Excel spreadsheets, were transferred to the graphing program Origin 2016 to create the figures presented herein.

STATISTICAL METHODS

All data for each species, either by cell position or by selected morphological measurements, were subjected to descriptive statistics and tests of both means and medians plus variances. General linear models (GLM) of analysis of variance (ANOVA), regression, and repeated-measures/paired *t* tests were developed and tests of full versus restricted models constructed. Assumptions were tested for each model and data transformed when necessary for either distributional or variance adjustment. For the ratio variables of cell length to cell diameter (L/D), we transformed to the difference of logarithms for testing. However, we report herein original values for clarity. For more than two groups, we examined one degree of freedom vectors and cite Scheffé's test results in text.

DNA EXTRACTION, PCR AMPLIFICATION, AND SEQUENCING

Genetic material was successfully obtained and amplified from 92 specimens in the herbaria BM, NCU, and US (Appendix Figure A1); herbarium acronyms follow Thiers (2017, continuously updated) and are defined therein. All protocols were performed following recommendations of Saunders and McDevitt (2012) and Hughey and Gabrielson (2012) to prevent contamination. Small fragments (~3 mm³) were removed from larger specimens left as herbarium vouchers. Under a stereomicroscope, fragments were inspected to remove algal epiphytes and later crushed to powder in clean foil. Extraction of total genomic DNA for specimens in the US and BM herbaria followed the modified protocol by Broom et al. (2008) of the Qiagen DNeasy Blood and Tissue Kit (Qiagen, Crawley, UK); for specimens in NCU, the protocol was as in Gabrielson et al. (2011).

Plastid-encoded *rbcl* and *psbA* genes were analyzed using negative controls. The *rbcl* gene was initially amplified by polymerase chain reaction (PCR) by two pairs of primers, F57 (forward) – R753 (reverse) and F753 (forward) – RrbcS start (reverse, Freshwater and Rueness, 1994). If none of these pairs resulted in a PCR product, we used a pair of primers, F1150Cor (forward, Sissini et al., 2014) and RrbcS (reverse, Freshwater and Rueness, 1994), to amplify a shorter fragment (trimmed to 296 base pairs). The *psbA* gene was amplified initially using the primers psbAF1 (forward) and psbAR2 (reverse, Yoon et al., 2002). If PCR product was lacking, a second run was made using primers

psbAF1 (forward) and psbA600R (reverse, Yoon et al., 2002). The PCR and sequencing mixes and thermocycler protocols followed Adey et al. (2015b).

The DNA analysis included type material from the holotype of *Phymatolithon investiens* (Foslie) Foslie, the holotype of *Phymatolithon laevigatum* (Foslie) Foslie, an isotype of *Phymatolithon rugulosum* W. H. Adey, an isotype of *Phymatolithon squamulosum* (Foslie) W. H. Adey, J. J. Hernandez-Kantun & P. W. Gabrielson, and the holotypes of the newly described species *Phymatolithon borealis* W. H. Adey, J. J. Hernandez-Kantun & P. W. Gabrielson sp. nov. and *Phymatolithon nantuckensis* W. H. Adey, J. J. Hernandez-Kantun & P. W. Gabrielson sp. nov. Sequences from previous publications included *Lithothamnion* spp., *Sporolithon tenue* R. G. Bahia, G. M. Amado-Filho, G. W. Maneveldt & W. H. Adey, and *Phymatolithon* spp. (Adey et al., 2015b; Peña et al., 2015b; Appendix Figure A2); the first two were used as the outgroup.

Data sets were initially produced for *psbA* and for *rbcl*, including all sequences from Genbank and those obtained from the North Atlantic. Removing identical sequences for both markers generated two more data sets. All datasets were aligned with ClustalW in Mega version 5 (Tamura et al., 2011) using default settings and refined by eye. This software was also employed to analyze *rbcl* and *psbA* data sets with identical sequences by using the unweighted pair group method with arithmetic mean (UPGMA) with uncorrected p-distances and 1,000 resamplings for statistical support. Phylogenetic analyses were applied to *rbcl* and *psbA* data sets without identical sequences using maximum likelihood (ML) in RAxML 1.3 (Mac version; Silvestro and Michalak, 2012). The *psbA* and *rbcl* datasets were partitioned by codon position and analyzed using the general time-reversible (GTR) model with invariant sites and gamma distribution for each of the partitions; bootstrap analyses with 1,000 resamplings were used for statistical support. The same mentioned partition strategy and model were used for Bayesian inference in MrBayes v. 3.2.2 (Huelsenbeck and Ronquist, 2001). Four Monte Carlo–Markov chains were run for 5 million generations, and tree sampling was done every 1,000 generations. Tracer v.1.5 (Rambaut and Drummond, 2007) was used to verify the stationary distribution of the runs; 1,250 trees were discarded as burn-in for the 50% majority rule consensus trees.

ULTRASTRUCTURE OF CARBONATE WALLS

Crusts were fractured using shears and mounted in superglue. After low-magnification imaging of fractured crusts, they were prepared as follows for scanning electron microscopy–energy dispersive spectroscopy (SEM-EDS) measurements. Samples were polished using 2,000 gsm (grams/square meter) wet or dry sandpaper, then sonic cleaned in unbuffered deionized water for 2 min. This cleaning method very lightly etches the surface, allowing differentiation between different magnesium calcite morphologies without altering the measured Mg content. Specimens were then coated with platinum.

TABLE 1. Presence of *Phymatolithon* by species and depth at stations in the Boreal–Subarctic transition zone of the North Atlantic. Abbreviations: Int = intertidal zone; rhodos = rhodoliths; Tr = trace. A dash (-) indicates not present or data not available; a question mark (?) indicates indeterminant specimen.

Station no.	Date	Location ^a	Latitude	Longitude
61-1	7/13/1961	Sally Island, off Corea, ME, USA	44 24.1N	67 56.7W
61-3	7/19/1961	Andrews Island, W Deer Isle, Thorofare, ME, USA	44 8.8 N	68 42.2W
61-4	7/20/1961	Benner Island, Muscongus Bay, ME, USA	43 52.8 N	69 19.3 W
61-5	7/22/1961	Small Point, Cape Small, ME, USA	43 42.2N	69 50.3W
61-6	7/23/1961	Richmond Island, Cape Elizabeth, ME, USA	43 32.4N	70 13.8W
61-7	7/24/1961	Smutty Nose Island, Isles Shoals, NH, USA	42 59.0N	70 36.4W
61-8	7/27/1961	Stellwagen ledge, Scituate, MA, USA	vic 42 16N	70 46 W
61-9	7/28/1961	Naushon Island, Buzzards Bay, MA, USA	41 30.1N	70 44.1W
61-10	7/29/1961	Vineyard Sound, Norton Rock, Martha's Vineyard, MA, USA	41 26.1N	70 42.3W
61-11	7/30/1961	Nashawena Island, S Central, MA, USA	41 25.2N	70 52.5W
61-12	8/1/1961	Nantucket Harbor, Coate & 2nd, MA, USA	41 18.0N	70 4.4W
61-13	8/4/1961	Newport Neck, Sheep Point, RI, USA	41 27.6 N	71 18.0 W
61-14	8/5/1961	Bartlet Reef, NNW Race, Long Island Sound, CT, USA	41 16.3 N	72 8.1 W
61-15	8/7/1961	East side Block Island, Grace Point, RI, USA	41 10.0N	71 32.6W
61-16	8/9/1961	High Pine ledge, off Plymouth, MA, USA	42 1.9 N	70 36.5 W
61-17	8/9/1961	Pickworth Point, off Manchester, MA, USA	42 33.7 N	70 45.9 W
61-18	8/10/1961	Cape Neddick, ME, USA	43 10.1N	70 35.6W
61-19	8/12/1961	Outer Heron Island, Boothbay Harbor, ME, USA	43 46.2N	69 35.1W
61-20	8/13/1961	Otter Island, off Vinalhaven, ME, USA	44 0.3 N	68 48.0 W
61-21 (+ 62-32,87)	8/17/1961	Western Head, Isle au Haut, ME, USA	44 0.4N	68 39.1W
61-22	8/20/1961	Shingle Island, W Jericho Bay, ME, USA	44 9.2 N	68 35.0 W
61-23	8/23/1961	Wooden Ball Island, off Penobscot Bay, ME, USA	43 53.5N	68 44.3W
61-24	8/23/1961	Wooden Ball Island, off Penobscot Bay, ME, USA	43 53.5N	68 44.3W
61-25	8/23/1961	Matinicus Rock, ME, USA	43 47.0N	68 51.4W
61-26	8/27/1961	Great Duck Island, SE Muscongus Bay, ME, USA	43 52.6N	69 7.3W
61-27	8/29/1961	Upper Herring, Steele Harbor Island, ME, USA	44 29.1 N	67 31.7 W
61-28	8/30/1961	SW Head, Grand Manan Island, NB, Canada	44 36.5 N	66 59.8 W
61-29	8/31/1961	Spruce Point, Cross Island, ME, USA	44 35.9N	67 18.7W
61-30	9/5/1961	Baccarro Point, Barrington Bay, NS, Canada	43 27.8N	65 29.6 W
61-31	9/6/1961	Beaver Point, Outer Beaver Harbor, NS, Canada	44 53.4	62 25.0 W
61-32	9/7/1961	Livingston Cove, Cape George, NS, Canada	45 52.1 N	61 58.9 W
61-33 & following	9/23/1961	Merchant Island, off Deer Isle, ME, USA	44 6.3N	68 39.3W
61-34	9/24/1961	Northwest Harbor, Deer Isle, ME, USA	44 13.7 N	68 41.2 W
61-35	9/30/1961	Merchant Island, off Deer Isle, ME, USA	44 6.3N	68 39.3W
61-36	10/5/1961	Hurricane Island, off Vinalhaven, ME, USA	44 2.0 N	68 53.5 W
61-37	10/7/1961	Lower head, Marshall Island, ME, USA	44 5.8 N	68 30.4 W
61-38	10/17/1961	Merchant Island, off Deer Isle, ME, USA	44 6.3N	68 39.3W
61-39	10/22/1961	Kimball Head, Kimball Island, ME, USA	44 4.5 N	68 40.3 W

TABLE 1. (Extended)

Int	Depth (m); x = depth zone collected							% <i>P. laevigatum</i>	% <i>P. rugulosum</i>	% <i>P. squamulosum</i>	% <i>P. nantuckensis</i>	% <i>P. borealis</i>	% <i>P. investiens</i>
	0-3	3-9	9-15	15-21	21-28	28-37	>37	0-25 m	5-30 m	Int-3 m	0-30 m	0-35 m	
-	-	x	x	-	-	-	-	12	17	-	-	-	-
-	x	x	-	-	-	-	-	0	0	-	-	-	-
x	-	-	-	-	-	-	-	-	-	Present	-	-	-
-	x	x	x	-	-	-	-	32	21	-	-	-	-
-	-	x	x	-	-	-	-	24	5	-	-	-	-
-	-	-	x	-	-	-	-	0	0	-	-	-	-
-	-	-	x	-	-	-	-	46	Tr	-	-	-	-
-	-	x	x	-	-	-	-	100	0	-	-	-	-
-	x	x	-	-	-	-	-	90	0	-	-	-	-
-	x	x	x	-	-	-	-	100	0	-	-	-	-
-	-	x	-	-	-	-	-	?	0	-	100	-	-
-	-	-	x	-	-	-	-	100	0	-	-	-	-
-	-	x	-	-	-	-	-	100	0	-	-	-	-
-	-	x	-	-	-	-	-	46	<1	-	-	-	-
-	x	x	x	-	-	-	-	28	1	-	-	-	-
-	x	x	x	-	-	-	-	14	12	-	-	-	-
-	-	x	x	x	-	-	-	28	5	-	-	-	-
-	-	x	x	x	-	-	-	4	15	-	-	-	-
-	-	-	x	-	-	-	-	-	-	-	-	-	-
-	x	-	-	-	-	-	-	-	-	-	-	-	-
x	x	-	-	-	-	-	-	-	-	Absent	-	-	-
-	-	-	-	x	x	-	-	0	0	-	-	-	-
-	-	x	x	-	-	-	-	6	5	-	-	-	-
-	x	x	x	-	-	-	-	2	3	-	-	-	-
-	-	x	x	x	-	-	-	11	2	-	-	-	-
-	-	x	x	x	-	-	-	1	Tr	-	-	-	-
-	-	x	x	x	-	-	-	2	<1	-	-	-	-
-	-	x	-	-	-	-	-	10	28	-	-	-	-
-	-	x	x	x	-	-	-	4	0	-	-	-	-
-	-	x	x	x	-	-	-	-	-	-	-	-	-
x	x	x	x	-	-	-	-	2	32	Absent	-	-	-
x	-	-	-	-	-	-	-	-	-	Absent	-	-	-
-	x	x	-	-	-	-	-	-	-	-	-	-	-
-	x	x	x	-	-	-	-	3	11	-	-	-	-
-	x	x	x	-	-	-	-	0.4	27	-	-	-	-
-	x	x	-	-	-	-	-	-	-	-	-	-	-
-	x	x	-	-	-	-	-	3	4	-	-	-	-

TABLE 1. (Continued)

Station no.	Date	Location ^a	Latitude	Longitude
61-40	10/23/1961	Northwest Harbor, Deer Isle, ME, USA	44 13.7 N	68 41.2 W
61-41	11/2/1961	Merchant Island, off Deer Isle, ME, USA	44 6.3N	68 39.3W
61-42,46; 62-4,21	11/5/1961	NW Great Spoon Island, ME, USA	44 2.7N	68 33.5W
61-43	11/17/1961	N Vineyard S, Woods Hole, MA, USA	41 31.0 N	70 39.4 W
61-44	11/19/1961	Halibut Point, Cape Ann, MA, USA	42 41.7 N	70 37.9W
61-45	12/2/1961	Merchant Island, off Deer Isle, ME, USA	44 6.3N	68 39.3W
61-46	12/3/1961	NW Great Spoon Island, ME, USA	44 2.7N	68 33.5W
62-1	1/3/1962	W Deer Isle, Dunham Point, ME, USA	44 13.3 N	68 44.0 W
62-2	1/6/1962	Merchant Island, off Deer Isle, ME, USA	44 6.3N	68 39.3W
62-3	2/10/1962	Merchant Island, off Deer Isle, ME, USA	44 6.3N	68 39.3W
62-4	2/16/1962	NW Great Spoon Island, ME, USA	44 2.7N	68 33.5W
62-5	2/28/1962	NW Deer Isle, ME, USA	44 16.0 N	68 40.5 W
62-6	3/5/1962	NW Little Deer Isle, ME, USA	44 18.5 N	68 44.8 W
62-7	3/7/1962	NW Harbor, Deer Isle, ME, USA	44 13.4 N	68 40.9W
62-8	3/11/1962	Lane Cove Breakwater, Cape Ann, MA, USA	42 40.8 N	70 39.7 W
62-9	3/16/1962	S Saddleback Island, W Jericho Bay, ME, USA	44 8.6 N	68 34.8 W
62-11L	3/17/1962	Brace Cove, SE Cape Ann, MA, USA	42 35.6 N	70 38.9 W
62-12	3/29/1962	Sheephead Island, off Deer Isle, ME, USA	44 12.3 N	68 34.0 W
62-13	3/30/1962	E Wbster Head, North Haven Island, ME, USA	44 11.1 N	68 50.6 W
62-14	4/3/1962	Rich's Point, Isle au Haut, ME, USA	44 5.2 N	68 36.0 W
62-15	4/11/1962	Fog Island, off Deer Isle, ME, USA	44 5.7 N	68 34.4 W
62-16	4/12/1962	Merchant Island, off Deer Isle, ME, USA	44 6.3N	68 39.3W
62-17	4/15/1962	Stave Island, Egemoggin Reach, ME, USA	44 17.3 N	68 41.3 W
62-18	4/17/1962	Pressey Cove to NW Harbor, Deer Isle, ME, USA	44 14.3 N	68 42.5 W
62-19,23	4/28/1962	NE Eagle Island, E Penobscot Bay, ME, USA	44 13.2 N	68 46.2 W
62-20	5/2/1962	Off Bartlett Harbor, North Haven Island, ME, USA	44 8.4 N	68 55.6 W
62-21	5/11/1962	NW Great Spoon Island, ME, USA	44 2.7N	68 33.5W
62-23	5/12/1962	NE Eagle Island, Penobscot Bay, ME, USA	44 13.2 N	68 46.2 W
62-24	5/16/1962	Orrs Cove, Cape Rosier, Penobscot Bay, ME, USA	44 19.6 N	68 49.4 W
62-25	5/17/1962	Negro Island, Bagaduce River, N Penobscot, ME, USA	44 24.2 N	68 46.4 W
62-26	5/17/1962	Turtle Cove, Long Island, Penobscot Bay, ME, USA	44 23.1 N	68 53.7 W
62-27	5/29/1962	NE Mount Desert Rock, ME, USA	43 58.2 N	68 7.6 W
62-28	5/31/1962	Great Spruce Thoro, Roque Island, ME, USA	44 33.9 N	67 30.7 W
62-29	5/31/1962	Cow Point, Mack Cove, Englishmen Bay, ME, USA	44 35.8 N	67 27.6 W
62-30	6/1/1962	W Almore Cove, off Cutler, ME, USA	44 39.7 N	67 11.2 W
62-31	6/2/1962	Deep Cove, Cobscook Bay, ME, USA	44 53.7 N	67 6.7 W
62-32,87	6/8/1962	E Western Ear, Isle au Haut, ME, USA	44 0.3 N	68 39.1 W
62-33	6/8/1962	Central S Isle au Haut, ME, USA	44 0.8 N	68 38.3 W
62-35	6/14/1962	Popplest Cove, Great Wass Island, ME, USA	44 27.5 N	67 34.2 W

TABLE 1. (Extended)

Int	Depth (m); x = depth zone collected							% <i>P.</i> <i>laevigatum</i>	% <i>P.</i> <i>rugulosum</i>	% <i>P.</i> <i>squamulosum</i>	% <i>P.</i> <i>nantuckensis</i>	% <i>P.</i> <i>borealis</i>	% <i>P.</i> <i>investiens</i>
	0-3	3-9	9-15	15-21	21-28	28-37	>37	0-25 m	5-30 m	Int-3 m	0-30 m	0-35 m	
x	-	-	-	-	-	-	-	-	-	Absent	-	-	
-	x	x	-	-	-	-	-	-	-	-	-	-	
-	x	x	x	-	-	-	-	6	13	-	-	-	
-	x	x	-	-	-	-	-	90	-	?	-	-	
-	x	x	x	-	-	-	-	22	6	-	-	-	
-	x	-	-	-	-	-	-	-	-	-	-	-	
-	-	x	-	-	-	-	-	-	-	-	-	-	
x	-	-	-	-	-	-	-	-	-	Present	-	-	
-	x	x	-	-	-	-	-	-	-	-	-	-	
-	x	x	-	-	-	-	-	-	-	-	-	-	
-	-	x	-	-	-	-	-	-	-	-	-	-	
x	-	-	-	-	-	-	-	-	-	Present	-	-	
x	x	-	-	-	-	-	-	11	6	Abundant	-	-	
x	-	-	-	-	-	-	-	-	-	Absent	-	-	
-	x	x	-	-	-	-	-	12	Tr	-	-	-	
-	x	x	-	-	-	-	-	0.9	13	-	-	-	
-	-	x	-	-	-	-	-	-	-	-	-	-	
x	-	-	-	-	-	-	-	-	-	Abundant	-	-	
-	x	-	-	-	-	-	-	2	10	-	-	-	
-	-	x	-	-	-	-	-	3	Tr	-	-	-	
-	x	x	-	-	-	-	-	0.5	2	Absent	-	-	
-	x	x	-	-	-	-	-	-	-	-	-	-	
x	-	-	-	-	-	-	-	-	-	Present	-	-	
x	x	x	-	-	-	-	-	0	20	Present	-	-	
-	x	x	x	-	-	-	-	7	4	-	-	-	
x	x	x	-	-	-	-	-	6	4	Present	-	-	
-	-	-	x	-	-	-	-	-	-	-	-	-	
-	x	x	x	-	-	-	-	-	-	-	-	-	
x	x	x	-	-	-	-	-	0.8	Tr	Abundant	-	-	
-	x	x	x	-	-	-	-	19	0	-	-	-	
x	x	x	-	-	-	-	-	31	0.5	Abundant	-	-	
-	-	-	x	x	-	-	-	7	1	-	-	-	
x	x	-	-	-	-	-	-	1	0	Absent	-	-	
x	x	x	x	-	-	-	-	4	0	Absent	-	-	
x	x	x	-	-	-	-	-	6	Tr	Absent	-	-	
x	x	x	-	-	-	-	-	Tr	2	Absent	-	-	
-	-	x	x	x	x	-	-	18	6	-	-	-	
-	x	x	-	-	-	-	-	0	6	-	-	-	
x	x	x	x	x	-	-	-	5	0	Absent	-	-	

TABLE 1. (Continued)

Station no.	Date	Location ^a	Latitude	Longitude
62-36	6/15/1962	Grand Manan Channel, East Head, NB, Canada	44 49.9 N	65 55.6
62-37	6/16/1962	Passamaquoddy Bay, Deer Isle, NB, Canada	44 47.5 N	66 57.0
62-38	6/17/1962	N Nancy Head, Campobello Island, NB, Canada	44 55.0 N	67 53.5
62-39	6/18/1962	Cambell Point, Dipper Harbor, Bay of Fundy, NB, Canada	44 5.2 N	66 24.6 W
62-40	6/21/1962	Macomber Point, Quaco Bay, Bay of Fundy, NB, Canada	45 21.4 N	65 31.0 W
62-41	6/22/1962	Quaco Ledge, Bay of Fundy, NB, Canada	vic 45 17 N	65 20 W
62-42	6/23/1962	Broad Cove, off Digby, NS, Canada	44 41.3 N	65 46.5 W
62-43	6/25/1962	N Swallowtail Point, Grand Manan, NB, Canada	44 46.4 N	66 45.0 W
62-44,50	6/26/1962	Arey Cove, Schoodic Point, ME, USA	44 20.0 N	68 3.6 W
62-45	6/20/1962	NE Butter Island, E Penobscot Bay, ME, USA	44 14.2 N	68 47.4 W
62-46	7/1/1962	SE Pickering Island, E Penobscot Bay, ME, USA	44 15.6 N	68 44.7 W
62-47	7/2/1962	Deer Isle Mill Pond, ME, USA	44 13.6 N	68 41.1 W
62-48	7/2/1962	SW Eagle Island, E Penobscot Bay, ME, USA	44 12.3 N	68 47.1 W
62-49	7/9/1962	SE Vinalhaven, ME, USA	44 1.9 N	68 49.0 W
62-50	7/12/1962	Arey Cove, Schoodic Point, ME, USA	44 20.0 N	68 3.6 W
62-51	7/13/1962	S Parker Head, Roque Island, ME, USA	44 34.7 N	67 32.4 W
62-52	7/14/1962	S shore Outer Wood Island, NB, Canada	44 36.3 N	66 49.1 W
62-53	7/16/1962	SW Cape Fourchu, West, NS, Canada	43 47.8 N	66 10.0 W
62-54	7/17/1962	SW St Ann Point, Pubnico, NS, Canada	43 35.7 N	65 48.6 W
62-55	7/18/1962	E Cat Point, Baccaro Point, NS, Canada	43 27.4 N	65 27.9 W
62-56	7/19/1962	E Cape Roseway, NS, Canada	43 37.7 N	65 15.7 W
62-57	7/20/1962	Green Point, W Port Latour, NS, Canada	43 29.9 N	65 31.7 W
62-58	7/23/1962	Whipple Point, Brier Island, NS, Canada	44 13.5 N	66 22.3 W
62-59	7/30/1962	Kimble Island, ME, USA	44 4.5 N	68 40.3 W
62-60	7/30/1962	Eggemoggin in Egg, Reach, ME, USA	44 18.6 N	68 44.0 W
62-61	8/3/1962	NW Flint Island, Flint Island Narrows, ME, USA	44 28.8 N	67 47.8 W
62-62	8/4/1962	Pinkham Island, Harrington Bay, ME, USA	44 32.6 N	67 49.8 W
62-65	8/11/1962	Deep Cove, Long Island, Blue Hill Bay, ME, USA	44 21.7 N	68 31.4 W
62-67	8/12/1962	Seal Cove, Bartlett Island, Blue Hill Bay, ME, USA	44 20.3 N	68 27.0 W
62-68	8/13/1962	Long Porc/Hop, Frenchmen Bay, ME, USA	44 24.6 N	68 9.3 W
62-69	8/12/1962	Freese's Island, W Deer Isle, ME, USA	44 12.3 N	68 43.3 W
62-70	8/16/1962	E Metinic Island, ME, USA	44 52.3 N	69 7.1 W
62-71	8/17/2015	Cranberry Island, Muscongus Bay, ME, USA	43 56.2 N	69 21.8 W
62-72	8/18/1962	Stage Island, Cape Porpoise, ME, USA	43 21.7 N	70 24.9 W
62-73	8/19/1962	Flat Point, E Cape Ann, MA, USA	42 38.9 N	70 35.4 W
62-74	8/20/1962	Center Hill Point, Cape Cod Bay, MA, USA	41 51.6 N	70 31.3 W
62-75	8/21/1962	N Clark Island, Duxbury Bay, MA, USA	42 0.8 N	70 38.2 W
62-76	8/21/1962	W Calf Island, off Boston Harbor, MA, USA	42 20.4 N	70 53.9 W
62-77	8/23/1962	Wood Island, off Biddeford, ME, USA	43 27.5 N	70 19.5 W

TABLE 1. (Extended)

Int	Depth (m); x = depth zone collected							% <i>P.</i>	% <i>P.</i>	% <i>P.</i>	% <i>P.</i>	% <i>P.</i>	% <i>P.</i>
	0-3	3-9	9-15	15-21	21-28	28-37	>37	<i>laevigatum</i> 0-25 m	<i>rugulosum</i> 5-30 m	<i>squamulosum</i> Int-3 m	<i>nantuckensis</i>	<i>borealis</i> 0-30 m	<i>investiens</i> 0-35 m
-	x	x	x	-	-	-	-	2	0.7	-	-	-	-
x	x	x	x	-	-	-	-	Tr	33	Absent	-	-	-
-	x	x	x	-	-	-	-	0.2	8	-	-	-	-
x	x	x	-	-	-	-	-	7	8	Absent	-	-	-
x	x	x	-	-	-	-	-	34	3	Absent	-	-	-
x	x	x	-	-	-	-	-	9	9	Absent	-	-	-
-	x	x	-	-	-	-	-	31	0.2	-	-	-	-
x	x	x	x	x	-	-	-	Tr	6	Absent	-	-	-
-	x	x	-	-	-	-	-	Tr	21	-	-	-	-
-	x	-	-	-	-	-	-	-	-	-	-	-	-
-	x	x	-	-	-	-	-	0	25	-	-	-	-
x	x	-	-	-	-	-	-	-	-	Absent	-	-	-
-	x	-	-	-	-	-	-	0	30	-	-	-	-
-	x	x	-	-	-	-	-	-	-	-	-	-	-
-	-	x	x	-	-	-	-	-	-	-	-	-	-
x	x	x	-	-	-	-	-	16	0	Absent	-	-	-
x	x	x	-	-	-	-	-	4	0	Absent	-	-	-
x	x	x	x	-	-	-	-	7	57	Abundant	-	-	-
x	x	x	-	-	-	-	-	58	1	Abundant	-	-	-
-	-	x	-	-	-	-	-	-	-	-	-	-	-
-	-	-	x	x	-	x	-	0.3	37	-	-	-	-
x	x	x	-	-	-	-	-	3	20	Present	-	-	-
x	x	x	-	-	-	-	-	4	0.8	Present	-	-	-
x	x	x	-	-	-	-	-	0.4	31	Absent	-	-	-
x	-	-	-	-	-	-	-	-	-	Present	-	-	-
x	x	x	-	-	-	-	-	3	Tr	Absent	-	-	-
x	-	-	-	-	-	-	-	-	-	Absent	-	-	-
x	x	x	x	-	-	-	-	1.7	20	Absent	-	-	-
x	x	x	x	-	-	-	-	4	65	Absent	-	-	-
x	x	x	x	-	-	-	-	Tr	23	Absent	-	-	-
x	-	-	-	-	-	-	-	-	-	Present	-	-	-
x	x	x	x	x	-	-	-	7	4	Abundant	-	-	-
x	x	x	-	-	-	-	-	1	0	Abundant	-	-	-
x	x	x	x	-	-	-	-	3	0	Absent	-	-	-
x	x	x	x	x	-	-	-	10	4	Abundant	-	-	-
x	x	x	-	-	-	-	-	79	0	Absent	-	-	-
x	x	x	-	-	-	-	-	48	0	Absent	-	-	-
x	x	x	-	-	-	-	-	5	0	Absent	-	-	-
x	x	x	x	-	-	-	-	45	Tr	Absent	-	-	-

TABLE 1. (Continued)

Station no.	Date	Location ^a	Latitude	Longitude
62-78	8/24/1962	N of Rockland Breakwater, W Penobscot, ME, USA	44 7.1 N	69 4.6 W
62-79A	8/26/1962	NW Moose Island, SW Deer Isle, ME, USA	44 9.0 N	68 41.2 W
62-79B	8/27/1962	Carter Point, Eggemoggin Reach, ME, USA	44 16.7 N	68 37.6 W
62-79C	8/27/1962	Naskeag Harbor, ME, USA	44 13.7 N	68 31.8 W
62-79D	8/20/1962	Harriman Point, Blue Hill Bay, ME, USA	44 18.1 N	68 31.9 W
62-79E	8/20/1962	Thompson Cove, Eggemoggin Reach, ME, USA	44 15.8 N	68 39.1 W
62-79F	8/21/1962	W Lazygut Island, off Deer Isle, ME, USA	44 10.9 N	68 33.9 W
62-79G	8/21/1962	SW E Mark Island, Jericho Bay, ME, USA	44 10.1 N	68 34.9 W
62-80	8/28/1962	W Bradbury Island, E Penobscot Bay, ME, USA	44 14.7 N	68 45.9 W
62-82	8/29/1962	W Cape St Mary, NS, Canada	44 5.3 N	66 12.9 W
62-83	8/30/1962	Cape D'or, Bay of Fundy, NS, Canada	45 18.1 N	64 45.7 W
62-84	9/1/1962	L'Etete Pass, Green Point, Passam, NB, Canada	45 2.4 N	66 53.6 W
62-87	9/4/1962	Western Ear, Isle au Haut, ME, USA	44 0.3 N	68 39.1 W
62-88	9/6/1962	Dice Head, N Penobscot Bay, ME, USA	44 22.9 N	68 49.4 W
E62-6	10/20/1962	N & Little Deer Isle, ME, USA	vic 44 17N	68 41W
63-1	7/17/1963	E Point off Scituate, MA, USA	42 12.4 N	70 43.0 W
63-2	7/18/1963	Orrs Island, Harpwell Sound, ME, USA	43 47.6 N	69 56.8 W
63-3	7/21/1963	S Merchant Island cove, ME, USA	44 6.3N	68 39.3W
63-5	7/22/1963	Pemaquid Point, ME, USA	43 50.1 N	69 30.4 W
63-6	7/24/1963	Brant Rock, Mass Bay, MA, USA	42 5.6 N	70 38.5 W
63-7	7/24/1963	Woods Hole, Marine Biological Lab Beach, MA, USA	41 31.6 N	70 40.5 W
63-8	7/14/1963	Cape Cod Canal, MA, at bridges, USA	vic 41 46 N	70 33.9 W
63-9	7/26/1963	Great Bald Head, Ogunquit, ME, USA	43 12.5 N	70 35.2 W
63-10	7/26/1963	Ogunquit, ME, shore off harbor, USA	43 14.0 N	70 35.2 W
64-1	6/6/1964	Harding Point off Port Hebert, NS, Canada	43 44.8N	64 57.5W
64-2	6/8/1964	SE Shannon Island, NS, Canada	49 27.4N	63 44.5W
64-3	6/9/1964	Bald Rock off Ship Harbour, NS, Canada	44 41 N	62 48.4 W
64-4	6/10/1964	Pass between Liscomb & Hemloe Island, NS, Canada	45 0.4N	61 58.5W
64-5	6/11/1964	Mill Cape, Bras D'Or Lakes, NS, Canada	45 49.5N	60 41.8W
64-6	6/15/1964	Pearl Island, Bay of Islands, NF, Canada	49 12.6N	58 15.8W
64-8	6/16/1964	Pearl Island, NF, Canada	49 14N	58 17W
64-9	6/21/1964	E Cape St George, NF, Canada	48 29.2N	59 7.3W
64-10	6/22/1964	SE Cape Ray, NF, Canada	47 37.2N	59 17.7W
64-11	6/23/1964	St Paul Island, NS, Canada	47 12.8N	60 8.2W
64-12	6/25/1964	Beaton Point, Mabou, Cape Breton, Canada	46 6.5N	61 28.8W
64-14	6/27/1964	E Macquarie Point, off Pictou, NS, Canada	45 47.2N	62 50W
64-15	6/28/1964	Cape Wolfe, W shore, PEI, Canada	46 43.5N	64 24.5W
64-16	6/29/1964	Fisherman Ledge, off Caraquet, NB, Canada	47 52.5N	64 53.25W

TABLE 1. (Extended)

Int	Depth (m); x = depth zone collected							% <i>P.</i> <i>laevigatum</i>	% <i>P.</i> <i>rugulosum</i>	% <i>P.</i> <i>squamulosum</i>	% <i>P.</i> <i>nantuckensis</i>	% <i>P.</i> <i>borealis</i>	% <i>P.</i> <i>investiens</i>
	0-3	3-9	9-15	15-21	21-28	28-37	>37	0-25 m	5-30 m	Int-3 m	0-30 m	0-35 m	
x	x	x	x	-	-	-	-	5	Tr	Abundant	-	-	-
x	-	-	-	-	-	-	-	-	-	Present	-	-	-
x	-	-	-	-	-	-	-	-	-	Present	-	-	-
x	-	-	-	-	-	-	-	-	-	Absent	-	-	-
x	-	-	-	-	-	-	-	-	-	Absent	-	-	-
x	-	-	-	-	-	-	-	-	-	Present	-	-	-
x	-	-	-	-	-	-	-	-	-	Absent	-	-	-
x	-	-	-	-	-	-	-	-	-	Absent	-	-	-
x	x	x	x	x	-	-	-	5	5	Abundant	-	-	-
x	x	x	-	-	-	-	-	-	-	Present	-	-	-
x	x	x	x	-	-	-	-	19	12	Abundant	-	-	-
-	x	x	-	-	-	-	-	0	31	-	-	-	-
-	x	x	x	x	-	-	-	22	7	-	-	-	-
-	x	x	-	-	-	-	-	2	12	-	-	-	-
x	-	-	-	-	-	-	-	-	-	Present	-	-	-
x	-	-	-	-	-	-	-	-	-	Absent	-	-	-
x	-	-	-	-	-	-	-	-	-	Abundant	-	-	-
x	-	-	-	-	-	-	-	-	-	Abundant	-	-	-
x	-	-	-	-	-	-	-	-	-	Abundant	-	-	-
x	-	-	-	-	-	-	-	-	-	Absent	-	-	-
x	-	-	-	-	-	-	-	-	-	Absent	-	-	-
x	-	-	-	-	-	-	-	-	-	Absent	-	-	-
x	-	-	-	-	-	-	-	-	-	Abundant	-	-	-
x	-	-	-	-	-	-	-	-	-	Present	-	-	-
x	x	x	x	-	-	x	x	10	51	Abundant	-	-	-
x	x	x	x	x	-	-	-	14	0.4	Abundant	-	-	-
-	-	-	x	x	-	-	x	2	1	-	-	-	-
-	-	x	-	-	-	-	-	29	0.2	-	-	-	-
-	x	x	-	-	-	-	-	100	0	-	-	-	-
x	x	x	x	x	x	x	-	5.0	0.1	Present	-	-	-
-	-	-	-	-	-	-	x	-	-	-	-	-	-
-	x	-	x	-	-	-	-	39	0	-	-	-	-
x	-	x	x	-	-	-	-	0	0	Absent	-	-	-
x	-	x	-	x	x	-	x	0	Tr	Absent	-	-	-
x	-	x	-	-	-	-	-	44	0	Absent	-	-	-
-	x	x	-	-	-	-	-	53	0	Abundant to 9 m	-	-	-
-	x	x	-	-	x	x	x	58	0	Present	-	-	-
-	-	x	x	x	-	x	-	22	0	-	-	-	-

TABLE 1. (Continued)

Station no.	Date	Location ^a	Latitude	Longitude
64-17	6/30/1964	NE Bonaventure Island, Quebec, Canada	48 29.8N	64 9.5W
64-18	7/1/1964	Fame Point, NE Gaspé, Quebec, Canada	49 7N	64 38W
64-19	7/2/1964	Ile Petite Basque, Quebec, Canada	50 8.3N	66 21.4W
64-20	7/3/1964	Off Seal River, Moisie Bay, Quebec, Canada	50 15N	65 46W
64-21	7/4/1964	Eskimo Island, off Havre St P, Quebec, Canada	50 12.9N	63 39.5W
64-22	7/5/1964	S Ile Longue, Quetachu Bay, Quebec, Canada	50 16.4N	62 48W
64-23	7/12/1964	North Arm Point, Bay of Islands, NF, Canada	49 11.2N	58 7.1W
64-24	7/15/1964	Bay of Islands, NF, Canada	49 4-12N	58 12-20W
64-26	7/21/1964	Bound Head, Humber Arm, NF, Canada	49 2.6N	58 6.8W
64-27	7/24/1964	Wapitagan Island, Quebec, Canada	50 11.7N	60 0.8W
64-28	7/25/1964	NE Great Mecatina, Mackinnon Island, Quebec, Canada	50 50.2N	58 50.6W
64-29	7/25/1964	Red Bay, Strait of Bell Isle, Labrador, NF, Canada	51 42.8N	56 25.8W
64-30	7/27/1964	NW Camp Islands, Labrador, NF, Canada	52 10.5N	55 39.9W
64-31	7/28/1964	White Bear Arm Labrador, NF, Canada	52 46.7N	56 0.7W
64-32	7/31/1964	Cape Harrison, Labrador, NF, Canada	54 52N	57 57W
64-33	8/1/1964	Hopedale Run, Labrador, NF, Canada	55 26.2N	59 49.1W
64-34	8/2/1964	Tunungayualuk Island, Labrador, NF, Canada	56 3.6N	61.13W
64-35	8/4/1964	Whale Island, Labrador, NF, Canada	56 32N	61 9.2W
64-36	8/5/1964	Kikkertasoak Island, Labrador, NF, Canada	57 14.3N	61 28W
64-37	8/7/1964	Saglek Bay, Labrador, NF, Canada	58 32.2N	62 39W
64-38	8/8/1964	Nachvak Fjord, Labrador, NF, Canada	59 5.5N	63 30.5W
64-39	8/9/1964	Eclipse Harbor, Labrador, NF, Canada	59 51N	64 10.5W
64-40	8/10/1964	Ekortarsuk Fjord, Labrador, NF, Canada	60 6N	64 22.4W
64-41	8/17/1964	Strait of Belle Isle, NF, Canada	51 32.6N	56 4.2W
64-42	8/18/1964	James Island, St John Bay, NF, Canada	50 55.5N	57 11.5W
64-43	8/20/1964	Bay Le Moine, NF, Canada	47 37.3N	58 40.3W
64-44	8/27/1964	Fish Head, Great Island, Ramea Island, NF, Canada	47 31.7N	57 20.3W
64-45	8/29/1964	Chap Rouge, Great St Lawrence, NF, Canada	46 53.8N	55 21.7W
64-46	8/30/1964	Great Island, off Valen, NF, Canada	47 30.0N	54 2.17W
64-47	9/1/1964	Outer Fermeuse Harbor, NF, Canada	46 57.2N	52 53.5W
64-48	9/2/1964	Bay Bulls, Baboul Rocks, NF, Canada	47 17.5N	52 46.8W
64-49	9/6/1964	Trinity Bay, King's Head Cove, NF, Canada	47 59N	53 19.2W
64-50	9/7/1964	Trinity Bay, Random Sound, NF, Canada	48 5N	53 38W
64-51	9/8/1964	Skervink Head, Trinity Bay, NF, Canada	48 22N	53 19.7W
64-53	9/11/1964	E side of Change Island, NF, Canada	49 37.5N	54 23W
64-54	9/13/1964	Cape St Martin, Hardy Harbor, NF, Canada	50 1.5N	55 53W
64-56	9/27/1964	Scatari Island, NS, Canada	46 1.1N	59 45.5W
64-57	9/29/1964	SW Arm, Green Island, NS, Canada	45 53.7N	59 59.5W

TABLE 1. (Extended)

Int	Depth (m); x = depth zone collected							% <i>P.</i>	% <i>P.</i>	% <i>P.</i>	% <i>P.</i>	% <i>P.</i>	% <i>P.</i>
	0-3	3-9	9-15	15-21	21-28	28-37	>37	<i>laevigatum</i> 0-25 m	<i>rugulosum</i> 5-30 m	<i>squamulosum</i> Int-3 m	<i>nantuckensis</i>	<i>borealis</i> 0-30 m	<i>investiens</i> 0-35 m
x	-	x	x	x	-	-	-	3	0	Absent	-	-	-
x	-	x	-	x	-	-	-	0	0	Absent	-	-	-
-	-	x	x	x	-	-	-	0	0	-	-	-	-
x	x	x	x	-	-	-	-	0	0	Absent	-	-	-
x	-	x	x	x	-	-	-	0	Tr	Absent	-	-	-
x	-	x	x	x	x	-	-	0	Tr	Absent	-	-	-
-	x	x	-	-	-	-	-	30	0	-	-	-	-
x	-	-	-	-	-	-	-	-	-	Present at 1/11 sites	-	-	-
-	x	x	x	-	-	-	-	24	0	-	-	-	-
x	x	x	x	x	x	x	-	Tr	0	Absent	-	-	-
x	-	x	-	x	x	-	x	0	0	Absent	-	-	-
-	-	x	-	x	-	-	x	0	0	-	-	-	-
x	-	x	-	x	x	-	x	0	0	Absent	-	-	-
x	x	x	x	x	-	-	-	0	0	Absent	-	-	-
x	-	x	-	-	-	-	-	0	0	Absent	-	-	-
-	-	x	x	x	-	-	-	0	0	-	-	-	-
x	x	x	x	x	-	-	-	0	0	Absent	-	-	-
-	-	x	-	x	x	-	-	0	0	-	-	-	-
-	-	x	-	x	x	-	x	0	0	-	-	-	-
-	-	-	-	x	-	-	-	0	0	-	-	-	-
-	-	x	x	x	x	-	-	0	0	-	-	-	-
-	-	x	x	x	-	-	-	0	0	-	-	-	-
x	x	x	x	-	x	-	x	0	0	Absent	-	-	-
x	x	x	x	-	x	-	x	18	0	Absent	-	-	-
x	x	x	x	x	x	-	x	2	0	Absent	-	-	-
-	x	x	x	x	x	-	x	3	0.2	Absent	-	-	-
-	x	x	x	x	x	-	x	0.3	3	-	-	-	-
x	x	x	x	x	x	-	-	14	2	Absent	-	-	-
x	x	x	x	x	x	-	x	0	0	Absent	-	-	-
-	-	x	x	x	x	-	x	0	0	-	-	-	-
-	-	-	-	-	x	-	-	0	0	-	-	-	-
-	x	x	x	x	x	-	x	8	0	-	-	-	-
x	x	x	x	x	x	-	x	0	0	Absent	-	-	-
x	x	x	x	x	x	-	-	13	Tr	Abundant	-	-	-
-	x	x	x	x	x	-	x	0.4	0	-	-	-	-
-	-	x	x	x	-	-	-	7	15	-	-	-	-
-	-	x	-	-	-	-	x	20	0	-	-	-	-

TABLE 1. (Continued)

Station no.	Date	Location ^a	Latitude	Longitude
64-58	9/30/1964	Chedabucto Bay, Durell Island, NS, Canada	45 21N	61 00W
64-60	10/1/1964	Bald Rock, Whitehaven, NS, Canada	45 12N	61 10.5W
64-62	10/3/1964	Nichol Island, off Ship Harbor, NS, Canada	44 44.5N	62 45W
65-2	7/24/1965	Shrewsbury Rocks, NE NJ, USA	40 20.5 N	73 57.1 W
66-10	6/5/1966	Hvalfjord, mid Iceland	64 20N	21 45W
66-11	6/6/1966	Hvalfjord, inner Iceland	64 22.5N	21 33W
66-12	6/10/1966	Kollufjord, Hofsvik, Iceland	64 15.3N	21 52.9W
66-13	6/17/1966	Breidhafjord, Kolgraf, Iceland	65 1.2N	23 1W
66-14	6/19/1966	Kolgrafafjord, SW arm, Iceland	64 56.5N	23 6.5W
66-15	6/25/1964	Steingrimsfjord, Hunafloi, Iceland	65 39N	21 29.5W
66-16	6/27/1966	Steingrimsfjord, Os, Iceland	65 44.4N	21 41.2W
66-17	6/28/1966	Kollafjord, Iceland	65 36.4N	21 22 W
66-18	7/5/1966	Hrutey in Hrutfjord, Iceland	65 16.4N	21 8.3W
66-19	7/13/1966	Sandesnes in Eyiafjord, Iceland	66 1.4N	18 31W
66-20	7/14/1966	W shore N of Hangenes, Eyiafjord, Iceland	65 55.9N	18 18.7W
66-21	7/15/1966	S of Grenivik, Eyiafjord, Iceland	65 56N	18 12.7W
66-22	7/16/1966	E Hrusey, Eyiafjord, Iceland	65 59.9N	18 21.7W
66-23	7/26/1966	Thernunes in Reydarfjordur, Iceland	64 58.9N	13 52W
66-24	7/29/1966	Holmanes, Reydarfjordur, Iceland	65 2.5N	14 0.6W
66-25	8/4/1966	Vattarnes, outer Reydarfjordur, Iceland	64 56.4N	13 41.5W
66-26	8/11/1966	Stadhur off Grindavik, Iceland	63 49N	22 31W
66-27	8/17/1966	Urdharvita, Heimey, Iceland	63 26N	20 15W
66-28	8/29/1966	Hammerfest-Kvaloy, Norway	70 44.5N	23 48.3E
66-29	8/31/1966	Kargeneset, Kvaloy, Norway	70 31.4N	23 44.2E
66-30	9/3/1966	Bringnes, Inner Porsangerfjord, Norway	70 31.5N	25 11E
66-31	9/4/1966	Kavholme, Langfjord, N Norway	70 06.5N	22 50E
66-32	9/8/1966	Nordbotn, Kvaloy (Tromso), N Norway	69 40.4N	18 46.2E
66-33	9/11/1966	Hokey (Tromso), N Norway	69 40.1N	18 50.2E
66-34	9/11/1966	Sandesund-Tromso, N Norway	69 41.7N	18 55E
66-35	9/13/1966	Tussoy, off Tromsoy, N Norway	69 41 N	18 7.8 E
66-36	9/17/1966	Landegodefjord, N of Bodo, Norway	67 20.5N	14 29.6 E
66-37	9/18/1966	Landegodefjord, off Skjelstad, Norway	67 22.4N	14 31 E
66-38,42, 43,1,3,4	9/30/1966	Digertmulen, Trondheimsfjord, Norway	63 27.2N	10 18.8E
66-39	10/13/1966	Beitstadfjord, in Trondheimsfjord, Norway	63 56.7N	11 14 E
66-40	10/27/1966	Sorfjord, Bergkalnes, Norway	63 43.9N	10 01.1 E
66-41	10/27/1966	Sorfjord, Bergkalnes, Norway	63 43.1N	10 0.3 E
66-42	11/23/1966	Digertmulen, Trondheimsfjord, Norway	63 27.2 N	10 18.8 E`
66-43	12/27/1966	Digertmulen, Trondheimsfjord, Norway	63 27.2N	10 18.8 E
67-1	2/1/1967	Digertmulen, Trondheimsfjord, Norway	63 27.2N	10 18.8E`

TABLE 1. (Extended)

Int	Depth (m); x = depth zone collected							% <i>P. laevigatum</i>	% <i>P. rugulosum</i>	% <i>P. squamulosum</i>	% <i>P. nantuckensis</i>	% <i>P. borealis</i>	% <i>P. investiens</i>
	0-3	3-9	9-15	15-21	21-28	28-37	>37	0-25 m	5-30 m	Int-3 m		0-30 m	0-35 m
-	-	-	-	-	x	-	-	-	-	-	-	-	-
x	x	x	x	x	x	-	-	26	3	Absent	-	-	-
x	x	x	-	-	x	x	x	23	2	Abundant	-	-	-
-	-	x	x	-	-	-	-	100	0	-	-	-	-
-	x	-	-	-	-	-	-	0	46	-	-	0	0
-	-	x	x	x	-	-	-	0	4	-	-	0	0
x	x	x	x	x	x	-	-	1	39	Abundant	-	0	0
x	x	x	x	x	-	-	-	0	2	Present	-	0	0
x	x	x	x	-	-	-	-	0	0	Abundant	-	0	0
-	x	x	x	x	x	x	x	0	0.2	-	-	0	0
-	x	x	x	-	-	-	-	0	0	-	-	0	0
x	x	x	x	x	x	x	-	0	0.4	Absent	-	0	0
x	x	x	x	x	x	x	x	0	0	Absent	-	0	0
-	-	-	x	-	-	-	-	0	0	-	-	0	0
-	x	x	x	-	-	-	-	0	0	-	-	0	0
x	-	x	x	x	-	-	-	0	0	Absent	-	0	0
-	-	x	x	x	-	-	-	0	0	-	-	0	0
x	x	x	x	x	x	x	x	0	0	Absent	-	0	0
-	x	x	x	x	x	x	-	0	0	-	-	0	0
x	x	x	x	x	x	x	x	0	0.1	Absent	-	0	0
x	x	x	x	x	x	x	-	0.3	36	Abundant	-	0	0
x	x	x	x	x	x	-	-	0	61	Abundant	-	0	0
x	x	x	x	x	x	x	x	0	Tr	Present	-	0	7
x	x	x	x	x	x	x	-	0	0	Present	-	0	7
x	x	x	x	x	-	-	-	0	0	Present	-	0	42
-	x	x	x	x	x	x	x	0	Tr	Tr	-	0	39
x	x	x	x	x	x	x	-	5	0	Present	-	-	rhodos, Tr
-	-	-	x	x	x	-	-	0	0	-	-	-	rhodos, Tr
-	-	-	-	-	x	-	-	-	-	-	-	-	rhodos, Tr
-	x	x	x	x	-	x	-	0	4	-	-	0	Tr
-	x	x	x	x	x	-	-	0	Tr	Present	-	-	17
x	-	x	-	x	-	-	-	-	-	Abundant	-	0	0
x	x	x	x	x	x	-	-	22	0.1	Abundant	-	2	10
x	x	x	x	x	x	x	-	35	0.6	Abundant	-	2	0
x	x	x	x	x	x	-	-	33	1	Abundant	-	-	0
-	-	x	-	-	-	-	-	-	-	-	-	0	0
x	x	x	x	x	x	x	-	-	-	-	-	-	Tr
-	x	x	x	x	x	-	-	-	-	-	-	-	-
-	x	x	x	x	x	x	-	-	-	-	-	-	-

TABLE 1. (Continued)

Station no.	Date	Location ^a	Latitude	Longitude
67-2	2/3/1967	Prestvaagen, inner Trondheimsfjord, Norway	63 48.7N	10 39.1E
67-3	3/11/1967	Digertmulen, Trondheimsfjord, Norway	63 27.2N	10 18.8E
67-4	4/22/1967	Digertmulen, Trondheimsfjord, Norway	63 27.2N	10 18.8E
67-5	7/16/1967	Sorfjord, N corner of Daleoren, Norway	63 43 N	10 0 E
67-6	7/18/1967	E side of Froya-Helskjaeret, Norway	63 45 29.2	8 55 40.4
67-7	7/21/1967	Nogvafjord-Kjeholmen, Norway	62 41.5 N	6 15.7 E
67-8	7/21/1967	Veddehl in Asefjord (Alesund), Norway	62 26.7N	6 15.2 E
67-9	7/26/1967	Lagoyfjord-Indre Solund Tobehl, Norway	61 9.2N	4 48.2 E
67-10	7/30/1967	Hardangerfjord-Kvindherredsfj, Norway	59 59.5 N	5 57 E
67-11	7/31/1967	Hardangerfjord-Samlenfjord, Norway	60 20.2N	6 20.5 E
67-12	8/2/1967	Espevaer-Ryggen skjaer, Norway	59 34.4N	5 7.9 E
67-13	8/7/1967	South coast Norway-Hille-Asgard, Norway	57 59.4 N	7 21.2 E
67-14	8/9/1967	Oslo Fjord, SW Molen, Norway	59 28.9 N	10 29.6 E
67-15	8/11/1967	Oslofjord Nesodden Baerodden, Norway	59 50.2 N	10 38.2 E
67-16	8/13/1967	Outer OsloFjord-Tjomoy-Bustein, Norway	59 6.4 N	10 29.5 E
68-27	9/5/1968	Gaasvaer, Norway	66 4.2 N	12 10.0 E
68-28	9/6/1968	Alstfjord-Haestadsund, Norway	66 1-2 N	12 28-30 E
68-29	9/8/1968	Ranfjorden-Leirviken, Norway	66 12.5 N	13 33.6 E
68-30	9/12/1968	Vestvagoy-Lofoten Island, Brandish, Norway	68 4.3 N	13 38.8 E
68-31	9/14/1968	E Fjord, Forsahavnet, Norway	68 17 N	16 36.5 E
68-32	9/18/1968	Hakoy-Sandnessund-Tromsoy, Norway	69 39.7N	18 46.5E
68-33	9/27/1968	Balsfjord, Hamarvoll, Norway	69 20.8 N	19 13 E
68-34	10/3/1968	Tromsoy, SW off Biological Station, Norway	69 38.1N	18 54.3E
68-35	11/13/1968	Tromsoy, SW off Biological Station, Norway	69 38.1N	18 54.3E
69-1/2	2/19/1969	Tromsoy, SW off Biological Station, Norway	69 38.1N	18 54.3E
69-8	6/24/1969	Revabotn; Rolfroysund, Norway	71 46.7 N	23 48.5 E
69-9	6/25/1969	Hjelmsøy-Akkarfjorden-Holmen, Norway	71 5.5 N	24 42 E
69-11	6/26/1969	Mageroy-Turfjorden-Kaka, Knive, Norway	71 7.1 N	25 31.4 E
69-12	6/28/1969	Porsangerfjord-Reinoy, Norway	70 44.4N	25 50.3 E
69-13	6/29/1969	Porsangerfjord-Osterbotn, Norway	70 6.5 N	25 15 E
69-14	7/2/1969	Syltefjord-Veidnesodden, Norway	70 32.5 N	30 8.5 E
69-16	7/4/1969	Sor-Varanger-Kjofjord Brasneset, Norway	69 44.8 N	29 39.7 E
69-17a	7/4/1969	Sor-Varanger, Stransnes, Norway	69 48.0 N	29 44.2 E
69-17b	7/4/1969	Kjofjord-Straumen, Norway	69 48.6N	29 45.6E

^a Location abbreviations: MA = Massachusetts, ME = Maine, NB = New Brunswick, NF = Newfoundland, NJ = New Jersey, NS = Nova Scotia, PEI = Prince Edward Island, RI = Rhode Island.

TABLE 1. (Extended)

Int	Depth (m); x = depth zone collected							% <i>P.</i>	% <i>P.</i>	% <i>P.</i>	% <i>P.</i>	% <i>P.</i>	% <i>P.</i>
	0-3	3-9	9-15	15-21	21-28	28-37	>37	<i>laevigatum</i> 0-25 m	<i>rugulosum</i> 5-30 m	<i>squamulosum</i> Int-3 m	<i>nantuckensis</i>	<i>borealis</i> 0-30 m	<i>investiens</i> 0-35 m
x	x	-	-	-	-	-	-	23	0	Abundant	-	-	-
-	x	x	x	x	x	-	-	-	-	-	-	-	-
-	x	x	x	x	x	x	-	-	-	-	-	-	-
-	x	x	x	x	-	-	-	-	-	-	-	0	0
x	x	x	x	x	x	x	x	Tr	0	Abundant	-	58	0
-	x	x	x	x	-	-	-	5	4	Present	-	35	?
x	x	x	x	x	x	x	x	10	0	Abundant	-	38	?
x	x	x	x	x	x	x	x	0	1	Absent	-	67	0
-	x	x	x	x	x	x	x	18	0	-	-	34	0
-	x	x	x	x	x	x	x	43	0	Abundant	-	10	0
x		x	x	x	x	x	x	0	0	Present	-	94	0
x	x	x	x	x	x	x	x	9	Tr	Present	-	57	0
x	x	x	x	x	x	x	-	20	0	Abundant	-	24	0
-	x	x	x	x	x	x	-	53	0	Abundant	-	21	0
-	x	x	x	x	x	x	-	50	0	Abundant	-	8	0
-	x	x	x	x	x	x	x	2	11	-	-	20	?
-	x	x	x	x	x	-	-	-	-	-	-	0	0
-	x	x	x	x	x	-	-	4	0.1	-	-	0	34
-	x	x	x	x	x	x	x	0	0	-	-	-	77
-	x	x	x	x	x	x	-	10	2	-	-	0	Tr
-	-	-	-	-	x	-	-	-	-	-	-	0	rhodos, Tr
-	x	x	x	x	x	x	-	0	0	-	-	0	rhodos, Tr
-	-	-	-	-	x	-	-	-	-	-	-	0	Tr
-	-	-	-	-	-	x	-	-	-	-	-	0	rhodos, Tr
-	-	-	-	-	-	-	-	-	-	-	-	0	Tr
-	-	-	-	-	-	-	x	0	0	-	-	0	Tr
-	x	x	x	x	x	-	-	0	0	-	-	0	34
-	-	-	-	-	x	x	x	-	-	-	-	-	37
-	-	-	-	-	-	x	x	-	-	-	-	0	0
-	x	x	x	x	x	x	-	0	0	-	-	0	0
-	-	x	x	x	x	x	-	0	11	-	-	0	7
-	x	x	x	x	x	x	x	0	0	-	-	0	0
-	-	-	-	-	x	x	-	0	0	-	-	0	0
-	-	-	-	-	x	x	-	0	0	-	-	0	0

For these analyses, we used a Zeiss UltraPlus field emission SEM equipped with an HKL electron backscatter diffraction (EDS) housed at the Australian National University, Centre for Advanced Microscopy. SEM-EDS was used for spot analyses to quantify the elemental composition of representative parts of the coralline crust. Usually eight to nine measurements were made for each carbonate type. For EDS the operating voltage was 15 kV with 11 mm working distance. A range of settings were used for imaging, including secondary electron and in-lens imaging to show topography, and backscatter electron imaging that shows higher magnesium areas as darker carbonate and is useful for rapid visual identification of mineral distribution. For details of analyses, see Nash and Adey (2017a,b).

RESULTS

GENETIC LINEAGES AND EVOLUTIONARY RELATIONSHIPS

Genetic information was successfully acquired from 98 specimens. Specimens with identical sequences were used to update morphological and distributional data (Appendix Figure A1). The plastid markers used, *psbA* and *rbcL*, recovered congruent topologies (Figure 1). The identification of specimens based on morpho-anatomical features versus identification from sequences of type material obtained a 95% success.

Lineages successfully identified by a DNA sequence from type material included *P. borealis* sp. nov., *P. calcareum* (Pallas) W. H. Adey & D. L. McKibbin (the generitype), *P. investiens*, *P. laevigatum*, *P. lamii* (Me.Lemoine) Y. M. Chamberlain, *P. lusitanicum* V. Peña, *P. nantuckensis* sp. nov., *P. rugulosum*, and *P. squamulosum* (Figure 1). Other lineages could not be assigned a name (Figure 1). There is no single clade containing all Boreal–Subarctic transition zone species. Rather, these and Boreal to warm temperate species are mixed in each clade (Figure 1) as follows: a clade of *P. lamii*, *P. lusitanicum*, and *P. rugulosum* is strongly supported by *psbA* and weakly to strongly by *rbcL*; a clade of *P. squamulosum* and specimens identified as *P. lenormandii* is fully supported by *rbcL* and weakly to strongly by *psbA*, as is a clade of *P. borealis*, *P. investiens*, and *P. laevigatum*; a clade only weakly supported by analyses of both markers contains *P. calcareum* and *P. nantuckensis*.

Phymatolithon Foslie 1898:4 nom. cons.

We present herein an amended generic description updated from Adey (1964).

Plants crustose; hypothallium growing subparallel to the substrate and arcing upward to form the perithallium, short dead-ended filaments turning down to the substrate; epithallium thin, 0–2 cell layers (mean ~0.5) and cell walls thinly calcified and not armored; below a single layer of intercalary meristem cells on average shorter than the first perithallial derivatives; perithallial cells gradually lengthening as they are buried; calcified cell walls 2–4 μm thick of two components, an inner wall of

small, narrow, high-magnesium grains oriented more or less perpendicular to the cell lumen and an interfilament layer 0.1–0.4 μm thick of very small tabular grains (typically 0.2–0.4 μm long and 0.05 μm in diameter) that form a glide plane for differential growth, and often produce vertical “stripes” seen on vertical thallus fractures; calcified walls gradually perforated with depth to form cell fusions. All conceptacle primordia formed adventitiously from cells 30–100 μm deep in the perithallium; as the conceptacles develop, overlying perithallium is raised and cut off as degenerating discs; mature conceptacles, with floors sunken below the crust surface and often with sunken roofs; bi-tetrasporangia with thick cap walls (i.e., conceptacles with many pores); pore canals not lined by distinctive cells; male and female conceptacle roofs formed by overgrowing of lateral perithallial tissue; spermatangia borne in dendroid clusters completely clothing conceptacle walls; carpogonial filaments unbranched, producing highly fragmented, dendritic fusion cells on fertilization and producing typically one-celled gonimoblast filaments bearing single large carposporangia, across the entire conceptacle floor. In some species, postmature conceptacle cavities are buried by new perithallial growth and remain as cavities in thick crusts. Species occur in a wide range of marine/polyhaline estuarine habitats.

TYPE SPECIES. *Phymatolithon calcareum* (Pallas) W. H. Adey & D. L. McKibbin, 1970:100.

ANATOMY

The North Atlantic Boreal–Subarctic transition zone *Phymatolithon* species are presented as three species pairs based on morpho-anatomical similarities, with *P. laevigatum* and *P. rugulosum* characterized by adherent thalli with thin hypothalli, *P. squamulosum* and *P. nantuckensis* sp. nov. characterized by leafy and imbricating thalli, also with thin hypothalli, and *P. borealis* sp. nov. and *P. investiens* by thick and leafy to cantilevered thalli with thick hypothalli (Figure 2A,B). By a paired, two-tailed Welch–Satterthwaite *t* test ($t = 5.89$, $df = 2.14$, $p < 0.005$), the thick/thin hypothallium differentiation is highly significant (Figure 2C).

Hypothallium

Hypothallial characteristics are critical to understanding these species in the North Atlantic Boreal–Subarctic transition zone, as is shown in a plot of hypothallial L/D cell ratio versus hypothallium thickness (Figure 2). Our ANOVA model showed that this relationship is significantly different across the species ($p < 0.001$). *Phymatolithon investiens* has by far the thickest hypothallium (98–350 μm ; mean 176 μm), which is thicker than *P. borealis* (50–140 μm ; mean 77 μm); the latter is thicker than *P. squamulosum* (15–75 μm ; mean 41 μm), which in turn is thicker than *P. laevigatum* (13–55 μm ; mean 27.4 μm) and *P. rugulosum* (8–50 μm ; mean 26.1 μm). Finally, *P. laevigatum* is significantly thicker than *P. nantuckensis*, the latter with a hypothallium only

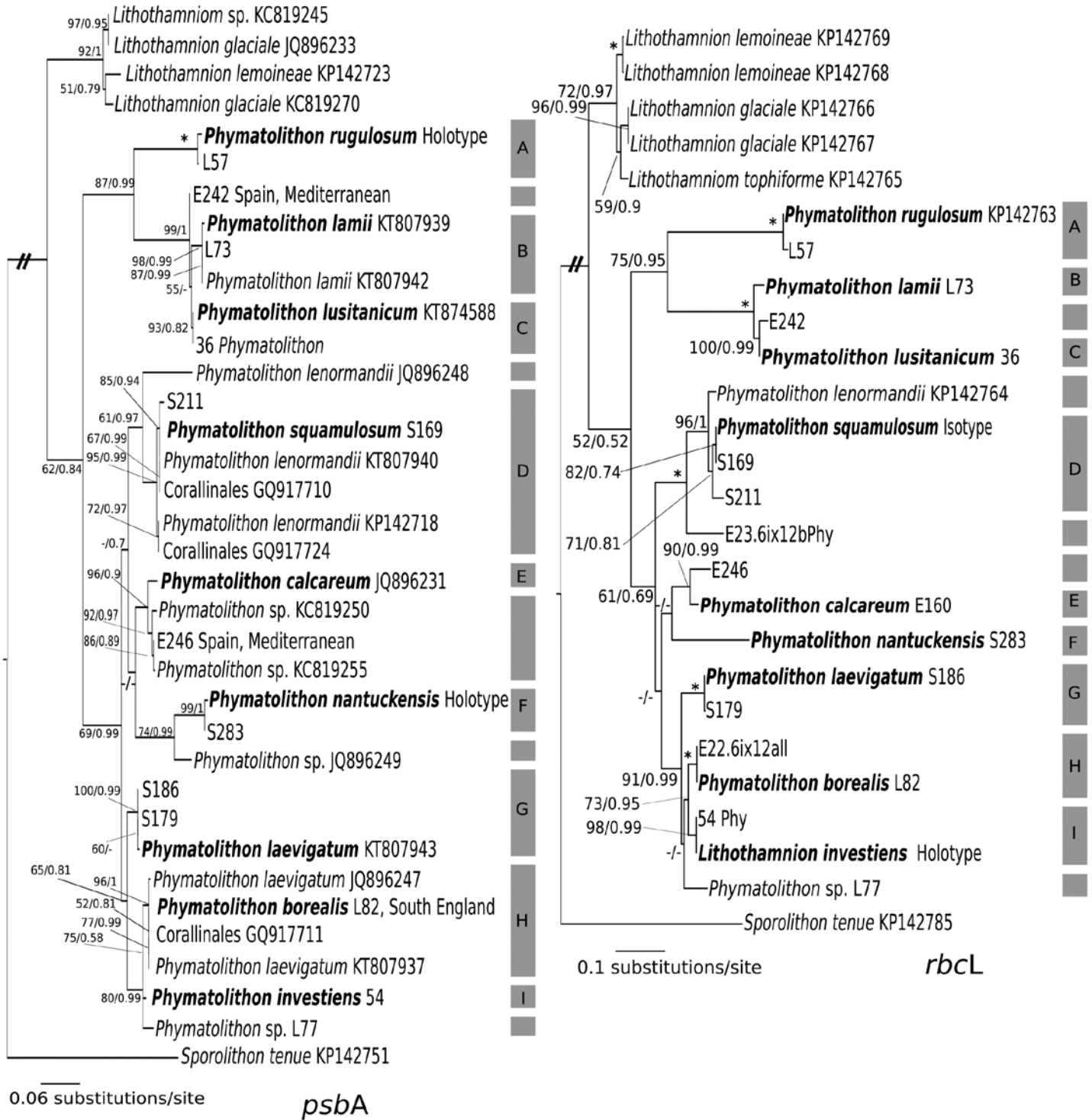


FIGURE 1. Phylograms inferred from maximum likelihood (ML) analyses of *psbA* (left) and *rbcL* (right) plastid markers for selected species of *Phymatolithon*, including all North Atlantic Boreal–Subarctic transition zone species. Names in bold indicate either type sample DNA or samples producing DNA that matches sequences from type material. Support values at nodes are bootstrap/posterior probabilities: only values above 50%/0.5 are shown. Samples indicated by alphanumeric or number codes after taxon names are also included in Appendix Figure A1. Dark gray bars on right of phylogram with letters indicate the extent of accepted taxa; unlettered dark grey bars are apparent unnamed *Phymatolithon* species. Figure by author JJHK.

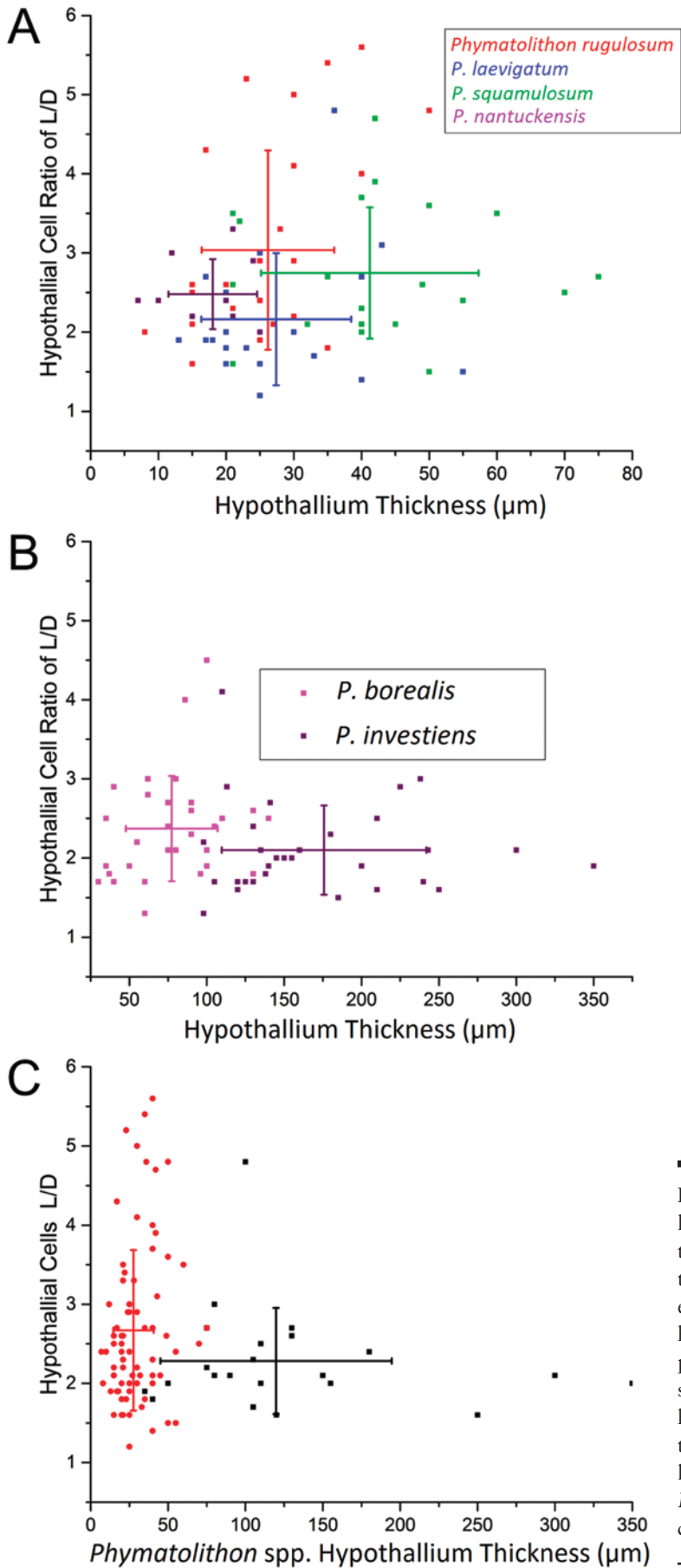


FIGURE 2. A, B. Mean hypothallial cell shape (ratio of cell length to cell diameter, L/D) as a function of hypothallial thickness for the *Phymatolithon* species of this paper. Note the scale change in hypothallial thickness from A to B. The eastern North Atlantic species, *P. borealis* and *P. investiens*, have considerably thicker hypothallia, although all species as populations have significantly different hypothallial dimensions. C. The two thick hypothallium species combined are highly significantly different from the combined thin hypothallium species (see text; red data points = thin hypothallia species: *P. rugulosum*, *P. laevigatum*, *P. squamulosum*, *P. nantuckensis*; black data points = thick hypothallia species: *P. borealis*, *P. investiens*). Figure by author WHA.

a few cells thick (7–25 μm ; mean 18 μm). However, although *P. rugulosum* and *P. laevigatum* have essentially the same hypothallial thickness, *P. rugulosum* has significantly more elongate cells than *P. laevigatum* ($p < 0.01$). All these species have overlapping dimensions (both hypothallium thickness and cell elongation), and only population/statistical testing can provide a cogent understanding of species differences.

Because hypothallium development with time is dependent upon progression across an irregular and perhaps even changing substrate, the characters of cell size and tissue thickness are inherently more variable than those of the perithallium, which lacks substrate contact. As we have shown, hypothallial characters can be quite valuable, and in some cases highly definitive, even on individual specimens (for example, differentiating *P. rugulosum* from *P. investiens*). However, in general, for larger-scale use, population/statistical analysis is necessary.

Perithallium

All *Phymatolithon* species have short, intercalary meristematic cells, ranging from approximately 1 to 8 μm long (mean 3.5 μm) in the species treated here, depending upon the division cycle. The perithallial cells are cut off at similar length, but consequent to subsequent growth, in species treated here, the cutoff cells range from approximately 2 to 9 μm (mean 4.6 μm). These perithallial cells continue to lengthen as they are buried by subsequent divisions of the meristematic cells (Figure 3A–C). Figure 3C shows the mean length of meristematic cells and the first 8 proximal perithallial cells for the five species with sufficient data to produce smooth curves (see below). A first-order curve fit to cells 1–4, by least mean squares, has a slope of 1.068 with a fit of $R^2 = 0.983$, with both slope and intercept fits, by a t test, of $p < 0.01$. A similar curve fit to cells 4–8 has a slope of 0.183 with a fit of $R^2 = 0.908$, with slope and intercept fit by a t test of $p < 0.01$. Thus, significant cell elongation is achieved by cell number 4, although some small additional elongation with depth occurs in most species. This pattern of division and elongation results in increased thickness of the perithallium. Mature cell length for cell positions 4–8 for each species is not significantly different from the others by Scheffé's and Student–Kuels tests. However, if the shorter pair (*P. rugulosum* and *P. laevigatum*) and separately the longer-celled set of *P. nantuckensis*, *P. squamulosum*, *P. borealis*, and *P. investiens* are combined, fitted first-order curves by t tests have significantly different slopes ($p = 0.04$) and highly significant intercepts ($p < 10^{-4}$). We return to this issue when we treat cell shape.

Figure 4 shows the coefficient of variation in cell length (CVL) as a function of cell position. In all *Phymatolithon* species, high levels of variation in cell length occur in the meristematic cells and in the first several rapidly growing perithallial cells, which is consistent with the independent division of meristematic cells and elongation of their derivatives relative to adjacent filaments and those in the species population. The two species with the least perithallial growth, giving rise to lesser crust thickness,

P. squamulosum and *P. nantuckensis*, have considerably lower meristem CVLs than the remaining species. It seems likely that this difference results from a lower rate of cell division in the meristem. Deeper in the perithallium, CVL values decrease to roughly half their rates nearer the meristem.

The change of cell diameter with depth in the perithallium (Figure 5) is much less than it is for cell length (Figure 3); this is logical considering that in crust species lateral extension is accomplished by hypothallial growth and the number of filaments per unit surface area is essentially fixed. (In Figure 5, we see that *P. nantuckensis* is highly erratic as compared to other species, and it seems likely that this results from the limited sampling in this case; 2 plants and 10 measurement sets versus 28–41 plants and 31–52 measurement sets in other species). In the following treatment of perithallial development, we do not include *P. nantuckensis*; this matter is treated in the Discussion. Statistical analysis of cell diameter, using GLM ANOVA models and Scheffé's tests, shows that mean cell diameter in *P. rugulosum* is narrower than in other *Phymatolithon* species, which are otherwise all similar to each other. The slopes of *P. borealis* and *P. investiens*, cells 4–8, are negative, but this is not significant by Scheffé's tests. However, as shown in Figure 5C, the combined thin hypothallia species have a highly significant positive slope (by $p < 0.001$). Because this is an expansion of the cell lumina, it is likely the result of a loss of inner cell wall carbonate; although this might be an artifact of cell fusions, the species with a thick hypothallium (*P. borealis* and *P. investiens*) both have slightly more fusions than the thin hypothallium species (see below) and apparently show a slight negative slope with depth.

Variation in cell diameter (Figure 6), following the cessation of cell division, shows roughly the same values as cell length (Figure 4). As expected, cell diameter CV is more or less constant with depth. However, when the two thick hypothallium species are combined, a first-order regression of CV, by GLM regression F test, has a highly significant positive slope. This result suggests that the nonsignificant negative slope of cell diameter for these species is probably correct. We treat this matter in the Discussion.

The ratio of cell length to cell diameter (L/D) with depth in the perithallium is shown in Figure 7. The resulting curves are similar to the growth curves, as might be expected, because change in diameter is minimal; however, the differences in L/D between the mature cells of the first three species are highly significant. Although all three have the same basic growth pattern with depth, cell shape, a character rarely applied in coralline literature, is the most defining feature of species differentiation based on cell dimensions in the mature upper perithallium (sub-elongation zone). Although mature postgrowth cells (cells 4–8) appear to have a “drift” in both length and diameter, as we presented earlier and treat in detail in the Discussion, all species (except *P. nantuckensis*, with inadequate data) have mature cells with remarkably stable L/D ratios (i.e., cell shape). *Phymatolithon rugulosum*, *P. borealis*, and *P. investiens* all have somewhat elongate cells, with a mature cell ratio of approximately 1.5

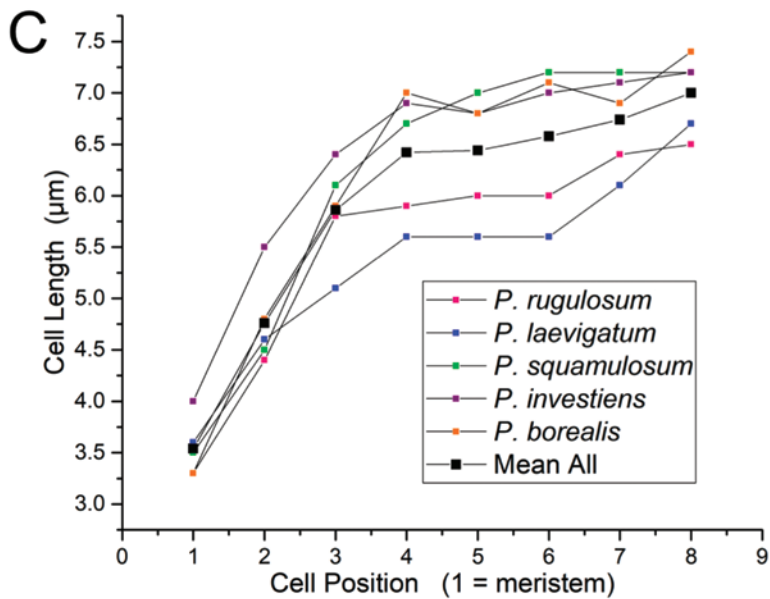
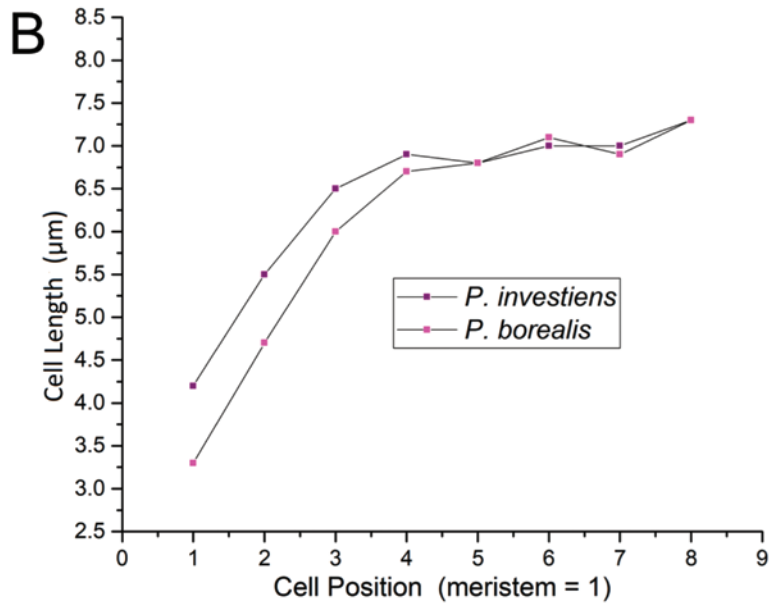
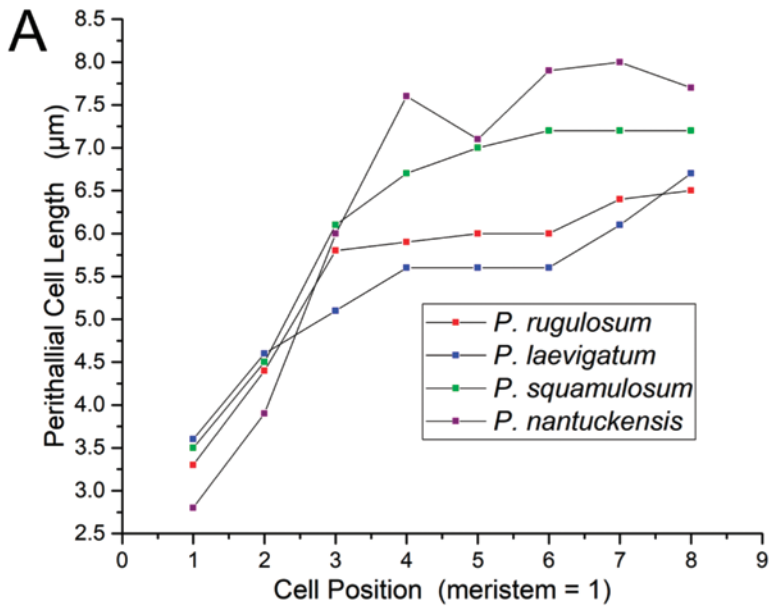


FIGURE 3. Change in mean cell length (pit to pit) of perithallial cells in all *Phymatolithon* species of this paper as a function of cell position. A. Thin hypothallium species. B. Thick hypothallium species. C. All species combined except *P. nantuckensis* (omitted because data were not sufficient to produce a smooth curve; see Discussion). Number of stations/plants/filaments measured (i.e., for each data point) as follows: *P. rugulosum*, 25/41/52; *P. laevigatum*, 33/44/47; *P. squamulosum*, 22/27/33; *P. nantuckensis*, 1/2/10; *P. investiens*, 17/29/31; *P. borealis*, 18/28/31. Figure by author WHA.

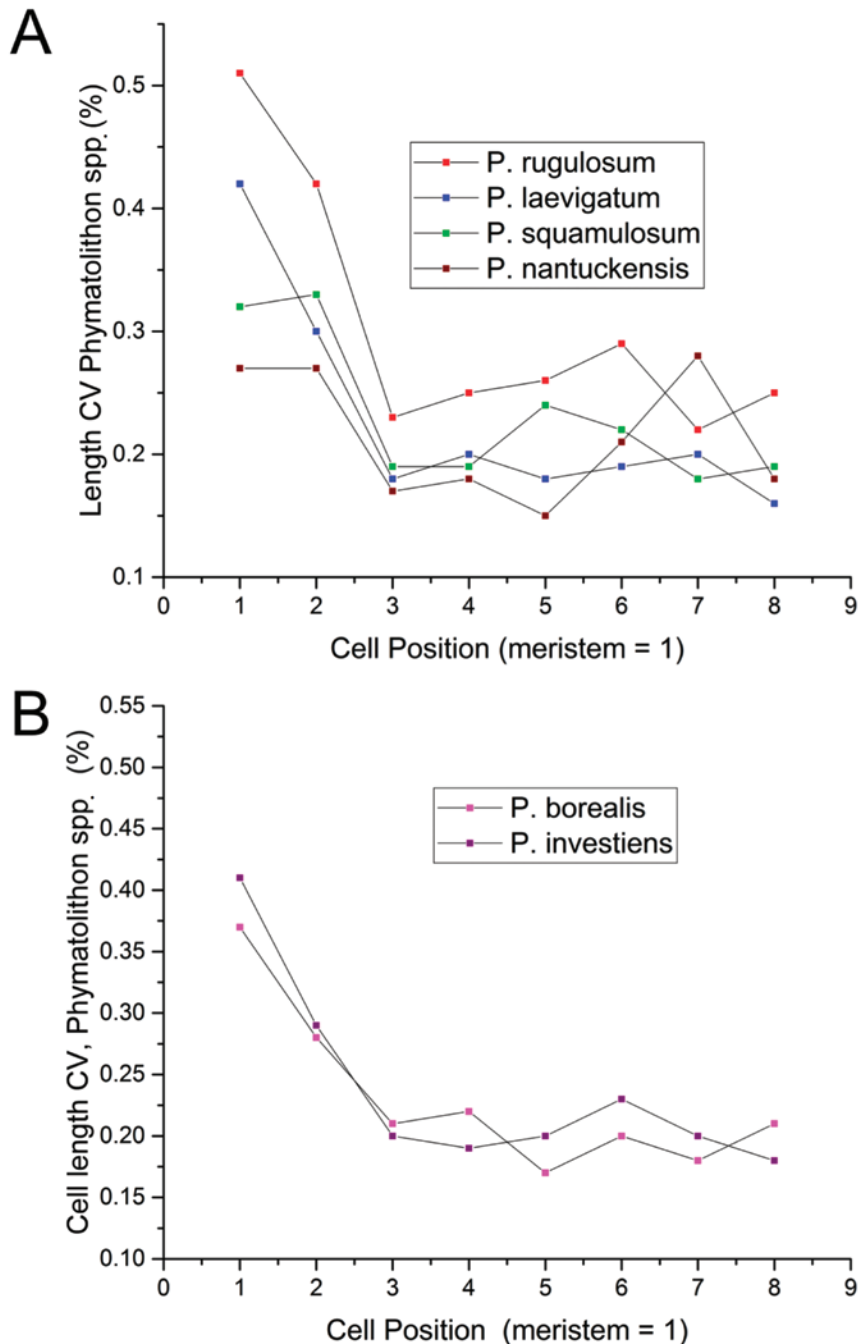


FIGURE 4. Coefficient of variation of cell length as a function of cell position in all the *Phymatolithon* species of this paper. A. Thin hypothallium species. B. Thick hypothallium species. Number of measurements as in Figure 3. Figure by author WHA.

(Figure 5). However, at $L/D = 1.25$ for *P. squamulosum*, and at $L/D = 1.03$ for *P. laevigatum*, the remaining species have shorter, ovoid, or even round cells in the latter case. This three-way separation is highly significant ($p < 0.001$) by ANOVA.

When L/D is plotted as a function of cell position in the perithallium (Figure 7), but showing the extension to the hypothallium, it is seen that L/D roughly doubles, making hypothallial cells generally more elongate than perithallial cells in the same species. However, the cell ratios between species are proportionally largely unchanged from the perithallium ratio.

The dissolution of usually narrow channels in cell walls between perithallial cells of adjacent filaments (typically referred to as fusions) are well known in the genus *Phymatolithon* (Adey, 1964, 1966a; Irvine and Chamberlain, 1994); these develop gradually with depth in the perithallium (Figure 8; Plates 1D, 6D, 8C). The term fusion may be a misnomer, as generally such cell connections are formed by dissolution of cell wall carbonate in well-defined tunnels of which the sides are eventually recalcified. As shown in Figure 8A, fusions rarely occur in the meristem, and only occur in less than 10%

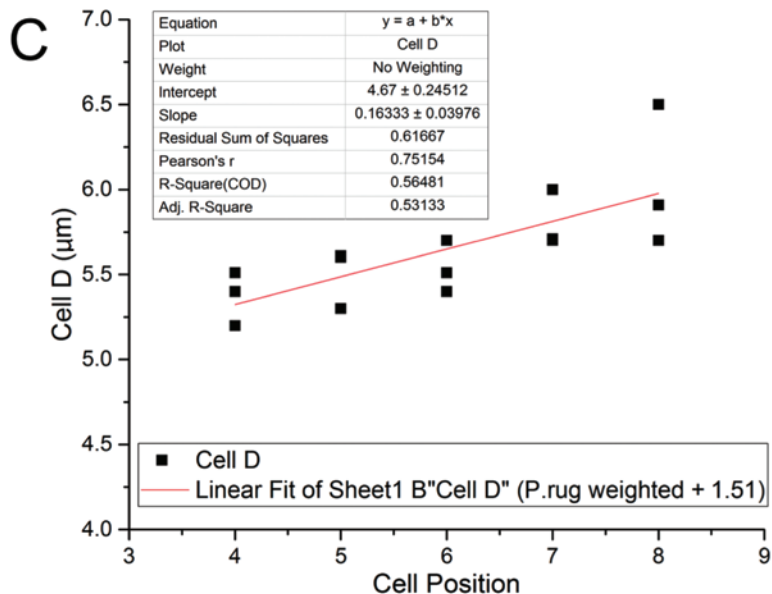
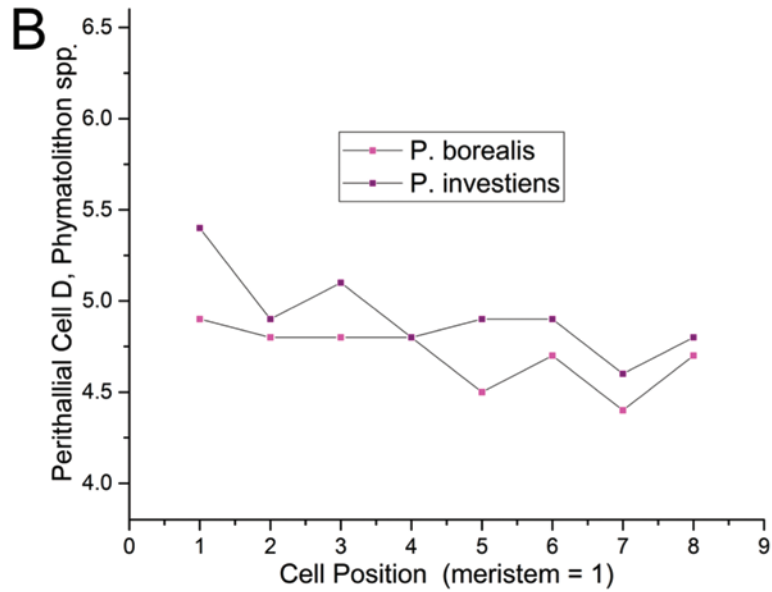
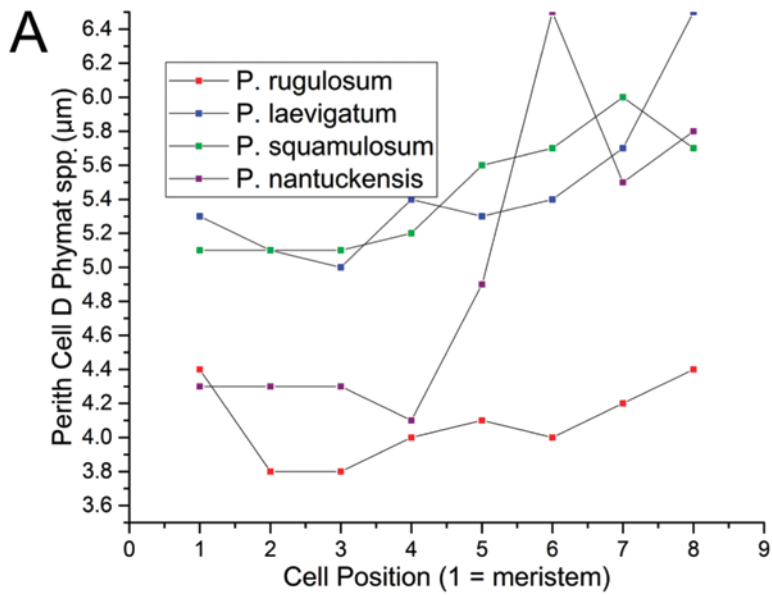


FIGURE 5. Change in mean cell diameter (width mid-cell lumen) as a function of cell position for the *Phymatolithon* species of this paper. A. Thin hypothallium species. B. Thick hypothallium species. Number of measurements as in Figure 3. C. Combined thin species cell diameter as a function of cell position with *P. rugulosum* weighted by means (*P. nantuckensis* not used, see above). At $R^2 = 0.56481$, the diameter increase is significant. By t test, the slope is highly significant. The negative slope of the two thick hypothallium species is not significant (however, see Figure 6). Figure by author WHA.

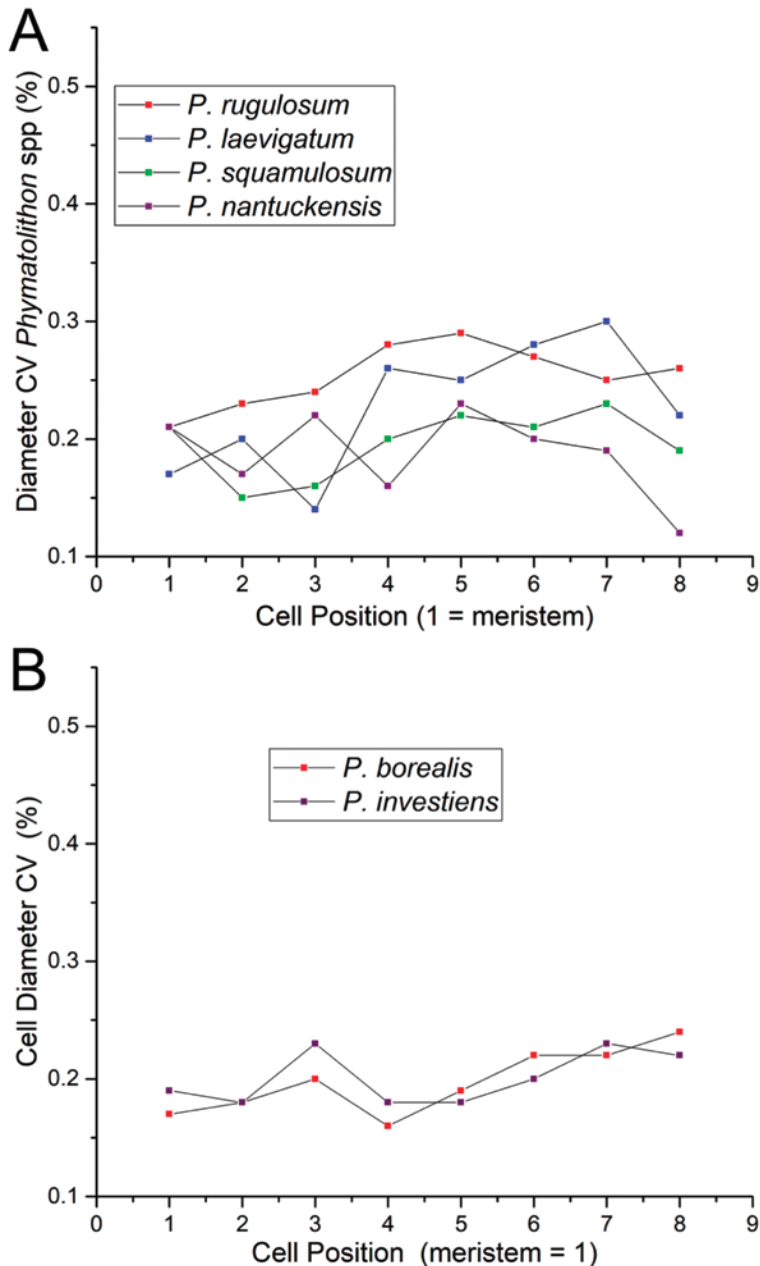


FIGURE 6. Cell diameter coefficient of variation (CV) as a function of cell position in all *Phymatolithon* species of this paper. A. Thin hypothallium species. B. Thick hypothallium species. Number of measurements as in Figure 3. After cell elongation ceases, the strongly positive slope of the thick hypothallium species cell diameter CV suggests that the nonsignificant decrease in cell diameter is likely real and is caused by addition of carbonate to cell lumen walls. Figure by author WHA.

of cells to a depth of cell 4. From that level deeper, they develop rapidly. As shown in Figure 8B, to a large extent growth and fusion development are independent; roughly three-quarters of fusions develop after significant cell elongation stops. By ANOVA, the differences between cells 1–3 and 4–8 are highly significant.

Most cold-water corallines produce starch storage globules that are readily visible in SEM mounts. However, as first described by Adey (1964) and further discussed by Irvine and Chamberlain (1994), some *Phymatolithon* species have additional globules that stain heavily with hematoxylin. Adey (1964)

referred to them as starch globules; however, these do not appear in SEM images and may be membranous oil globules that break down on drying. Although not always very abundant, these “staining bodies” can usually be located, especially in hypothallial cells, and, in *Phymatolithon*, only in the species of the *P. laevigatum*–*P. borealis*–*P. investiens* subclade, the three most closely related *Phymatolithon* species of this paper. Staining bodies tend to develop rapidly in the growth phase of the perithallium (Figure 9), suggesting that this is also the zone of strongest photosynthesis with the formation of storage food. Presumably the staining bodies in the hypothallium develop at plant margins

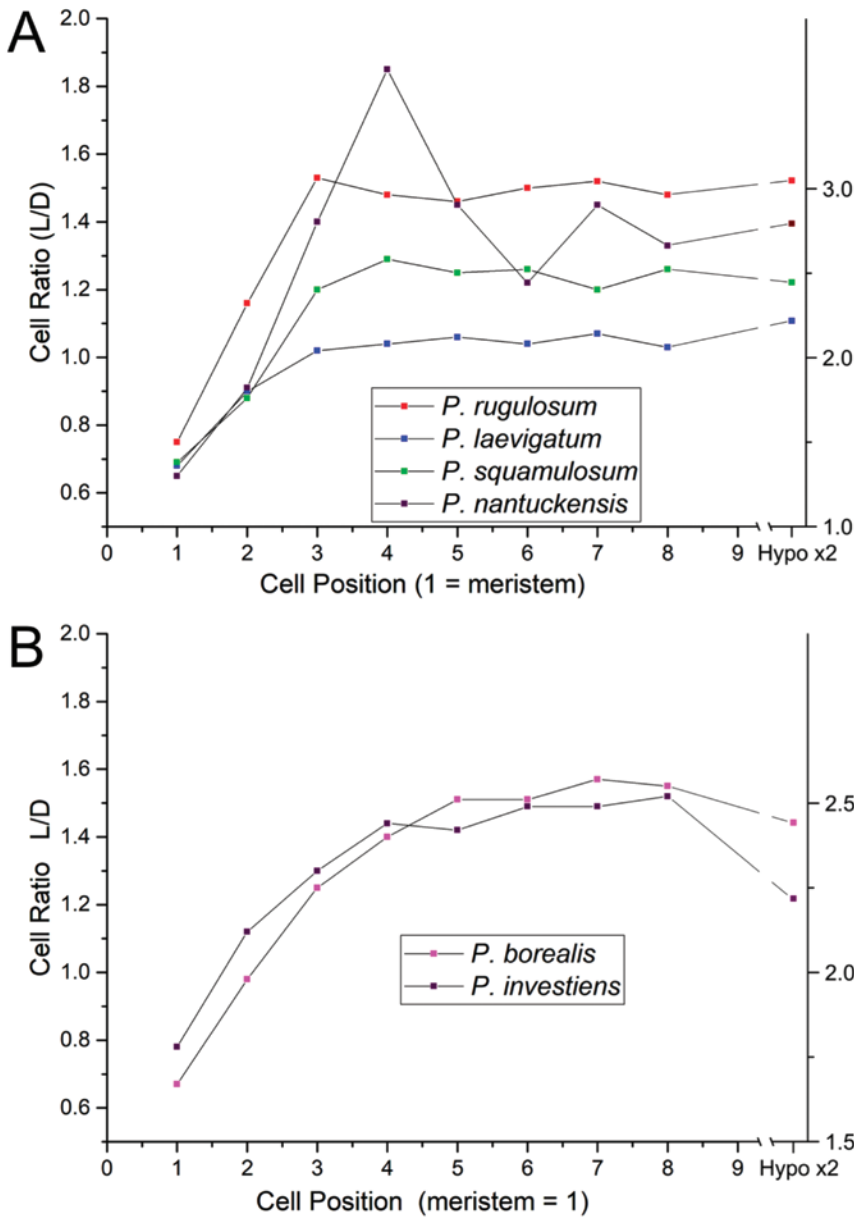


FIGURE 7. Ratio of cell length to cell diameter (L/D) as a function of cell position for all the *Phymatolithon* species of this paper. A. Thin hypothallium species. B. Thick hypothallium species. Number of measurements as in Figure 3. Note that each hypothallial value (two times perithallium value) is the mean of three cells rather than a single cell (e.g., for *P. rugulosum* the data source is 25/41/156). Except for the highly variable *P. nantuckensis*, with 10 measurement sets from two plants, L/D in the perithallium is proportional to that in the hypothallium for each species. Figure by author WHA.

when the overlying photosynthetic perithallium is thin and photosynthate is being transported to the rapidly growing hypothallium. We have not researched this matter. In any case, in the North Atlantic Boreal–Subarctic transition zone, this is a diagnostic character for separating this subgroup from the remaining species of the genus.

Tissue Variation and Wall Mineralogy

As Adey et al. (2005, 2013) showed for Arctic–Subarctic *Lithothamnion* and *Clathromorphum* spp., and as Nash and Adey (2017a,b) show for Arctic *Leptophytum*, *Kvaleya*, and Boreal–Subarctic transition zone *Phymatolithon* spp., the

high-magnesium calcite cell walls have an inner wall (IW, the wall) with radial calcite granules (Plates 9–11). Adjacent filaments of cells are separated by a calcitic formation, called interfilament (IF, middle lamella; Plates 9B,D; 10C,D; 11C–F), that is distinctive but highly variable in thickness, structure, and magnesium content among genera, among species within a genus, and even among the hypothallium, perithallium, and wound tissue of an individual crust. *Phymatolithon* species generally have a thin IF layer that probably functions at least partially as a glide plane, allowing differential elongation between cells of adjacent filaments; however, the variation between tissue subtypes is considerable (Plates 9–11), and this we describe in detail below. In the *Phymatolithon* species presented in this paper,

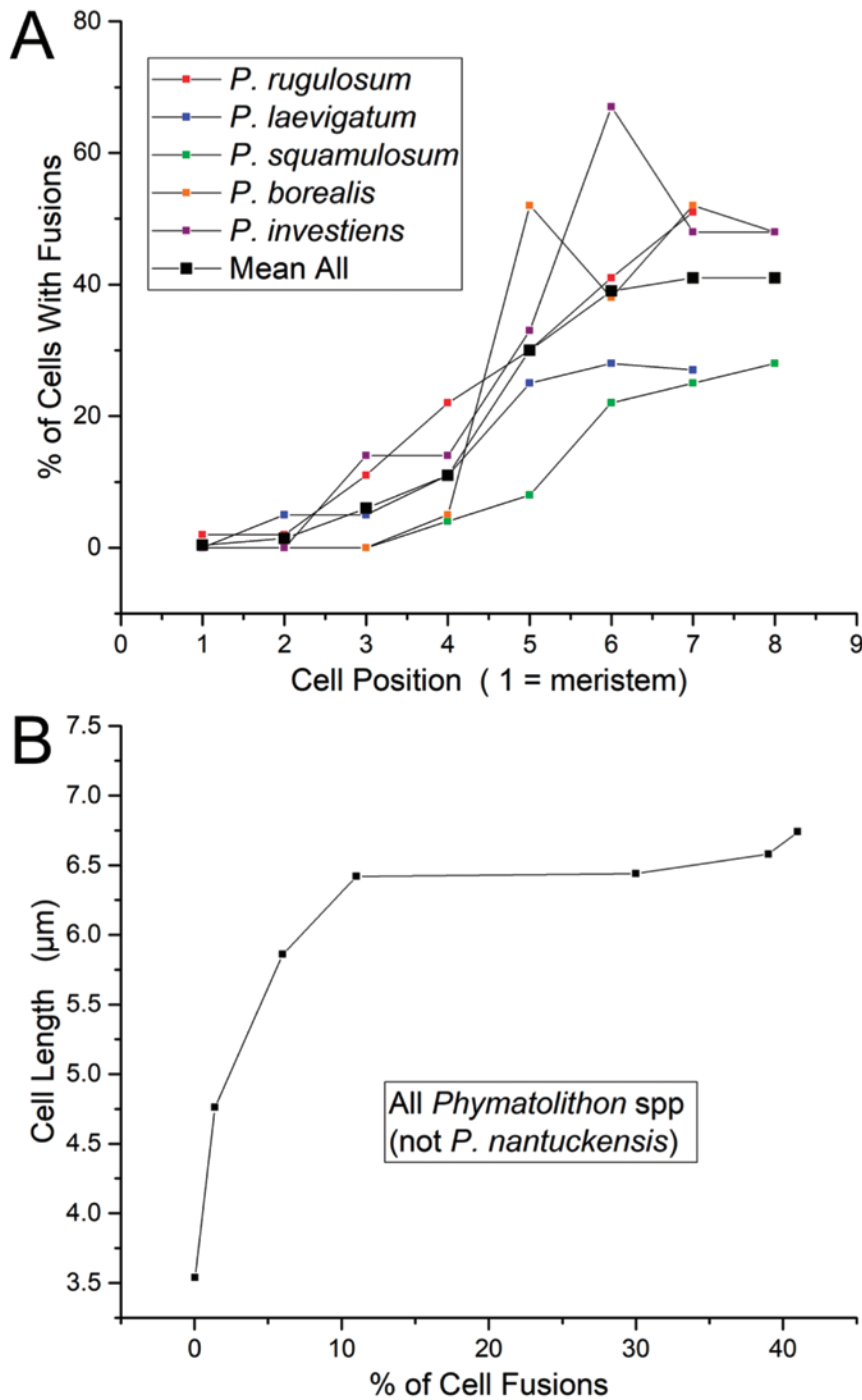


FIGURE 8. A. Percent of cells with fusions as a function of cell position for all the *Phymatolithon* species of this paper except *P. nantuckensis* (see text). Number of measurements as in Figure 3. B. Mean cell length (of all species, as shown in A) at each cell position as a function of the cell fusions at that position. Number of measurements as in Figure 3. Figure by author WHA.

crust perithallia typically have a complex of subtissues, mostly relating to “injury” caused by grazers or other surface damage (Plates 1A; 2C; 4F; 6A,B; 7E); however, this can also result from the breakout and regrowth over or within post-mature conceptacles. Typically, such “wound tissue” consists of more rapid cellular growth necessary to repair crustal damage (usually a hole); such tissue usually consists of longer, thinner-walled cells, with decreased interfilament calcification and increased magnesium

(in the high-Mg-calcite walls). We discuss cell wall variation in greater detail below. There are other subtissues typically present in the perithallia of *Phymatolithon* species, including secondary hypothallia, but we do not examine these in detail in this paper. Conceptacles, both bi-tetrasporangial and gametangial, also have supporting tissues, including two types of roof growth and nurse tissue in the bi-tetrasporangial conceptacles (Adey et al., 2013).

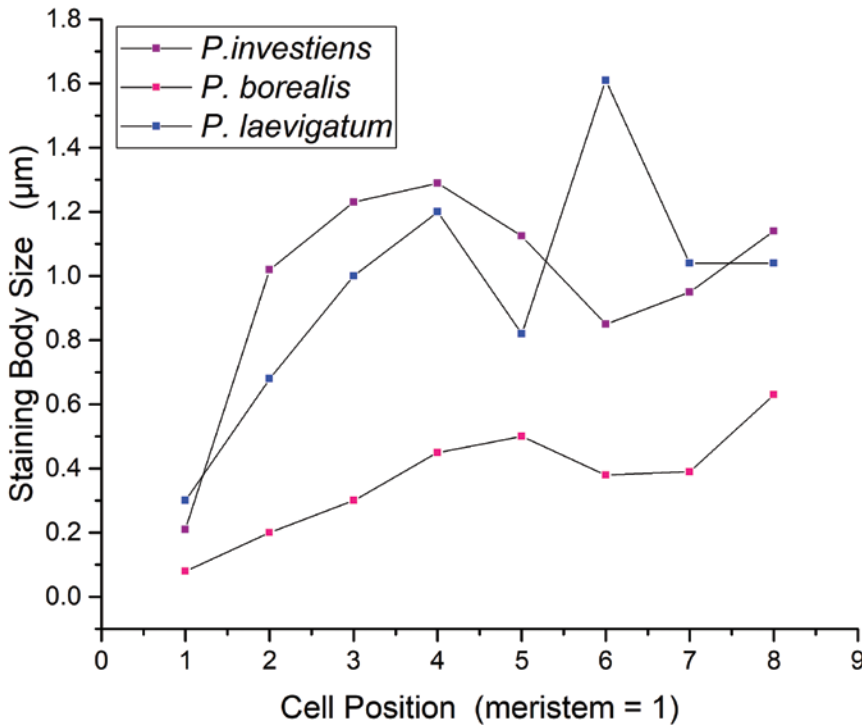


FIGURE 9. Mean staining body size (diameter, μm) (absence = 0; see text) as a function of cell position. Number of measurements as in Figure 3. *Phymatolithon* species of this paper not included do not have staining bodies. All three species shown belong to a single clade of the larger *Phymatolithon* tree (see Figure 1). Figure by author WHA.

REPRODUCTION

General

The extraordinary adventitious development of *Phymatolithon* conceptacles, from primordial discs several to tens of cells below the intercalary meristem in the perithallium, has been earlier described and occurs in the species newly presented in this paper (e.g., Plate 7A,C,D). Adey (1964, 1966a) demonstrated this process, both diagrammatically and photographically, for the three species in this paper that occur in the Gulf of Maine. Here we add the new species, *Phymatolithon nantuckensis*, described from Nantucket Island in the western North Atlantic, *Phymatolithon borealis* sp. nov. (replaces *P. polymorphum* Foslie; Adey 1970b, 1971; Irvine and Chamberlain, 1994), and *Phymatolithon investiens* from central and eastern North Atlantic.

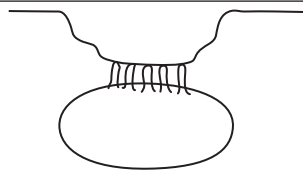
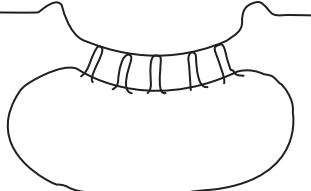
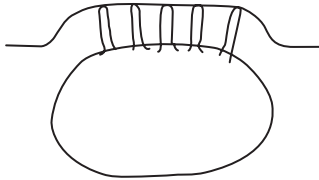
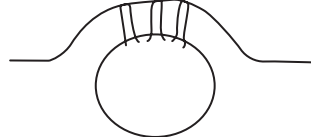
Bi-tetrasporangial Plants

In this paper, we use the term bi-tetrasporangial conceptacles instead of asexual conceptacles as in the earlier literature. Although bisporangial conceptacles are probably part of an independent asexual loop in a reproductive cycle and are the most common conceptacles for most Arctic and Subarctic species, tetrasporangial conceptacles, more common in Boreal to tropical corallines, provide the chromosomal reduction division of sexual cycles. Many of the *Phymatolithon* species studied earlier presented quantitatively well-defined yearly asexual reproductive

cycles, with peaks in the winter and early spring; two of the newly added species, *P. borealis* and *P. investiens*, appear to have very similar cycles, never producing bi-tetrasporangial conceptacles in summer. Adey and Adey (1973) developed similar curves of reproductive cycles for these species as a combined *P. polymorphum*; because data for *P. investiens* were very limited, these curves likely represented *P. borealis* sp. nov. *Phymatolithon squamulosum* apparently remains an exception, with no well-defined yearly cycle. The more distantly related *P. nantuckensis* sp. nov. has conceptacles of all types during the summer. We have only summer collections for this species, but it would appear that, similar to *P. squamulosum*, it does not have a defined yearly reproductive cycle.

In Table 2, we numerically and pictorially present the essential mean dimensions of bi-tetrasporangial conceptacles for the six species in this paper; cross sections are mean dimensions, all to the same scale. Although some of these species were treated previously in regional publications and there is little change in the essential parameters, in this paper these data are derived from across the North Atlantic range of each species. Note that in *Phymatolithon squamulosum* (Plate 4D,F) and *P. nantuckensis* (Plate 3B,C), mature conceptacles have roofs that are raised above the surrounding vegetative crust, which derives from two factors: the depths of formation of the conceptacle primordia are less than those in all the thicker species (generally 4–8 cells as compared to 15–25 cells below the surface); however, in addition, upward growth of the surface of these crusts is considerably less pronounced than crusts of the generally thicker species.

TABLE 2. Mean dimensions (μm) of asexual conceptacles of *Phymatolithon* species in the North Atlantic Boreal–Subarctic transition zone. Drawings by W. H. Adey.

#stats	#plants	#concs	Pore Plate Diam (CV)	Cavity Diam (CV)	Pore Plate Elev +- (CV)	Cavity Height (CV)	
							200 μm
11	14	43	82 (0.26)	153 (0.19)	-40 (0.46)	73 (0.19)	
14	16	43	148 (0.24)	239 (0.18)	-32 (0.74)	93 (0.24)	
12	14	31	150 (0.23)	187 (0.20)	+74 (0.44)	108 (0.20)	
1	2	10	95	140	+52	88	
4	4	16	103 (0.25)	184 (0.20)	-58 (0.46)	125 (0.18)	
1	1	6	97	158	-57	102	

Bi-tetrasporangial conceptacle elevation relative to the crust surface results only in part from internal conceptacle development and derives also from the relative growth (or lack of it) in the surrounding perithallus (Adey et al., 2013).

In Figure 10, we plot bi-tetrasporangial conceptacle height as a function of conceptacle cavity diameter. By the Welch-Satterthwaite t test, the thin hypothallial species (Figure 10A) are all significantly different from each other ($t = 6.4$, $df = 40.1$, $N = 14-45$, $P < 0.001$) in the key conceptacle cavity diameter dimension, whereas the thin imbricate species have elevated mature

conceptacles and the thicker adherent crust species at maturity remain considerably sunken; at $p < 0.001$ ($t = 18.8$, $df = 50.4$, $N = 35-45$), these height differences are highly significant. By the same test, the two thick hypothallium species, *P. borealis* and *P. investiens*, are also significantly different ($t = 3.8$, $df = 20.6$, $N = 6-20$, $p < 0.01$) from each other in cavity diameter. In the thick hypothallial species *P. borealis* (Figure 10B; Plates 5C, 6A), conceptacles are sunken at maturity. Although the pore plate is not significantly deeper than in *P. rugulosum* and *P. laevigatum* (Figure 10A), the mature conceptacle cavity floors of the latter

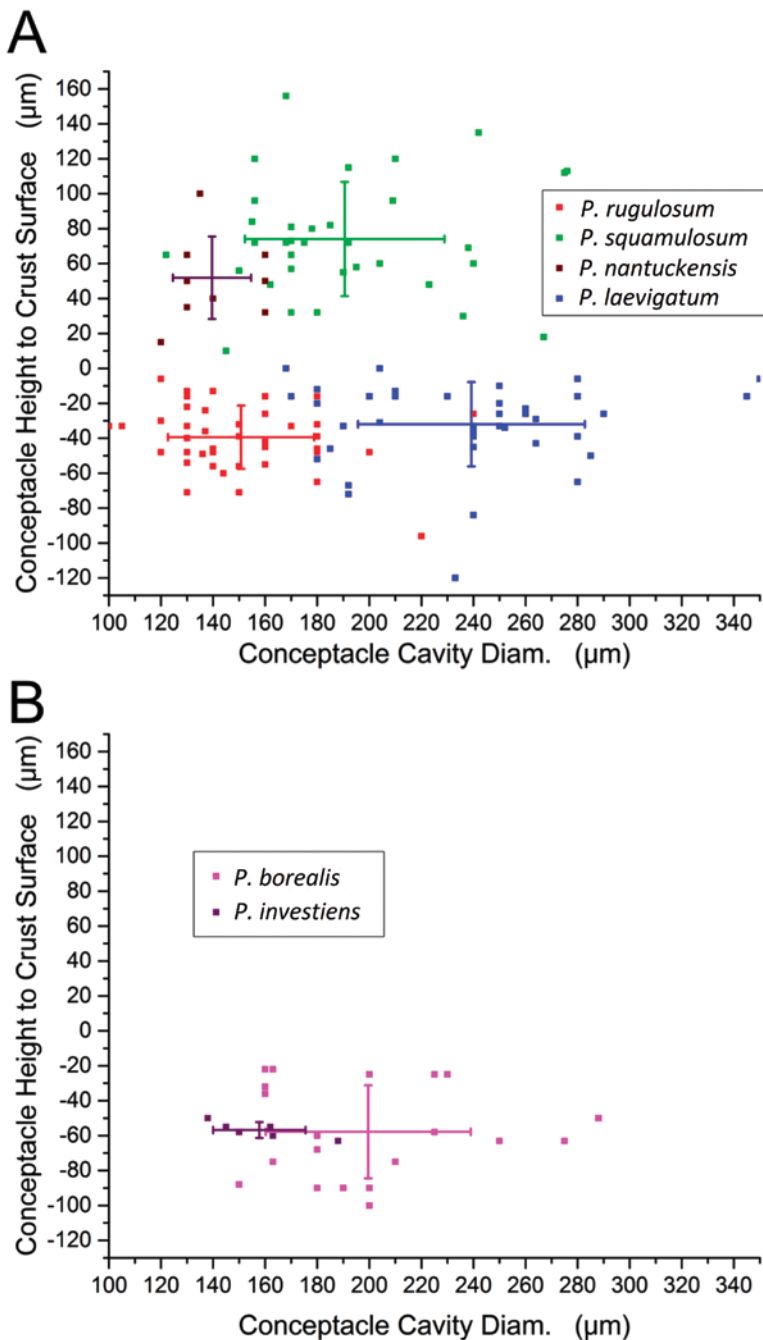


FIGURE 10. Bi-tetrasporangial conceptacle height to crust surface (pore plate surface height above or below crust surface) as a function of conceptacle cavity diameter for all the *Phymatolithon* species of this paper. A. Thin hypothallium species. B. Thick hypothallium species. Number of stations/plants/conceptacles (each data point from a single conceptacle) as follows: *P. rugulosum* 11/13/52; *P. squamulosum* 14/16/35; *P. nantuckensis* 1/2/10; *P. laevigatum* 14/16/43; *P. borealis* 5/5/20; *P. investiens* 1/1/6. (See also Table 2.) Figure by author WHA.

species are considerably deeper than in *P. borealis* (Table 2). The rapid growth in *P. borealis* of surrounding perithallial tissue relative to conceptacle development is also reflected in the high percentage of conceptacle cavities deeply embedded in the crust (Plates 5B, 6F). *P. borealis* bi-tetrasporangial conceptacles are intermediate in conceptacle cavity diameter between *P. rugulosum* and *P. laevigatum*. Although *P. investiens* conceptacles are dimensionally similar to those of its sister species, *P. borealis* (conceptacle cavities are somewhat smaller), with only six conceptacles from one plant of *P. investiens* measured, the similarity

is somewhat uncertain. The larger conceptacle cavity diameters are directly and significantly a function of pore plate diameter as shown in Figure 11 for *P. laevigatum*. In agreement with the figures shown in Irvine and Chamberlain (1994), and in contrast to the superficially similar *Leptophytum laeve*, all these species lack distinctive pore cells in conceptacle roofs (and, as we present below, have short gonimoblast filaments across the conceptacle floor in mature carposporangial conceptacles, as compared to the laterally placed long gonimoblast filaments of *Leptophytum*; Adey, 1966a).

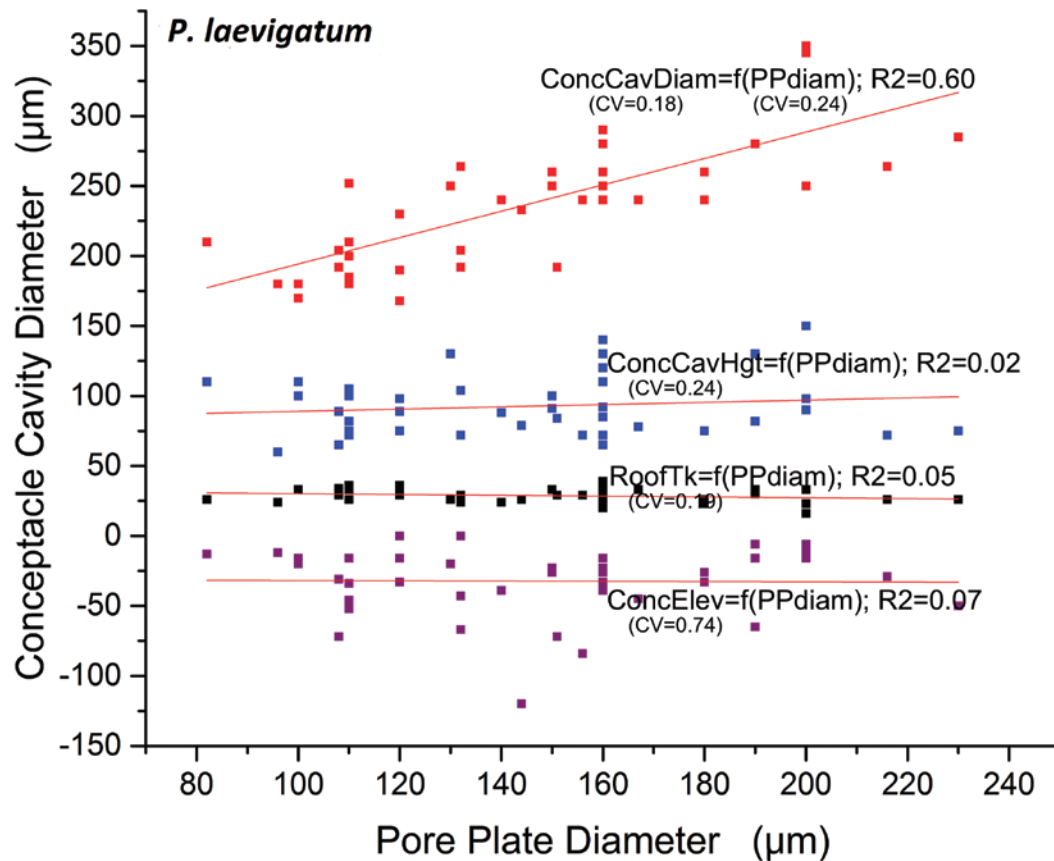


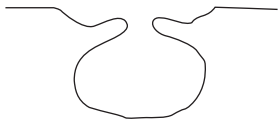
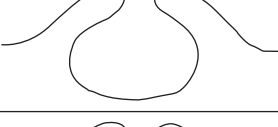
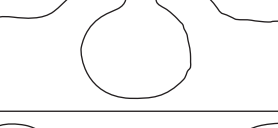
FIGURE 11. Conceptacle dimensions (ConcCavDiam; ConcCavHgt; RoofTk [roof thickness]; ConcElev) as a function of conceptacle pore plate diameter (PPdiam) for *P. laevigatum*. Conceptacle cavity dimensions have a direct first-order relationship with the conceptacle pore plate diameter (which in turn is determined by the conceptacle primordial disc diameter). Other conceptacle dimensions are independent of primordial disc diameter. See text for full explanation. Figure by author WHA.

Gametangial Plants

In general, in *Phymatolithon*, gametangial conceptacles are rarer than bi-tetrasporangial conceptacles, and predictable annual reproductive cycles have not been reported. In Tables 3 and 4, we present the mature shape and dimensions of both female and carposporangial conceptacles of the Boreal-Subarctic transition zone *Phymatolithon* species (Plates 3D-F; 5E,F; 7C-F). Single-pored female (carpogonial) conceptacles are equal to or considerably smaller than their bi-tetrasporangial counterparts; yet they are either raised or only weakly sunken, even in the *Phymatolithon* species with strongly sunken bi-tetrasporangial conceptacles. This situation is the result of two key factors: the roof and sporangial filaments of bi-tetrasporangial conceptacles in the Melobesioideae stop growing in mid-development, once sporangia mother cells are formed, while the roofs of sexual conceptacles continue to grow until either breakout or reimmersion into vegetative tissue, if the conceptacle is buried. Except for

P. rugulosum, the conceptacle roofs are generally twice the thickness of the bi-tetrasporangial conceptacle roofs because of the continued overgrowing, hypothallial-like character of their roof tissue. Male conceptacles have been found in all these species except *P. nantuckensis* and *P. investiens*, for which our sample number is considerably smaller than for the other species. In general, male conceptacles are rare in our collections, perhaps because they are short lived and mostly produced in winter. In each species in which they have been described, spermatia are produced on extensive dendritic arrays on all surfaces of the very small conceptacle cavities (Plate 5D). *Phymatolithon borealis* routinely buries its conceptacles in older crust (Plates 5B; 6A-F). In female crusts, unfertilized, buried, female conceptacles are common, suggesting that spermatia frequently do not achieve their target, either because of timing, or inadequate production, or density of reproductive plants. In *P. investiens* such conceptacles, although present, are usually replaced with new wound tissue (Plate 8E).

TABLE 3. Dimensions (μm) of female conceptacles of *Phymatolithon* species in the North Atlantic Boreal–Subarctic transition zone. Drawings by W. H. Adey.

	outer conc dia	cav dia	pore hgt	cav floor depth	cav hgt	roof tk	
<i>P. rugulosum</i> 1 station 9 conc	(190)	131	(–18)	–119	(85)	(15)	
<i>P. laevigatum</i> 1 station 4 conc	194	139	17	–112	72	43	
<i>P. squamulosum</i> 3 stations 5 conc	(270)	120	68	–56	75	47	
<i>P. nantuckensis</i> 1 station 3 conc	198	111	44	–84	82	44	
<i>P. borealis</i> 3 stations 8 conc	245	153	–29	–140	93	58	
<i>P. investiens</i> 5 stations 15 conc	318	179	73	–90	89	62	

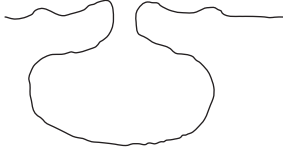
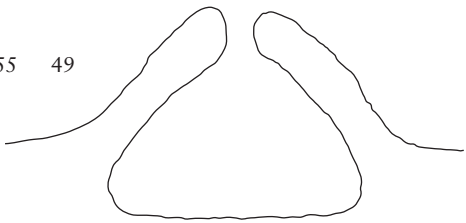
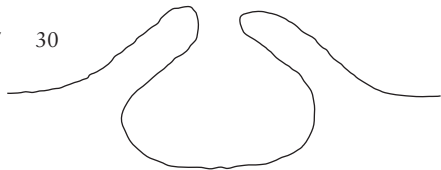
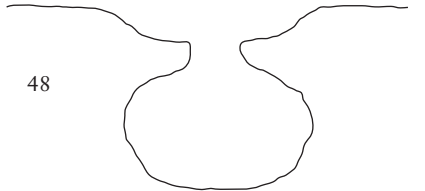
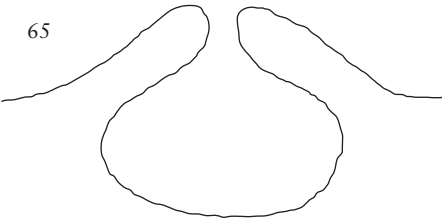
In Figure 12 and Plates 3E,F, 5E,F, and 7C–F, we present new information on female pre- and postfertilization development from procarps to mature carposporangia as a mosaic of *P. investiens*, *P. borealis*, and *P. nantuckensis*. As we discuss later, these patterns are consistent with the previously described structures and developmental patterns for *P. rugulosum*, *P. squamulosum* (as *P. lenormandii*), and *P. borealis* (as *P. polymorphum*) (discussion in Suneson, 1943; Adey, 1964, 1966a; Irvine and Chamberlain, 1994). Carpogonial branches are short (3 or 4 cells including the carpogonium; they bear a single carpogonium, sometimes with an additional single sterile cell borne on the hypogynous cell (Figure 12). We have not observed two carpogonia side by side on a single branch. After fertilization, all cells of the carpogonial branch fuse, producing fusion cells that are small and very irregular, including several adjacent, unfertilized, carpogonial branches. Many single-celled gonimoblast filaments are then produced across

the fertile disc, each producing a single large carposporangium. As in the bi-tetrasporangial conceptacles, after fertilization the developing carposporangia appear to release an acid that dissolves the carbonate walls in cells lateral to and beneath the conceptacles (and sometimes the lower parts of the new roof tissue). Following cell wall dissolution, the conceptacles considerably enlarge in cavity volume as the carposporangia expand, in *P. squamulosum*, *P. nantuckensis*, and *P. investiens* increasing in volume by several fold.

BIOGEOGRAPHY AND ECOLOGY

Adey and Steneck (2001) used the bottom cover data for all crustose coralline species as a “first level proof” for the thermogeographic model (in this paper we only refer to the cover data for *Phymatolithon* spp.). Later, Adey and Hayek (2011)

TABLE 4. Dimensions (μm) of cystocarpic conceptacles of *Phymatolithon* species in the North Atlantic Boreal–Subarctic transition zone. Drawings by W. H. Adey.

	outer conc dia	cav dia	pore hgt	conc floor	cav hgt	roof tk	200 μm
<i>P. laevigatum</i> 1 station 4 conc	183	164	18	-118	95	41	
<i>P. squamulosum</i> 4 station 8 conc	388	240	139	-68	155	49	
<i>P. nantuckensis</i> 1 station 10 conc	306	184	78	-80	107	30	
<i>P. borealis</i> 2 station 7 conc	205	177	-32	-169	122	48	
<i>P. investiens</i> 1 station 1 conc	315	223	85	-123	125	65	

developed a successful “second test” for the western North Atlantic, using multivariate statistics, for all macroalgae. It is those papers that support the southwest–northeast trending Boreal region across the northern North Atlantic around which this paper was organized. By restricting our southern limits to the Norwegian coast (that is, the colder Boreal), we have avoided the complexity of Lusitanian and Mediterranean species of *Phymatolithon* that enter the flora from the south in the British Isles. Here we alternatively present the geographic data for each *Phymatolithon* species as abundance at each station (Figures 13–17). The cover value (% of coralline total cover) for each species at each station is also given in Table 1. Note that only stations that

would likely support the presence of the indicated species are plotted (e.g., stations that only have depths below 3 m are not plotted for absence of *P. squamulosum* [Figure 15], as that species is almost entirely intertidal and uppermost sublittoral in its occurrence). Similarly, stations having only an intertidal zone are not presented as absent for *P. rugulosum* (Figure 14) when it is not found.

Except for the localized *P. nantuckensis* species that occurs in the large, pebble-bottomed “harbor” of Nantucket Island south of Cape Cod in the western Atlantic, and the very leafy *P. investiens* of northernmost Norway (Figure 17), the species of this paper are geographically widespread, primarily on rock

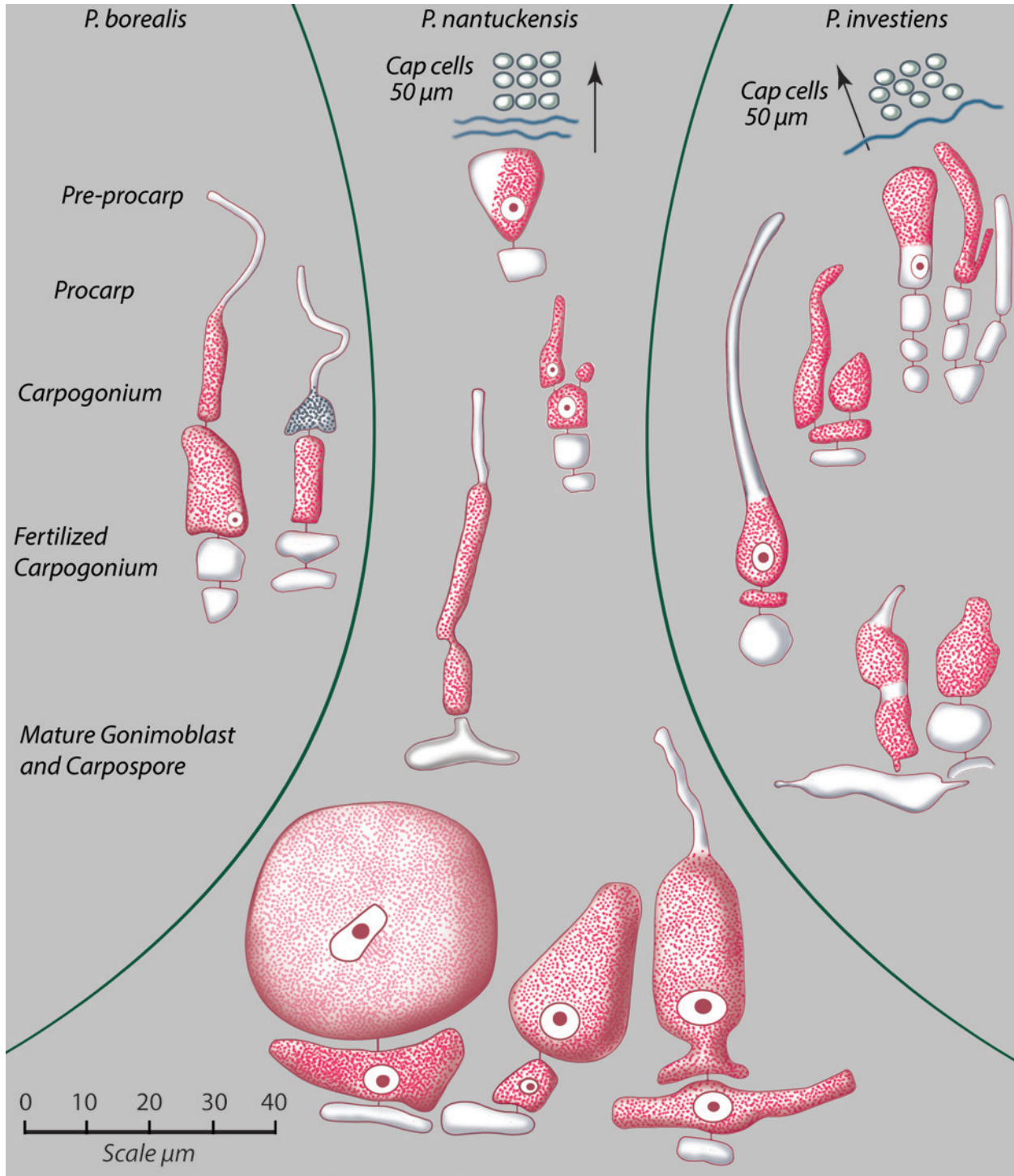


FIGURE 12. Development of female carpogonium from formation to carpospores after fertilization. The presentation is centered on the new species *Phymatolithon nantuckensis* with the poorly known *P. investiens* (right) and *P. borealis* (left) as backup. The mature, and early fertilized, carpogonium of *P. borealis* (left) is presented to back up the fuller presentations by Suneson (1943), as *Lithothamnion polymorphum*, and Irvine and Chamberlain (1994), as *Phymatolithon purpureum* (see text for fuller explanation). Drawn by WHA from microtome slides stained with phosphotungstic hematoxylin; digital image finished by Alice Tangerini for Smithsonian Institution.

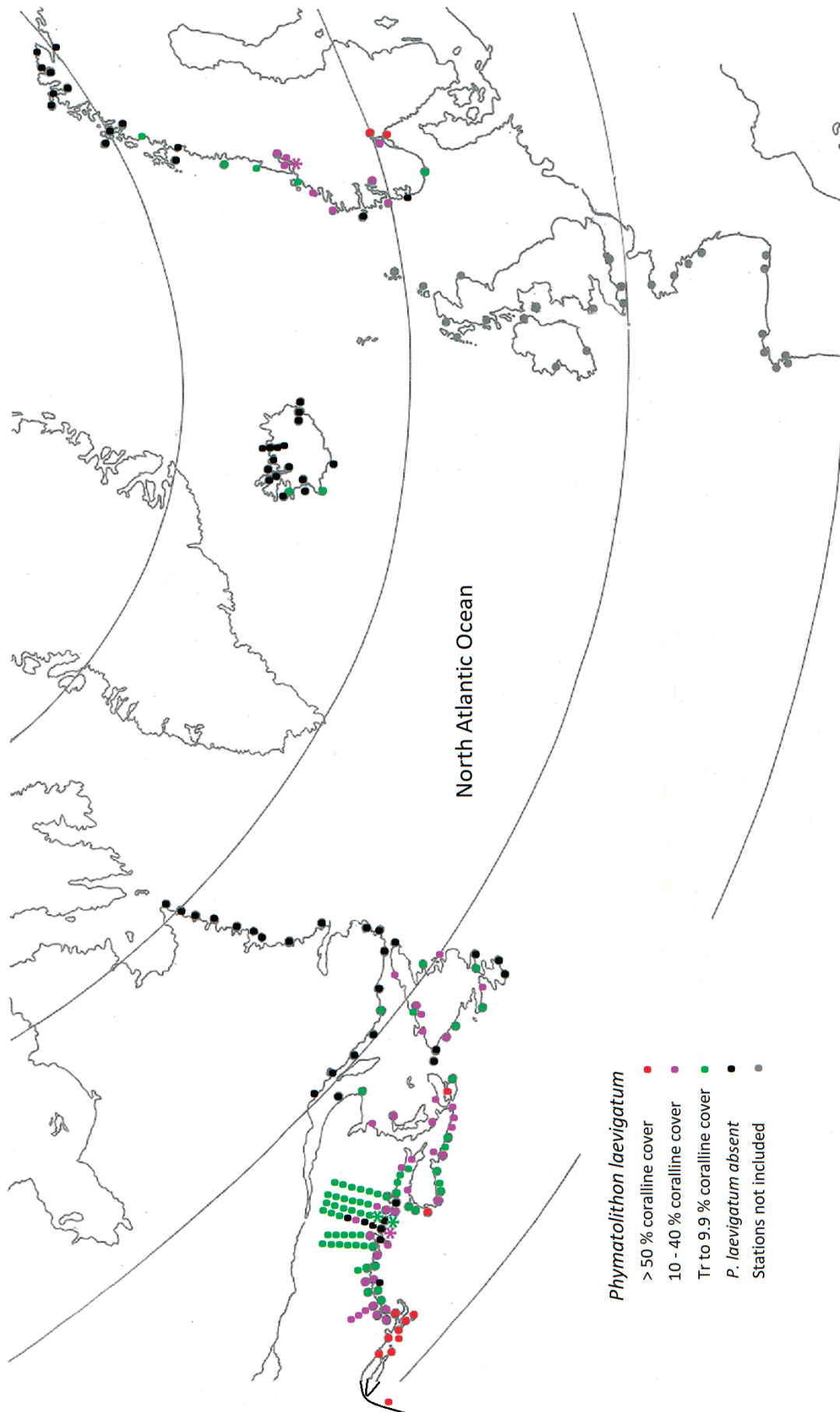


FIGURE 13. Distribution of *Phymatolithon laevigatum* in Boreal-Subarctic Atlantic. Gray dots = stations outside the Boreal-Subarctic Atlantic and not considered in this paper; black dots = species absent; at stations where substrate collections of crustose corallines obtained and within depth range of species, for abundance see legend on figure. The cover value (% of coralline total cover) at each station is given in Table 1. Figure by author WHA.

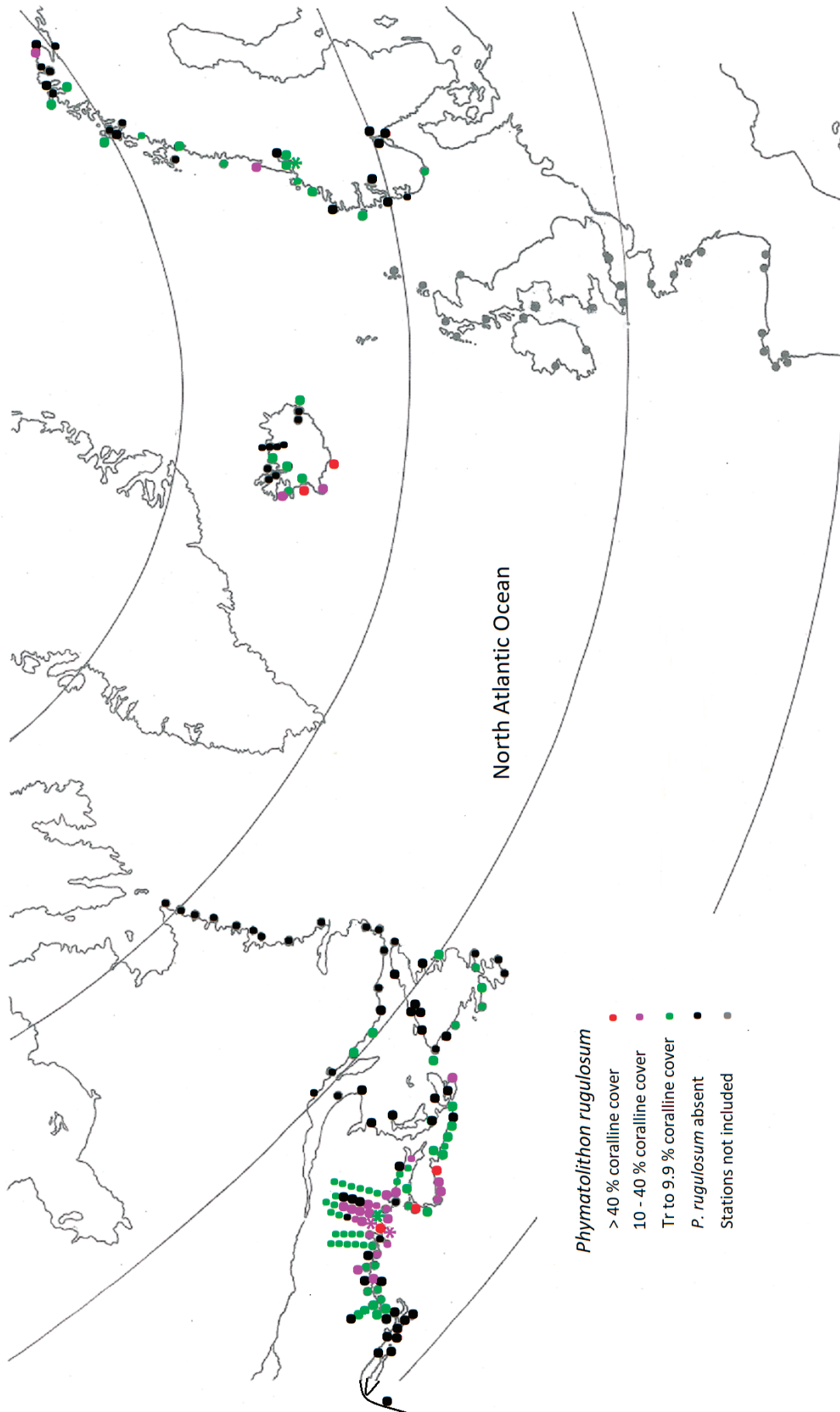


FIGURE 14. Distribution of *Phymatolithon rugulosum* in Boreal–Subarctic Atlantic. Gray dots = stations outside the Boreal–Subarctic Atlantic and not considered in this paper; black dots = species absent; at stations where substrate collections of crustose corallines obtained and within depth range of species, for abundance see legend on figure. The cover value (% of coralline total cover) at each station is given in Table 1. Figure by author WHA.

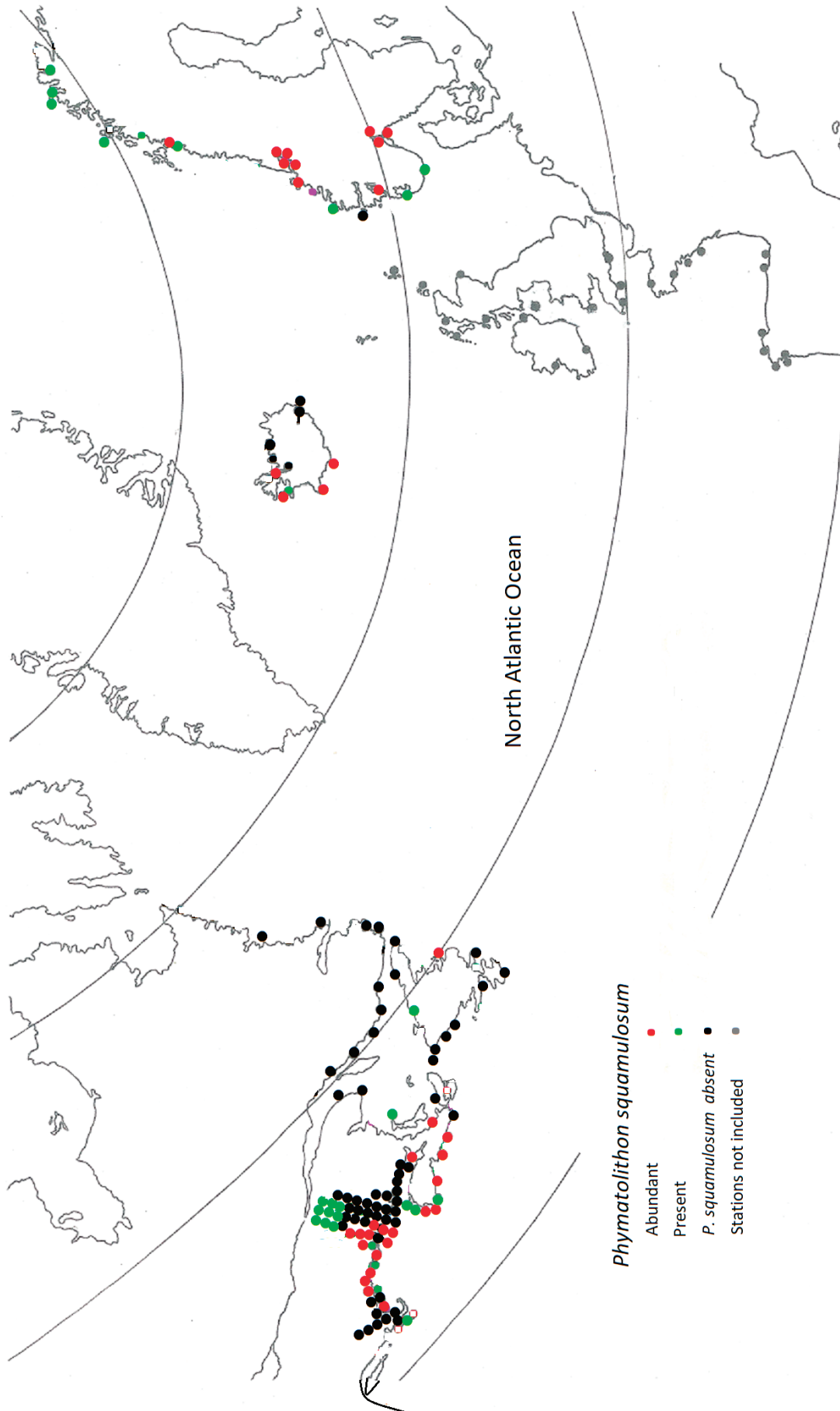


FIGURE 15. Distribution of *Phymatolithon squamulosum* in Boreal-Subarctic Atlantic. Gray dots = stations outside the Boreal-Subarctic Atlantic and not considered in this paper; black dots = species absent; at stations where substrate collections of crustose corallines obtained and within depth range of species, for abundance see legend on figures. The cover value (% of coralline total cover) for each species at each station is given in Table 1.

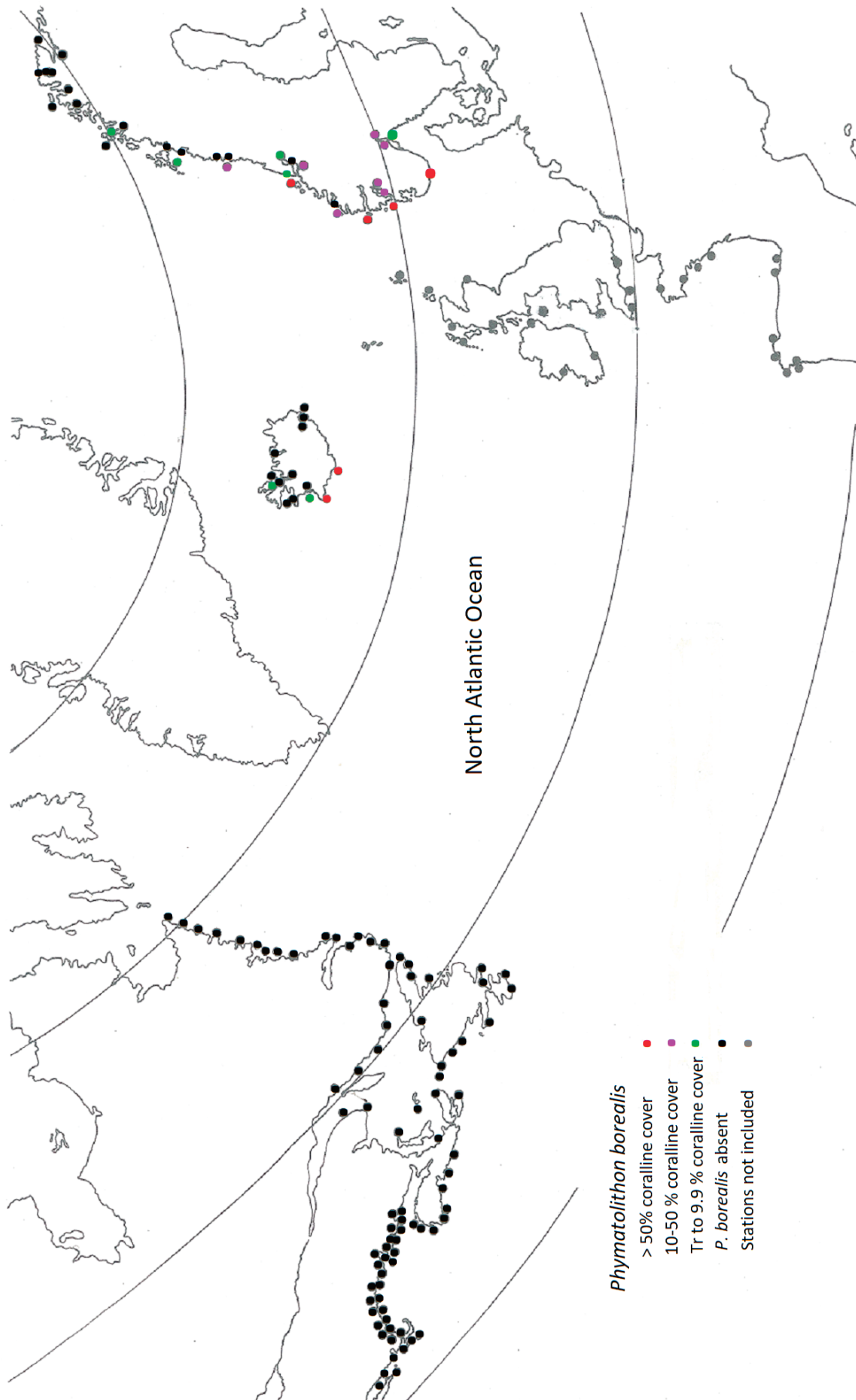


FIGURE 16. Distribution of *Phymatolithon borealis* in Boreal-Subarctic Atlantic. Gray dots = stations in the eastern N. Atlantic outside the Boreal-Subarctic Atlantic and not considered in this paper, also western N. Atlantic where *P. borealis* was not found at any station; black dots = species absent; at stations where substrate collections of crustose corallines obtained and within depth range of species, for abundance see legend on figure. The cover value (% of coralline total cover) at each station is given in Table 1. Figure by author WHA.

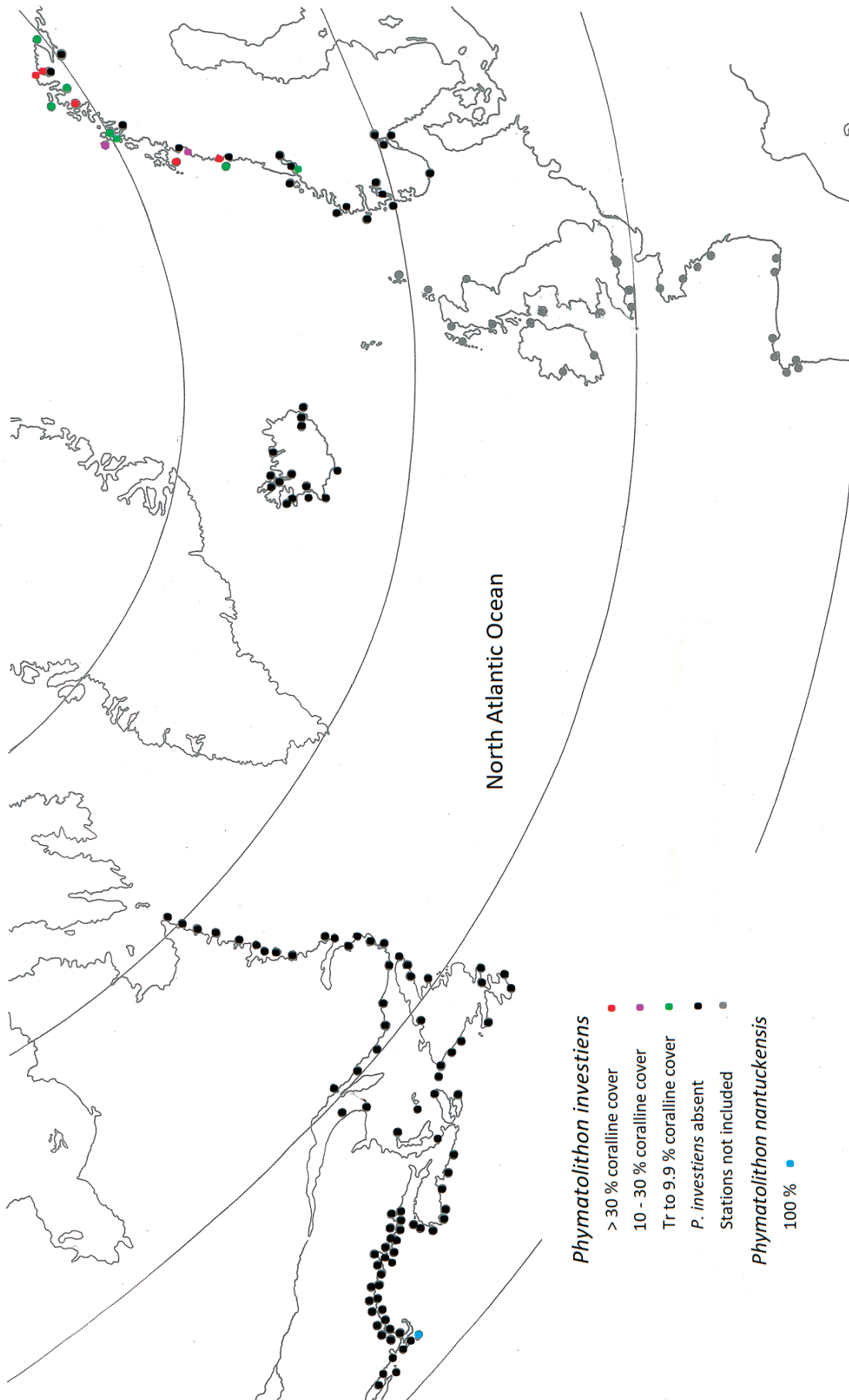


FIGURE 17. Distribution of *Phymatolithon investiens* and *P. nantuckensis* in Boreal–Subarctic Atlantic. *P. nantuckensis* found at a single locality in the western N. Atlantic (Nantucket Island). Gray dots = stations outside the Boreal–Subarctic Atlantic and not considered in this paper, also western N. Atlantic where *P. investiens* was not found at any station; black dots = species absent; at stations where substrate collections of crustose corallines obtained and within depth range of species, for abundance see legend on figure. The cover value (% of coralline total cover) at each station is given in Table 1. Figure by author WHA.

surfaces. Only rarely does *P. borealis* (Figure 16), and occasionally *P. investiens*, occur abundantly within rhodolith beds, and only *P. investiens* forms “potato-chip” type rhodoliths. *Phymatolithon squamulosum* is primarily an intertidal species, and it does not compete well with other subtidal corallines, even in intertidal pools. However, like many corallines, it also does not withstand significant drying at low tide. Thus, unlike other species in this flora, it tends to be patchy geographically and dependent on extensive fucoid cover (mostly *Ascophyllum* Stackhouse); some rock types (smooth granite) are very inhibitive, whereas porous, schistose rock can support the species even when minimal fucoid cover is present. Its great abundance from Cape Ann, Massachusetts, northeastward to western Penobscot Bay in the Gulf of Maine, followed by a virtual absence from Blue Hill Bay eastward to Passamaquoddy Bay (Figure 15), relates to the change from often schistose or layered sedimentary rocks in the more western areas and primarily granitic rocks eastward. Further northeast, in Nova Scotia, the species again becomes common. *Phymatolithon squamulosum* is common in southwestern Iceland and on the entire coast of Norway, being especially abundant in the south.

Phymatolithon laevigatum (Figure 13) tends to be limited to the upper half of the subtidal photic zone and occasionally occurs in larger tide pools. However, it is conspicuous that *P. laevigatum* has a considerable ability to thrive in lower salinities and at higher temperatures. Near the northern end of its range in the brackish waters of the Cape Breton Bras D’Or “Lakes,” it is abundant and appears to be the only coralline present; similarly, in the estuary of Humber Arm, in western Newfoundland, it is relatively abundant. At the other temperature extreme (summer temperatures $>20^{\circ}\text{C}$), on the western North Atlantic coast, ranging from Nantucket Sound to Long Island Sound, it is the dominant coralline species. Off northern New Jersey, the most southerly known site bearing rock ledges before the 800 km sandy coast barrier to corallines extending to south of Cape Hatteras, it is the only coralline present on the scattered rock ledges. Although sharply limited in the northern Gulf of St. Lawrence and absent in Arctic–Subarctic Labrador, *P. laevigatum* is abundant in the warm summer waters of the southern Gulf of St. Lawrence. Although virtually absent from Icelandic waters, and there present only on the warm southwestern coast, this species becomes abundant again in southern Norway and becomes the dominant species in the Norwegian Skagerrak and Oslofjord. In contrast, *P. rugulosum* (Figure 14) is most strongly developed at midphotoc depths in the subtidal and does not occur at lower salinities and in warmer waters within the western Atlantic region. It is locally abundant in southwestern Iceland and at scattered localities on the outer Norwegian coast; as a widespread dominant, it is primarily a species of the western North Atlantic.

Neither of the species with a thick hypothallium has been found in the western North Atlantic. *Phymatolithon borealis* occurs abundantly in southern Iceland and Norway. In Iceland it is reduced on the northwestern coast and is absent or rare in the colder, Subarctic north and east Iceland. *Phymatolithon borealis*

is the dominant rock-encrusting coralline on the outer coast of southern Norway; it is considerably more limited in the fjords, where it is replaced by Subarctic species from Trondheimsfjord northward and *P. laevigatum* further south. *Phymatolithon investiens* is a dominant species on the outer north Norwegian coast; on the central outer coast, it co-occurs with *P. borealis* and is sometimes epiphytic on that species or epizotic on barnacles and bryozoans. *Phymatolithon investiens* is moderately abundant as “potato chip” rhodoliths in the sounds of the outer coast of northern Norway where strong currents and moderate depths favor rhodolith formation. Along with other *Phymatolithon* species, it is sharply reduced in the inner fjords, being replaced by Subarctic species (Adey, 1971).

SPECIES DESCRIPTIONS

Perithallial cell measurements reported below are based on cells 4–7, with 1 being the meristematic cell, 2 the first perithallial cell below, etc. Measurements are given as $L_{47/44} = 2.8\text{--}10\ \mu\text{m}$ (5.7) [1.1], where L = cell length; $_{47/44}$ = 47 cell series measured from 44 plants; 2.8–10 μm = minimum–maximum cell length; (5.7) = mean cell length; and [1.1] = standard deviation. Perithallial cell length, diameter, ratio, and coefficient of variation (CV) with depth are given in Figures 3–7.

Phymatolithon laevigatum (Foslie) Foslie 1898:8

Basionym: *Lithothamnion laevigatum* Foslie 1895:167.

Heterotypic Synonym: ?*Lithothamnion embolooides* Heydrich 1900:74.

Lectotypus: TRH C25-3749, Helgoland, Germany, not dated, leg. Kuckuck. Designated by Adey and Lebednik (1967).

Morphology and Habitat: Encrusting, epilithic thalli firmly attached, thin, to 1 mm, lightly rugose, often with whitish surface swirls; pink when freshly collected; on boulders and bedrock, intertidal pools to 25 m depth; can tolerate warmer waters to 22°C and lower salinities to 18 ppt.

Anatomy: Epithallium as for genus (Plate 1C); perithallial cells $L_{47/44} = 2.8\text{--}10\ \mu\text{m}$ (5.7) [1.1]; $D_{47/44} = 2.2\text{--}10\ \mu\text{m}$ (5.5) [1.5] (Figures 4–9); hypothallium thin, 13–55 μm thick (mean 27.4, SD 11.8; Figure 2; Plate 1A).

Reproduction: Bi-tetrasporangial conceptacles flush with surface or sunken, bowl shaped with a distinctive raised rim (Table 2; Plate 1E,F); conceptacle cavity diameter (diam) $_{43/16} = 168\text{--}350$ (239) [43] μm (Figure 10); roofs (0–120 μm below surrounding surface). Gametangial conceptacles sunken, rare, and more poorly known; see Tables 2–4.

Distribution: Widespread in the Boreal–Subarctic transition zone (Figure 13) and south into the Boreal region in the North Atlantic.

Comments: Topotype material from Helgoland, Germany (Figure A2a) has been sequenced that morpho-anatomically matches the lectotype specimen. Among the other North Atlantic *Phymatolithon* spp., *P. laevigatum* can only be confused with *P. rugulosum* with which it shares considerable distribution

overlap (see Figures 13, 14). *Phymatolithon laevigatum* is distinguished by its coarser surface ridges, bi-tetrasporangial conceptacle roofs with a bowl shape and a distinctive raised rim, its less elongate perithallial cells, and statistically significantly greater mean cell diameter and higher mean bi-tetrasporangial cavity diameter compared with *P. rugulosum*.

***Phymatolithon rugulosum* W. H. Adey 1964:381**

Holotypus: MICH 701752, southwest Merchant Island, East Penobscot Bay, Maine, USA, 2.xi.1961, 3–5 m below mean low water, *leg.* W. H. Adey, 61-41A-3.

Isotypus: S-163, US 171023.

Morphology and Habitat: Encrusting, smooth, epilithic thalli firmly attached, thin to 4 mm, with fine rugulose surface; bluish-pink when freshly collected; on boulders and bedrock, depth 0–40 m (peak abundance at ~5–10 m).

Anatomy: Epithallium as for genus; perithallial cells $L_{53/41} = 3\text{--}11.4\ \mu\text{m}$ (6.1) [1.5]; $D_{53/41} = 2\text{--}8.6\ \mu\text{m}$ (4.1) [1.1] (Figures 4–9); hypothallium thin, 8–50 μm thick (mean 26.5, SD 9.6) (Figure 2).

Reproduction: Small, bi-tetrasporangial conceptacles, cavity diam_{45/13} = 100–220 μm (151) [28] (Figure 10); conceptacle roofs sunken (6–96 μm below surrounding surface) with a distinctive lateral shelf (Table 2; Plate 2C–F). Gametangial conceptacles rare, and more poorly known (Tables 3, 4).

Distribution: Widespread in the Boreal–Subarctic transition zone; in the Northwest Atlantic not reported south of Cape Cod Bay, Massachusetts, USA, and extending north through all but northernmost Newfoundland; absent in Labrador; most common on east coast of Iceland, but present throughout; not reported east of Vardø, northern Norway (Figure 14), extending south in the Boreal region throughout Ireland, Scotland, Wales, and England; not confirmed from France (see under comments below).

Comments: This species was placed in synonymy under *P. lamii* apparently on the basis of its morphological similarity and the apparent overlapping measured features such as cell length and diameter, conceptacle diameters, height and cell roof thickness, and tetrasporangial cell lengths and widths (Chamberlain, 1991: tbl.1). Irvine and Chamberlain (1994) described *P. lamii* as lacking a distinctive rim, whereas *P. rugulosum* has a highly distinctive sunken shelf lateral to the pore plate. Unfortunately, current available numerical data for *P. lamii* do not make a statistical comparison possible. DNA sequences, however, indicate that these are distinct species, with *P. lamii* more closely related to the recently described *P. lusitanicum* than to *P. rugulosum*. At present, *P. rugulosum* and *P. lamii* are separated biogeographically, with *P. rugulosum* not reported south of England and *P. lamii* not north of France.

In the Boreal–Subarctic transition zone across the entire Atlantic Ocean (Figure 14), vegetative *P. rugulosum* can only be confused with the similarly smooth and closely adherent *P. laevigatum*. But when fresh, and with attention, surface markings and color can distinguish these species. Surface ridges when

present are finer in *P. rugulosum* compared to *P. laevigatum*. When reproductive, in winter, *P. rugulosum* conceptacles are smaller and more sunken than in *P. laevigatum*, and they also possess a diagnostic lateral shelf compared to the bowl-shaped roof and raised rim of *P. laevigatum*.

***Phymatolithon nantuckensis* W. H. Adey, J. J. Hernandez-Kantun & P. W. Gabrielson sp. nov.**

Holotypus: US 171011, Nantucket Harbor, Nantucket Island, Massachusetts, USA; 41°18'15.51"N, 70°2'42.60"W; 1.viii.1961; shallow to 5 m; *leg.* W. H. Adey 61-12-1.

Morphology and Habitat: Encrusting, epilithic thalli firmly attached, thin and imbricating, to 600 μm thick by multiple self-overgrowth (Plate 3B); abundant on small pebbles 3–10 cm in diameter at 2–3 m depth; pink when freshly collected.

Anatomy: Epithallium as for genus; perithallial cells $L_{10/2} = 4.9\text{--}12.6\ \mu\text{m}$ (7.7) [1.6], $D_{10/2} = 3\text{--}9.1\ \mu\text{m}$ (5.3) [1.0] (Figures 4–9); hypothallium thin (Plate 3A,B) 7–25 μm thick (mean 18 μm , SD 6.2; Figure 2).

Reproduction: Small, mature bi-tetrasporangial conceptacles, cavity diam_{10/2} = 120–160 μm (140) [14] (Figure 10); conceptacle roofs raised (32–100 μm), but conceptacle floor 18–86 μm below crust surface (Table 2); gametangial conceptacles (Tables 3, 4; Plate 3E,F).

Distribution: Known only from the type locality, the harbor (lagoon) of Nantucket Island, USA (Figure 17).

Comment: The existence of this entity was known by the senior author for 55 years, but it was thought to be perhaps an introduced European species, as a result of the extensive use of Nantucket Harbor as a major whaling port in the late eighteenth and early nineteenth centuries. DNA sequencing has revealed this to be a distinct species, not matching with any European *Phymatolithon* species. Whether it is restricted to this area of a few square kilometers or is more widely distributed in very small numbers in the Northwest Atlantic remains to be determined. The area south of Cape Cod is environmentally isolated from both the Gulf of Maine and the more tropical region to the south; in addition Nantucket Harbor is large (more a bay created by an extensive sand bar), and the island itself is relatively isolated. Thus the possibility of this being a relict species cannot be discounted. Whaling ships travelled very widely in the late eighteenth and early nineteenth centuries, and a North Pacific origin might be considered. However, current DNA-based research has failed to locate any *Phymatolithon* species in the North Pacific. Furthermore, based in its distribution, and considerable DNA analysis, *Phymatolithon* is probably a Tethyan genus.

***Phymatolithon squamulosum* (Foslie) W. H. Adey, J. J. Hernandez-Kantun & P. W. Gabrielson comb. nov.**

Basionym: *Lithothamnion squamulosum* Foslie 1895:155, pl. 19, figs. 24–26.

Homotypic Synonym: *Lithothamnion lenormandii* (Areschoug) W. H. Adey f. *squamulosum* (Foslie) Foslie.

Holotypus: TRH B5-1962, Stensund [now Steinsund], Sulen [now Sula], indre [= inner], Sogn, Norway, vii. 1894; ned-erst lit. reg, beskyttet [= lowest littoral region, protected], leg. Boye (Woelkerling et al., 2005:267).

Isotypus: BM000044670, Box 434; collection data as above.

Morphology and Habitat: Thalli thin, imbricating and leafy, smooth when young, becoming squamulose with self-overgrowth and buried conceptacles, to 300 μm thick; violet when freshly collected; common on intertidal bedrock to uncommon in uppermost subtidal (<3 m depth), frequently under *Asco-phyllum* or on schistose rock (retains moisture), not in tide pools; occurs with *Clathromorphum circumscriptum* (Strömfelt) Foslie, rarely with *P. laevigatum*.

Anatomy: Epithallium as for genus; perithallial cells $L_{33/27} = 3.5\text{--}11.9 \mu\text{m}$ (7.0) [1.5], $D_{33/27} = 3.5\text{--}8.4 \mu\text{m}$ (5.7) [1.2] (Figures 4–9); hypothallium 15–75 μm thick (mean 40.5, SD 15.4; Figure 2).

Reproduction: Mature bi-tetrasporangial conceptacles common, cavity diam_{10/2} = 122–276 μm (190) [38] (Figure 10); conceptacle roofs raised (10–135 μm (74) [33]) but with conceptacle floor approximately 75 μm below crust surface (Table 2). Gametangial conceptacles uncommon (see Tables 3, 4; Plate 4).

Distribution: Geographically patchy in the Boreal–Subarctic North Atlantic transition zone; from northernmost to southernmost Norway; eastern and southern Iceland; uncommon in Newfoundland, absent northern Gulf of St. Lawrence and Labrador, patchily abundant Nova Scotia south to Woods Hole, Massachusetts, USA (Figure 15). In Boreal waters around Ireland and the UK, and confirmed as far south as Trévignon, France.

Comments: We sequenced an isotype specimen of *Lithothamnion squamulosum* (type locality: Sogn, Norway) in BM, because a partial *rbcL* sequence provided by Dr. Viviana Peña from an isoelectotype specimen of *Melobesia lenormandii* Areschoug [basonym of *Phymatolithon lenormandii* (Areschoug) W. H. Adey, type locality: Arromanches-les-Bains, Calvados, France] in CN, was distinct at the species rank from field-collected material that we had called *P. lenormandii*. *rbcL* sequences from our field-collected material were identical to the isotype specimen of *L. squamulosum*; thus we made the new combination, *P. squamulosum*. It was relatively recently that Babbini and Bressan (1997) placed *L. squamulosum* in synonymy under *P. lenormandii* without comment.

With its primarily intertidal habitat and thin hypothallus, *P. squamulosum* cannot be confused with any other *Phymatolithon* species in the Boreal–Subarctic transition zone. In the Boreal part of its range, we do not know how it differs from *P. lenormandii*, as no one has found field-collected material that matches the *rbcL* sequence obtained for type material of *P. lenormandii*. It is likely that the description in Irvine and Chamberlain (1994) includes both species or, perhaps, is solely *P. squamulosum*.

Phymatolithon borealis W. H. Adey, J. J. Hernandez-Kantun & P. W. Gabrielson

Holotypus: US 170979, Heimey, Westmanneyjar, Iceland, 17 viii 1966, leg. W. H. Adey, 66-27, 0-10K.

Morphology and Habitat: Encrusting, smooth, weakly leafy, unless overgrowing substrate irregularities, rarely cantilevered, becoming thick (to 5 cm), often with buried postmature bi-tetrasporangial conceptacles; violet when freshly collected, often becoming greenish-yellow when dry; abundant on bedrock 0–30 m.

Anatomy: Epithallium as for genus; perithallial cells $L_{124/29} = 3\text{--}11 \mu\text{m}$ (6.9) [1.3], $D_{124/29} = 3\text{--}7.5$ (4.6) [0.9] (Figures 4–9); hypothallium 30–140 μm thick (mean 77, SD 25.2; Figure 2; Plate 5).

Reproduction: Mature bi-tetrasporangial conceptacles 22–100 μm (58) [27]) in diameter, roofs fully sunken with a raised rim but without a circumferential shelf (Table 2), cavity diam_{20/5} = 150–288 μm (199) [39] (Figure 10). Gametangial conceptacles (see Tables 3, 4). Postmature conceptacles often buried and remaining as yearly layers in the crust (Plates 5B, 6A,F).

Distribution: In the Boreal–Subarctic transition zone, only in Iceland and southern Norway (Figure 16). Common in Boreal waters around Ireland and the UK.

Comment: Despite its abundance in shallow subtidal (<15 m) waters in Iceland and southern Norway and its occurrence in mid-, but mostly low, intertidal and shallow subtidal habitats in Boreal waters, this species appears not to have been named. In Boreal–Subarctic transition zone waters, *Phymatolithon borealis* can only be confused with the other thick hypothallium species, *P. investiens*, but these two species only overlap in distribution along the central coast of Norway, and *P. investiens* is, in general, a deeper-water species. In European Boreal waters, *P. borealis* appears most similar to *Phymatolithon purpureum*. Type material of *P. purpureum* has not been sequenced, to our knowledge. Based on the descriptions in Woelkerling and Irvine (1986) and Irvine and Chamberlain (1994), *P. borealis* appears distinct from *P. purpureum*, primarily on the basis of bi-tetrasporangial conceptacle characters: slightly sunken to slightly raised in *P. purpureum* versus always sunken in *P. borealis*, conceptacles with wide, raised rims to 100 μm wide in *P. purpureum* versus narrow (30–40 μm) and raised in *P. borealis* and concave conceptacle pore plates in *P. purpureum* versus flat conceptacle pore plates in *P. borealis*.

Phymatolithon investiens (Foslie) Foslie 1905:81

Basionym: *Lithothamnion investiens* Foslie 1895:129, pl. 22, figs. 2–5.

Lectotypus: TRH C26-3785 in US (fragment), Lyngö, north of Tromsø, Norway, no date, leg. Foslie.

Morphology and Habitat: Primary thalli on rock, coral-line and shell substrate, moderately thick (to 1 mm), but extensively overgrowing by leafy cantilever, forming loose structures and breaking off to develop rhodoliths to 10–20 cm in diameter; violet when fresh.

Anatomy: Epithallium as for genus; perithallial cells $L_{124/28} = 4.5\text{--}12\ \mu\text{m}$ (6.9) [1.4], $D_{124/28} = 3\text{--}7\ \mu\text{m}$ (4.8) [0, 9] (Figures 3–9); hypothallium 98–350 μm thick (mean 176, SD 65; Figure 2; Plates 7, 8).

Reproduction: Mature bi-tetrasporangial conceptacles small, 55–60 μm (57) [4], with a raised rim but without a circumferential shelf (Table 2; Plates 7A,B, 8D); roofs sunken; cavity diameter $\text{diam}_{6/1} = 138\text{--}188\ \mu\text{m}$ (158) [16] (Figure 10). Gametangial conceptacles (Tables 3, 4; Plates 7C–F, 8E,F). Post-mature conceptacles rarely buried.

Distribution: Abundant in coastal northern Norway, especially in deeper water (10–30 m) as rhodoliths (Figure 17).

Comments: Both *Phymatolithon investiens* and its basionym, *Lithothamnion investiens*, are considered illegitimate names, because *Lithothamnion investiens* is said to be a superfluous name for *Lithophyllum zonatum* Foslie (1890: 10). This argument assumes, however, that *Lithophyllum zonatum* and *Lithothamnion investiens* are the same species. Foslie (1895) believed that they were, as he listed *Lithophyllum zonatum* as a synonym under *Lithothamnion investiens*, but convincing evidence is lacking. We have sequenced the *Lithothamnion investiens* lectotype specimen designated by Adey in Adey and Lebednik (1967: 72), and that sequence is an exact match to field-collected material. We have not sequenced the holotype of *Lithophyllum zonatum*, and thus we use the name *P. investiens*.

As noted above under *P. borealis*, *P. investiens* can only be confused with that species where they co-occur in central Norway, but *P. investiens* typically occurs in deeper water (10–30 m) where it is common, especially as rhodoliths.

DISCUSSION

For the Boreal–Subarctic transition zone *Phymatolithon* species treated herein, there is excellent congruence between the DNA sequence data and the identity of specimens and species delimitations based on previous morpho-anatomical studies by the senior author (Adey, 1964, 1965, 1966a), as well as new information in this paper. This agreement is in contrast to nearly all other coralline geniculate (Gabrielson et al., 2011; Hind and Saunders, 2013; Hind et al., 2014a,b, 2015) and non-geniculate genera and species (Basso et al., 2015; Hernandez-Kantun et al., 2014, 2016; Sissini et al., 2014; van der Merwe et al., 2015; Hind et al., 2016), wherein type specimens have been matched to field-collected material based on DNA sequences. The major reasons for this are fourfold with respect to non-geniculate corallines: (1) most coralline morpho-anatomists have relied on small sample sets stored in museums, and rarely have population analyses supported by statistical analysis been employed; (2) during the past 60 years since scuba has been widely available, few have taken the opportunity to intensively study these organisms in their natural habitat; (3) the gross morphology of a species can vary widely with substrate characteristics, such as

local fleshy algal cover, depth, and wave and current action; and (4) specimens often are bulky, especially when collected with their substrate intact, and are often mosaics of crusts of several different species; rarely has enough coralline-covered substrate been returned to museum collections to allow the evaluation of infra- and interspecific variation in relationship to the original environment.

Included in this group of species, where the morpho-anatomical and DNA sequence data are not congruent, are the Northeast Atlantic Boreal–Lusitanian *Phymatolithon* species (primarily UK, Ireland, France, and Spain). Thus far, we have no match in any database, including our unpublished sequences, to the sequence from the isolectotype specimen of *P. lenormandii* nor to the material excluded from the type of *Lithophyllum hibernicum* Foslie (the rhodolith lacking cup-forming terminal branches; Hernandez-Kantun et al., 2015: fig. 6A, top-right specimen), both of which belong in *Phymatolithon*. All the *Phymatolithon* species type specimens whose localities are in Boreal Europe need to be sequenced, as well as many more field-collected specimens, before we can confidently apply names as well as understand the ecology and distributions of these species. At present, all reports of *P. lenormandii* outside the Boreal Northeast Atlantic (Guiry and Guiry, 2017) are likely misapplications of this name.

HYPOTHALLIA

Hypothallial thickness and cell shape are useful characters for separating Boreal–Subarctic transition zone *Phymatolithon* species (Figure 2). Hypothallial overgrowth of initially thin crusts, including occasional burial and frequent refilling of conceptacle cavities by secondary hypothallia, can only be ascribed to *P. squamulosum* or the geographically and ecologically restricted *P. nantuckensis*. These species occupy unstable substrate where rapid growth over new surfaces, self-overgrowth, and constant conceptacle production have more adaptive value than building crust thickness.

At the other extreme, *P. borealis* and *P. investiens* have very thick hypothallia, typically two to five times that of the thin hypothallium *Phymatolithon* crusts (Figure 2); these are crusts that are leafy or “rolling” in character, with the thicker hypothallus more able to negotiate holes or valleys in the substrate. In *P. investiens*, with hypothallia mostly more than 100 μm thick, and sometimes more than 300 μm , crusts can become cantilevered over considerable holes and valleys in the substrate. When *P. investiens* crusts break free of the substrate, continued marginal growth and overgrowth can produce rhodoliths with a “potato chip” morphology.

Phymatolithon investiens is the only crustose Boreal–Subarctic transition zone *Phymatolithon* species to have significant rhodolith potential. In rhodolith habit it was only found well north of the Arctic Circle, although still in Boreal–Subarctic transition zone waters (Adey, 1971). In northern Norway land elevations

are generally lower than in the southern part of the coast. As a result, water depths in the sounds between outer fjords are often less than 30 m, are within the photic zone, and large areas are more or less flat-lying with strong tidal currents providing favorable conditions for extensive rhodolith development.

Although in the individual epilithic crusts of *P. investiens* overgrowths are more substantial and less frequent compared to *P. squamulosum* and *P. nantuckensis*, *P. investiens* is morphologically similar to these species as compared to the other Boreal–Subarctic transition zone species that more rarely overgrow their own crusts. For *P. borealis* and *P. investiens*, the advantages to being able to occupy very irregular surfaces with thick marginal primary crusts that can function without continuous substrate support seem more or less obvious. However, that these should be restricted to the warm winter (eastern Atlantic and southwestern Iceland) part of the North Atlantic Boreal–Subarctic transition zone remains more obscure. This locale restriction may result from biogeographical history, or possibly from the slow growth occasioned by long winters near 0°C on the colder side of the North Atlantic.

Intermediate between these two morphologically extreme growth forms are *P. laevigatum* and *P. rugulosum*. These species have moderately thick hypothallia (Figure 2), but are so tightly adherent to their typical rock substrate that removal from their habitat with hammer and chisel often brings rock fragments attached to their bases. They build long-lived crusts (perhaps decades in age) in stable environments; however, as we discuss below, they occupy rather different environmental niches.

PERITHALLIA

Non-geniculate corallines, in general, do not produce fixed-size cells within their carbonate matrix; intercalary meristematic cells divide and the ventrally produced perithallial cells continue to elongate and add wall carbonate for at least several cells deep in the perithallium. More deeply in the perithallial tissue, cells clearly add (and remove) carbonate within the walls. It is standard in coralline taxonomy to provide a set of cell measurements, as a range of dimensions, without statistical data and without specifying location (other than perithallium); this approach generally provides data having little value in discriminating species or in understanding their growth physiology.

Genera in the Hapalidiales present three general types of cell elongation in the perithallium below the intercalary meristem (Adey et al., 2005, 2015b). All *Phymatolithon* species are of the “progressive type,” elongating gradually, mostly over the first three to four cells below the meristematic cells, with relative stabilization thereafter (Figure 3). Thus, in *Phymatolithon*, typically cells four to seven below the meristem have the least variability and provide the best measure for potential species identification. In this range, cell elongation (upward crustal extension) has been completed and the cell shape changes associated with depth in the perithallium have not yet been expressed. Although cell lumen diameter changes far less, it

tends to increase or decrease a small amount below the level of length stabilization (Figure 5).

Among the *Phymatolithon* species treated herein, statistically significant numerical differences in cell length and particularly cell diameter in the stable cell range (cells 5–7) have been shown (Figure 5). Except in *P. nantuckensis*, cell shape (L/D) varies least within species and is consistently diagnostic among species, even when this measure is extended to the generally more elongate hypothallial cells (Figure 8). The thin hypothallial species, *P. rugulosum*, and the thick hypothallial species, *P. borealis* and *P. investiens*, have relatively long and narrow perithallial cell lumina, whereas *P. laevigatum* has spherical cells, and *P. squamulosum* is intermediate in this respect. *Phymatolithon nantuckensis* shows considerable perithallial cell elongation below cell 4 (Figure 4) that may be the result of its very thin crusts (typically 70–400 µm), the beginning of the transition from the hypothallium and, in large part, fewer sampled specimens. The tendency for perithallial cell diameter to increase slightly with depth in the thin hypothallium species (Figure 5) could be an artifact of the development of cross-filament fusions with depth below cell 3 (Adey, 1964; also see Figure 8). However, the thick hypothallium species, *P. borealis* and *P. investiens*, also have numerous cell fusions; they show the opposite trend, and both the positive and the negative slopes are statistically significant. CV values for perithallial cell diameter remain equivalently low as compared to cell length for the shallow cells (Figure 6). However, except for the consistently erratic values for *P. nantuckensis*, all species have a strong tendency for CV values to increase with depth, further indication of the dynamics of cell wall carbonate with depth.

Significant perithallial growth over several years may also occur, producing a more regular seasonal pattern of calcified walls of longer, thicker-walled cells in summer and shorter, thinner-walled cells in winter. This tendency is most pronounced in *P. borealis*, but it also occurs in *Clathromorphum* species, where the IF layer can be thicker than the IW wall, and varies seasonally, being typically much thicker in summer (Adey et al., 2013). In *Clathromorphum*, the calcite crystals are large, deltoid in shape, and typically oriented vertically or diagonally (Adey et al., 2013, 2015b). Additional sub-perithallial tissue types develop in the conceptacle roofs of both bi-tetrasporangial and gametangial conceptacles, although these could be considered tissue types of conceptacles.

Perithallium: A Complex of Tissues

Historically, corallines had been considered to have two basic tissue constructions: perithallium and hypothallium. In the 1960s, Adey (1964, 1965, 1966a), showing a great range of development in what had been previously referred to as cover cells (or deckenzellen), introduced a third tissue type, epithallium. These tissues vary widely in different genera and species. Herein, and in earlier papers (Adey et al., 2005, 2013, 2015b), we have demonstrated a pattern of perithallial cell development and modification with

depth. However, there is a higher level of organization within perithallial tissue that develops when cells of different shape and calcified wall chemical composition form. These anatomical changes occur when the normal intercalary meristem and elongating cell patterns are disrupted by more rapid growth relating to damage and return to morphological stability (Plates 1B, 2C, 3B, 4C,F, 6A,F, 8E). The changes are produced by the coordinated action of a local group of filaments and occur in response to grazing or when conceptacles break out after spore release. Such “wound” tissue results from deep grazing or from conceptacle breakout and produces a localized and coordinated rapid regrowth of distinctive and changing cell morphology (Siobhan Williams, W. Adey, J. Halfar, A. Kronz, P. Gagnon, D. Belanger, and M. Nash, unpublished manuscript [in review], “Effects of light and temperature on Mg uptake, growth, and calcification in the proxy climate archive *Clathromorphum compactum*,” Biogeosciences), cell wall microstructure, and Mg content (Nash and Adey, 2017a,b). The regrowth continues until the typical crust surface is attained. When the morphological anomaly is repaired, the cells return to their normal growth rate and shape.

In addition, *Phymatolithon* species conceptacles have at least two supporting tissues, those of conceptacle roofs (both bi-tetrasporangial and gametangial) and of nurse tissues, cells surrounding developing bi-tetrasporangia and carposporangia whose carbonate walls have been dissolved and the cells crushed. Transfer of photosynthate from nurse tissue to developing sporangia has not been demonstrated, but the very large size of the quickly developed sporangia indicates that photosynthate must be transferred from elsewhere, and the surrounding and underlying crushed tissue is a likely source (Adey et al., 2013).

More or less narrow fusion channels formed between adjacent cells by cell wall dissolution can, and probably do, have many roles in coralline metabolism. These channels also provide one key to understanding the basic process of cell wall calcification. Corallines produce high magnesium calcite of specific but varying magnesium content in their complex cell walls, but they also have the capacity to dissolve away that calcite, with some precision, at other points in their skeleton. As shown in Figure 8, calcification and wall dissolution rarely occur in the same cell, or the same local area of tissue, at the same time.

Some species of *Phymatolithon* have structures internal to cells, called staining bodies. The chemical structure of these bodies has not been investigated, but in the North Atlantic Boreal–Subarctic zone species they occur only in a single clade, that composed of the species *P. laevigatum*, *P. borealis*, and *P. investiens* (Figure 1), and can be useful in identification when reproductive structures are not present or when too few specimens are available for statistical analysis. The only other species in the North Atlantic Boreal–Subarctic known to have these distinctive staining bodies are *Lithothamnion tophiforme* Unger and *Lithothamnion sonderi*, but the former typically has a branching morphology and the latter is a thin, tightly attached deep-water species (>20 m) occurring mostly in southern Norway and the British Isles. *Lithothamnion tophiforme* and

P. investiens do occur together in the outer sounds and fjords of northwestern Norway, the former as rhodoliths and the latter as epiphytic crusts on these rhodoliths. Similarly, in deeper waters (>20 m) of southern Norway, *P. borealis* and *L. sonderi* can co-occur. Even when this is the case, the highly distinctive armored epithallial cells and elongate meristem cells, as seen in thin sections and SEM images of both *Lithothamnion* species, should easily serve to separate the species in section. In a hand specimen, *L. sonderi* is not only a very thin crust, but frequently has distinctive, raised white conceptacles, or rim remnants of conceptacles; it would not likely be confused with a *Phymatolithon* species.

REPRODUCTION

Adaptations to Grazing

In spite of the calcified thallus, non-geniculate corallines are often subject to considerable surface grazing by scraping invertebrates, especially chitons, limpets, and sea urchins. Thus, many corallines have evolved special adaptations to reduce the effects of grazing, particularly on their conceptacles. *Phymatolithon* species protect their developing conceptacles by initiating their conceptacle primordia adventitiously, more or less deeply (30–100 µm) in the perithallium. In nearly all other non-geniculate corallines, conceptacle primordia are produced from the intercalary meristem just below the crust surface, and these taxa have evolved other protective mechanisms. *Clathromorphum* species are truly extraordinary as they have developed a thick photosynthetic epithallium and have a symbiotic relationship with limpet grazers. When grazing is prevented, epithallial cells build up and, along with settled epiphytes, can cause the death of a crust (Adey, 1973; Steneck, 1982, 1992; Adey et al., 2013). Most *Lithothamnion* species have very thick-walled epithallial cells (presenting an armored effect; Adey et al., 2005) as well as branches, the latter having been shown to reduce grazing (Steneck, 1982, 1992), whereas others develop sunken conceptacles.

Many corallines in the Subarctic and the Boreal–Subarctic transition zone, including most *Phymatolithon* species (Adey, 1964), produce their bi-tetrasporangial conceptacles in winter, when grazer activity is minimal. *Phymatolithon* species that are not restricted to winter reproduction occupy environments which are largely grazer reduced. Phenological data and grazing experiments from cold-water anti-Boreal and Antarctic crustose corallines would be an interesting comparison. Recently, while carrying out laboratory experiments with *C. compactum*, we learned that if temperatures are raised while the conceptacles are maturing, chitons that are present in the experimental system, which would normally graze just the epithallium, gouge deeply into the conceptacles, removing sporangia as well as surface crust, a behavior never seen in situ (Williams et al., unpublished). Thus, grazer and coralline crust interactions are complex and can be significant (see also Steneck, 1982, 1992).

Bi-tetrasporangial Conceptacles

For all non-geniculate coralline taxa in Subarctic and Boreal–Subarctic transition zone waters, bi-tetrasporangial conceptacles are far more common than gametangial conceptacles (Adey, 1964, 1965, 1966; Adey and Adey, 1973); in most cases, they are initiated in autumn and produced in winter. As we have shown with population/statistical techniques, conceptacle dimensions are generally a reliable character for separating congeneric species within these regions, and this distinction has been widely accepted in the field over the past century. However, not all species are separated by conceptacle dimensions, and in some cases one has to rely on multivariate analysis for confident species differentiation (Figure 10). Perhaps more importantly, in spite of the high levels of statistical confidence for conceptacle parameters, all the Boreal–Subarctic transition zone *Phymatolithon* species have overlapping dimensions. Although this characteristic had been demonstrated for many genera in some earlier studies (e.g., Adey, 1964, 1965, 1966a; Adey and Adey, 1973), it has been routine in other coralline studies to utilize dimensional ranges for all characters. Rarely will this approach supply confident differentiation of species, especially when comparing species from different biogeographical regions.

The shapes and sizes of *Phymatolithon* bi-tetrasporangial conceptacles are statistically species specific (Table 2; Figure 10). However, there is also considerable overlap in dimensions for some species in all characters (Figure 10); although the measurements of a few conceptacles to distinguish *P. laevigatum* from *P. nantuckensis* would suffice, either numerous measurements or the use of a multi-character display (Adey, 1964) would be required to numerically separate *P. laevigatum* from *P. rugulosum*. On the other hand, the raised rim of the former species, as compared to the inner shelf of the latter, are highly diagnostic characters. The well-sunken conceptacles of the *P. borealis* and *P. investiens* clade, with their distinctive upper rim, is diagnostic, as is the rounded “bowl” shape of the large conceptacles of *P. laevigatum*. The conceptacle of *P. investiens* is smaller than *P. borealis*, and the tiny, sunken conceptacle of *P. rugulosum* bears the equivalent of the raised rim of the *P. borealis* clade; however, it occurs as a quite diagnostic sunken shelf.

In Table 2, for each species for which we have large data sets, we have given CV values for each conceptacle dimension. Most parameters have characteristically low CV values (0.19%–0.26%), but the height (or depth) of the pore plate, above or below the vegetative surface, has a large CV (0.44%–0.74%). [Note: we have not shown conceptacle roof values in the table to reduce complexity, but roof CV values for all species are also low (0.19%–0.24%)]. As has been demonstrated for many *Phymatolithon* species, the diameter of the conceptacle pore plate is species specific, and is essentially the same diameter as the primordial disc. Also, the conceptacle cavity diameter, although larger, is directly and significantly a function of pore plate diameter (Adey, 1964), as shown in Figure 11 for *P. laevigatum*. However,

the remaining conceptacle vertical characters (conceptacle cavity height, roof thickness, and conceptacle elevation) are independent of the horizontal characters. The horizontal character dimensions are determined by primordial disc diameter, whereas the vertical dimensions are controlled primarily by rate of development of conceptacle maturation relative to the growth of the vegetative surface. The remaining species have very similar plots for all parameters and are not presented.

Pore plate diameter and cavity diameter of the bi-tetrasporangial conceptacles are tightly linked (as derived from the primordial disc; Figure 11; Table 2) and are clearly genetically controlled. Conceptacle cavity height and roof thickness are independent variables; as they have low variability (Table 2), it is likely that they are separately genetically controlled, probably as sporangium dimensions. On the other hand, conceptacle elevation is independent of the lateral conceptacle dimensions (pore plate/cavity diameter) and has a high level of variability that relates not only to the rate of sporangial development but also to the rate of growth of the surrounding vegetative perithallium. After sporangial mother cells have fully formed, vertical elongation of sporangia, including their thick cap wall with the surrounding structural filaments of the roof, ceases. The sporangia now induce a dissolution of surrounding, and to a lesser extent underlying, cellular carbonate; their division and expansion crushing the cells, now without their carbonate walls. Although we have insufficient data to securely link the depth of the primordial disc to mature roof height (depth), casual observation suggests that such a link is only partly responsible for mature conceptacle elevation; perithallial growth during conceptacle development and maturation is a key factor (Adey et al., 2013). As we noted previously in our treatment of perithallium, conceptacle nurse and roof tissues form part of the diversity of tissues in these crusts.

This link of surrounding perithallial growth to conceptacle development and height was shown diagrammatically for *Clathromorphum compactum* by Adey et al. (2013). In *P. rugulosum* and *P. laevigatum*, for which we have abundant primordial disc data, approximately half the ultimate conceptacle cavity height is accommodated by upward perithallial growth and half by the crushing of perithallial cells beneath the sporangia (Plates 2, 3, 5) However, these are moderately thin crusts, with minimum upward growth, so the 5–10 μm increase in crust thickness during the 6 months while the conceptacles are developing is considerably less than the approximately 100 μm produced by the Subarctic *Clathromorphum* crust during 9 months of development. In the thin crust species, *P. squamulosum* and *P. nantuckensis*, conceptacles become raised at maturity, which derives from two factors: the depths of formation of the conceptacle primordia are less than those in all the thicker species (generally 4–8 cells as compared to 15–25 cells below the surface); in addition, upward growth of the surface of these crusts is considerably less than crusts of the generally thicker species. Bi-tetrasporangial conceptacle elevation relative to the crust surface results only in

part from internal conceptacle development; it derives also from the relative growth of the surrounding perithallus (Adey et al., 2013). The key element relevant to taxonomic characters is that the depth of conceptacle primordial formation is genetically controlled. The height of mature conceptacles, however, is far more complex, controlled in part by perithallial growth, in part by different genes, and in part by environmental conditions.

In the thick hypothallial species, *P. borealis* (Figure 10B), conceptacles are sunken at maturity; although the pore plates are somewhat deeper than in *P. rugulosum* and *P. laevigatum* (see Table 2), the mature conceptacle cavity floors are considerably deeper than in the former species (Table 2). The rapid growth in *P. borealis* of surrounding perithallial tissue relative to conceptacle development is also reflected in the high percentage of conceptacle cavities deeply embedded in the crust. *P. borealis* bi-tetrasporangial conceptacles are intermediate in conceptacle cavity diameter compared to *P. rugulosum* and *P. laevigatum*. Although *P. investiens* conceptacles appear dimensionally close to those of its sister species, *P. borealis*, with the conceptacle cavity appearing somewhat smaller, with only six conceptacles observed from one plant of *P. investiens* the correct relationship remains somewhat uncertain. In agreement with the figures shown in Irvine and Chamberlain (1994), and dissimilar to *Lep-tophytum leave*, all these species lack distinctive pore cells in the bi-tetrasporangial conceptacle roofs.

Among *Clathromorphum* species in the western Atlantic Subarctic, conceptacle shape and placement are indistinguishable, but patterns of degeneration and breakout, or lack thereof, are sometimes highly distinctive (Adey, 1964; Adey et al., 2013). *Clathromorphum circumscriptum* occupies the high-energy and extremely disruptive intertidal tide pools and shallow subtidal zones. Spore release occurs each spring with the breakout of fields of conceptacles, with the resulting loss of considerable crust; sometimes this process extends far below the intercalary meristem, and crusts die in the process. However, this species occupies an unstable environment where new, unoccupied substrate is often available and long-term space competition has minimum value. The massive and certain release of all produced spores provides the greatest opportunity to settle the abundant rock surface newly available each year. In deeper water, its sister species *C. compactum* maintains its conceptacles year after year, the conceptacles being buried, and often spores remain and are lost to reproductive potential. There is rarely a die-off, and the individual plants continuously occupy rock space for extended periods (typically to hundreds of years, but known to 1900 years; Adey et al., 2015a). *Clathromorphum compactum* occurs in a more stable environment, where competition for space by a host of encrusting invertebrates is extreme; once cover is established, it is more important to maintain that cover than to provide new spores, most of which will find few opportunities to settle. Nevertheless, as Adey (1965) demonstrated, when new artificial substrate is placed in the *C. compactum* environment in midwinter when grazers are largely inactive, rapid settlement occurs and

the sporelings are rarely grazed. *Phymatolithon borealis*, alone among the *Phymatolithon* species treated herein, reliably buries its conceptacles in the perithallia. This structure allows differentiation with its close relative *P. investiens*, but equally important, because it is characteristic of broad bedrock surfaces where space competition is extensive, as in the *Clathromorphum* species cited above, it indicates the importance of long occupation of these surfaces once successful attachment is achieved. This *Clathromorphum* example, along with our previous discussion for *Phymatolithon* spp., also shows that many reproductive adaptive factors are in play in addition to conceptacle size and shape.

The shape and elevation of *Phymatolithon* conceptacles relative to the crust surface demonstrates considerable niche specialization. Species in harsher environments (the non-tide-pool intertidal environment for *P. squamulosum* and unstable substrate for *P. nantuckensis* and *P. investiens*), where invertebrate grazers are at a disadvantage, have elevated conceptacles (only female/carposporangial conceptacles for *P. investiens*). Here, the production of excess crust with carbonate structure requires energy and time, produces excess weight, and is a disadvantage from burial in pebbles or finer sediment or drying or freezing on a long tidal cycle at an inopportune time. Species with tightly adherent, relatively thick crusts, in more stable environments, where grazers (limpets, chitons, and sea urchins) have an advantage, produce deeply sunken conceptacles.

Gametangial Conceptacles

These conceptacles are less reliable as species indicators, probably in large part because they are far more rare. Presently, we do not have enough information to pursue how gametangial conceptacles relate to strategies for survival. The available data are presented in Tables 3 and 4, primarily to indicate genetic affinities in support of DNA sequence data. In *Phymatolithon* gametangial conceptacles, where the roof is produced by a hypothallium-like overgrowth (rather than the nonreproductive ephemeral filaments between the developing carpogonia or the highly productive spermatial filaments), the link between conceptacle primordial depth and mature conceptacle height is reduced. In *P. investiens*, *P. squamulosum*, and *P. nantuckensis*, in which perithallial growth is more limited, the result is elevated sexual conceptacles, even though the original primordia were sunken in the perithallium. Simple use of the terms raised or sunken conceptacles is likely inadequate in most cases as a taxonomic character, with greater biological understanding being needed for accurate utilization.

ECOLOGY

In this section we bring together our ecological analyses for *Phymatolithon* species across the entire North Atlantic Boreal–Subarctic transition zone; we also offer testable hypotheses for the environmentally controlling factors.

Across the Boreal–Subarctic transition zone, the six *Phymatolithon* species occur largely in different environmental niches. Leaving aside the localized *P. nantuckensis* (which is monotypic at its type locality), the remaining species have overlapping distributions, but intraspecific competition is clearly limited to those in overlapping habitats. It is difficult to identify a morphological characteristic that affords near-total dominance to *P. laevigatum* in warmer, polyhaline, brackish waters; indeed, it may be entirely physiological. On the other hand, the highly imbricate structure of *P. squamulosum* allows water retention, and in its intertidal habitat it is typically the only coralline present. Also, the presence of overlying rockweed or a porous rock surface allows the plant to become highly abundant locally. Neither *P. borealis* nor *P. investiens* has crossed to the western North Atlantic, most likely because of low winter temperatures (neither species has a significant presence in the inner Norwegian fjords, which often freeze over in winter (Adey, 1971; Adey and Hayek, 2011). This restriction provides a niche for *P. rugulosum*, which although not competitive with Subarctic species further north in Labrador, becomes a dominant in the coastal Gulf of Maine, with its cold winters (0°–2°C). In Iceland, where winter water temperature grades strongly, from cold (near 0°C) in the north and east to quite warm (6°C) on the southern coast, *P. rugulosum* becomes abundant in the transition zone of the west coast. It occurs only at scattered localities on the Norwegian outer coast. It seems likely that a finer meshwork of stations along central Norwegian fjords would show that it is most abundant in mid-fjord regions, with *P. borealis* replacing it seaward and *Clathromorphum circumscriptum* replacing it landward.

BIOGEOGRAPHY

The North Atlantic marine biota, including seaweeds and corallines, was biogeographically derived from two very different source regions following the opening of the North Pacific Bering Strait in the late Pliocene. The Arctic and Subarctic coralline flora is primarily North Pacific (especially the Okhotsk to Bering Sea regions) in origin, whereas the Atlantic Boreal, Lusitanian, and Mediterranean coralline floras are primarily Tethyan (pre-Mediterranean) in origin (Adey and Steneck, 2001; Adey and Hayek, 2005, 2011; Adey et al., 2013). Even considering the north–south movement of biota during Pleistocene climate fluctuations, warm-water (tropical western Atlantic/Caribbean and Carolinean) corallines were not able to cross the long sandy and muddy coast that is continuous from roughly Cape Hatteras to Long Island in the western North Atlantic. The shallow waters of the eastern North American coast south to Florida further inhibited the development of a significant hard bottom coralline flora, further preventing the entry of warm-water corallines from the tropical and subtropical western North Atlantic into the Boreal coralline flora of New England. Thus, Boreal corallines from the eastern North Atlantic, mostly in shallower water, mix with Subarctic corallines from Rhode Island to the southern

Gulf of St. Lawrence. *Phymatolithon laevigatum* on highly scattered patches of hard bottom reaches to the northern New Jersey coast. From Newfoundland north, Subarctic and Arctic species form the coralline flora.

In the eastern North Atlantic, *Phymatolithon* species dominate the cold-water Boreal coralline flora because of the influence of the Gulf Stream (and continuing Norwegian and Irminger Currents). The Subarctic coralline flora only reaches northern and eastern Iceland and the more northern inner fjords of Norway, where the continental influence provides cold winters and ice-bound waters (Adey, 1968, 1971; Adey and Adey, 1973). Further south on the warmer western European coasts, several additional *Phymatolithon* species, along with many *Lithophyllum* species, dominate the warmer Boreal and Lusitanian floras (Irvine and Chamberlain, 1994). However, to the north and northeast, the Boreal boundary rather sharply, but complexly, interdigitates with the Subarctic coralline flora dominated by *Lithothamnion*, *Clathromorphum*, and *Leptophyllum* species. As we discussed earlier, in the cold-water Boreal, *Phymatolithon* species are largely ecologically and biogeographically partitioned so that there is little interspecific competition.

Phymatolithon laevigatum occurs across the entire region, although it is rare in Iceland; it occurs abundantly primarily in warmer waters, where temperatures reach more than 15°C in summer, and especially in waters of lower salinity (to 15 ppt). It is highly abundant in the warmer, lower-saline waters of the southern Norwegian coast and in the Skagerrak, and the holotype derives from Helgoland. It would be particularly interesting to examine the genetics of *P. laevigatum* populations from the eastern and western North Atlantic, to determine when the cross-ocean transit took place, as has been done with the rockweed *Fucus serratus* (Johnson et al., 2012). *Phymatolithon rugulosum* occurs in deeper and colder full coastal salinity waters where summer temperatures generally do not exceed 15°C; it is abundant only in southwestern Iceland and the central western North Atlantic.

Phymatolithon borealis occurs abundantly on hard rock substrate in southern Iceland and the North Sea outer coast of southwestern Norway, where winter temperatures do not drop below about 3°C; it is mostly replaced by *P. laevigatum* when entering southern and Skagerrak waters where salinities are lower and winter temperatures, especially in fjords and other inshore waters, can drop below 0°C. Its sister species, *P. investiens*, is primarily an outer coast northern Norwegian species, where in spite of the high latitude, winter temperatures are above 3°C. *Phymatolithon investiens*, with its expansive leafy habit, often occurs as an epizoic on calcified invertebrates and epiphytically on other corallines; it occupies mostly looser substrate, sometimes occurring in rhodolith beds, which, because of the change in topography and shallower inter-fjord and sound waters, are more abundant in northern Norway. The two species overlap on the outer central Norwegian coast, primarily between Bodø and Tromsø.

Calcification

Currently, we do not have a definitive understanding of the biophysical and chemical process of calcification in corallines. However, we do have a considerable amount of structural and physiological information that provides boundaries to the process. In the following, we assume that all corallines, and certainly those of the colder Boreal–Subarctic regions, have the same basic calcification process. Because many tropical genera of crustose corallines (Mastophoroideae and Lithophylloideae included) have meristem/growth patterns similar to that of *Lithothamnion* (Adey, 2005, 2015b; Nash and Adey, 2017a,b), it is likely that the patterns we describe are universal. Most critically, we know, from experimental and field studies (Adey et al., 2013), that *Clathromorphum* does not require light to calcify, although ultimately stored energy from photosynthesis is required. Also, there are non-photosynthetic coralline parasites, such as *Kvaleya* in the North Atlantic and Arctic (Adey and Sperapani, 1971; also Ezo on *Lithophyllum*; Adey et al., 1974) that show the same basic calcified wall structure as free-living corallines; in these cases the calcified walls are developed using photosynthate derived from their hosts (Nash and Adey, 2017a). Thus, calcification is almost certainly metabolically driven (Adey, 1998) rather than supported by pH elevation during photosynthesis.

All crustose corallines (ranging from Arctic to tropical) that we have examined with high-magnification SEM (5,000–100,000 \times), have two distinct types of cell wall calcification: inner wall (IW) and interfilament (IF) (Plates 9–11). IW calcification occurs broadly across the Corallinophycidae as short, narrow, radial crystals (approximately 0.1 μm in section; Plates 9B–D; 10A,B; 11B,C). At magnifications exceeding 10,000 \times , these crystals can be seen to be multi-lobed and 0.5–1.0 μm long, oriented more or less perpendicular to the cell lumen (Plate 9B–E). In contrast to *Clathromorphum*, in which all perithallial (and epithallial) calcification occurs in a very narrow band roughly in the middle of meristem cells (the meristem split; Adey, 1965; Adey et al., 2015b), *Phymatolithon* calcification is diffuse along the side walls of both the meristem cell and perithallial cells 2–4, where elongation occurs. IF calcification can be highly developed (as in *Clathromorphum*; Adey et al., 2013, 2015b), but in most progressive growth corallines (particularly all *Phymatolithon* spp.) the IF calcite consists of a few layers of more or less tabular crystals that are approximately 0.1 μm square and 0.5–1.0 μm long; typically, they are randomly oriented, but generally lying parallel to the cell lumen wall (Plates 9B,C,E; 10A–F; 11B–F). As differential elongation occurs in cells on both sides of the IF, we call these surfaces glide planes; in most progressive growth species, these glide planes can strikingly present visually in vertical fractures as extensive vertical surfaces the width of the cells. Of the species we treat in this paper, *P. rugulosum* has an unusually well-developed IF (Plate 11), and for the species treated in this paper this species also appears in a separate subclade (Figure 1).

Corallines routinely both calcify and de-calcify metabolically in the same plant, at the same time, but probably not in the same cell (or perhaps even the same cell grouping). Both processes occur in the vegetative perithallium and hypothallium and in reproductive tissues (conceptacles). The dissolution of usually narrow channels in walls between perithallial cells of adjacent filaments (typically referred to as fusions) is well known in *Phymatolithon*. The term fusion, although a misnomer as applied to the process in corallines (the fusion channels are typically quite narrow, more like tunnels), is nevertheless a widely applied shorthand term that we continue to use. These fusions develop progressively with depth in the perithallium, but mostly after cell elongation ceases (Figure 8B; Adey, 1964, 1966a). On average, roughly 75% of fusion cell formation occurs shortly after cell elongation (with IW calcification) stops (Figure 8).

In the strongly attached crusts of *P. rugulosum* and *P. laevigatum*, the cell lumina expand in diameter with depth. Because in most cases such expansion must be accompanied by removal of carbonate cell wall, we are currently exploring whether the carbonate metabolites are transferred to the actively growing surface. However, it is conspicuous that the two species with thick hypothallia (*P. borealis* and *P. investiens*), and in the latter case a larger-scale leafy habit, develop significantly smaller cell lumina with depth. As this development must result from thickening of carbonate cell walls, perhaps with a stronger development of IF, this would enhance crust strength to allow the cantilevered growth achieved by these plants. Such changes in density, tied to the production of interfilament carbonate, have been demonstrated for *Clathromorphum compactum* (Chan et al., 2017), and it would be valuable to perform such studies in the species presented here.

In general, growth and calcification in cold-water corallines is dependent on temperature and light (Adey, 1970c; Adey and McKibbin, 1970; Williams et al., unpublished). However, each species, and to some extent each genus, has its own patterns of dependency. There are coralline species that grow, calcify, and reproduce with seawater temperatures never exceeding 3°C and with a half year of no sunlight. Other species, with the same basic wall structure, but a somewhat different carbonate chemistry, never see seawater temperatures below 20°C, and probably reach 40°C and succeed with exposure to full tropical sunlight, although likely always wetted by wave-breaking spray.

Magnesium Content

As we have shown, in the perithallium of the *Phymatolithon* species (Nash and Adey, 2017b), IF calcite has the lowest Mg (8.9%), whereas the cell walls have significantly higher Mg (13.4%); the carbonate of hypothallial cells has even higher Mg content (17.1%). The cell walls in the tissues that regrew from broken-out conceptacles as wound tissue also had high Mg content (18.6%), not significantly different from hypothallial cells. As wound tissue has cells that are morphologically similar in size

and cell wall structure to hypothallial cells, and clearly result from growth that is more rapid than the surrounding perithallium, with equivalently higher Mg content, it is suggestive that Mg content in specific cells and tissues is related to growth rate. Nevertheless, within specific tissues Mg content is clearly dependent upon temperature (Nash and Adey, 2017a,b).

Finally, especially in hypothallial cells of tropical coralline crusts, very high magnesium content can occur, exceeding 40%; in this context we note that the level of a shift from high magnesium calcite to the crystal dolomite has been described (Nash et al., 2012). Although this may not generally be applicable to cold-water corallines, dolomite has been described in a *Clathromorphum* crust from Greenland (Nash and Adey, 2017b). These Mg variations are in agreement with the Mg offsets obtained for the cell wall, IF, and hypothallial cells in *Leptophytum laeve* and *Kvaleya epilaeve* from Arctic Labrador (Nash and Adey, 2017a). The elevated Mg in perithallial cell walls compared to IF (called interstitial) has also been noted for *Lithothamnion glaciale* (Ragazzola et al., 2016). Climate archiving, using Mg concentration (and other wall chemistry) as a proxy for seawater temperature (and other variables) at the time of wall formation has become an important tool in paleoclimatology (e.g., Halfar et al., 2013). Greater precision can likely be achieved in coralline climate archiving by considering these tissue and cellular variations in Mg content. Most *Phymatolithon* species have too little vertical growth to be climate archives, although yearly layers are often seen in *P. borealis*, and this species could have limited use in paleoclimatology.

CONCLUSIONS

As we describe in the Introduction, many nineteenth and twentieth century coralline identifications by a wide range of phycologists, based on classical coralline systematic studies, have often not been confirmed in the DNA sequence analyses of the past decade. Here, however, we have demonstrated a very

high degree of conformity between sequence analyses and morphological and reproductive analyses when large geographically extensive collections and population-level analyses, supported by statistical treatments, are utilized.

In the classical literature, coralline crusts were presented as composed of two tissues, perithallium and hypothallium, with little recognition of the underlying carbonate wall structure. However, as we briefly review in the Introduction, recent literature has tended to describe corallines as a cushion of independent calcified filaments, lacking tissue level or carbonate wall differentiation. Here we have shown a high diversity in both tissue type and high magnesium carbonate wall structure. Similarly, in the past, conceptacles (the reproductive structures) have been treated as entities largely independent of vegetative construction. Here, analyses of conceptacle development in *Phymatolithon* have demonstrated the linkage between genetic control and vegetative growth, parameters that interact to produce considerable variation in some characters of final gross morphology but not in others.

As demonstrated in an earlier publication on the unrelated Arctic and Subarctic genus *Clathromorphum* (Adey et al., 2013), we have also shown in species of *Phymatolithon* a dynamism in the development of vegetative anatomy, carbonate structure, and reproductive features, with a complex of tissues and interacting modes of formation. This depiction belies a simplistic model for this geographically and ecologically important subclass (Floridiophyceae) of red algae. With this study, augmenting earlier analyses that included the other dominant genera (*Clathromorphum*, *Lithothamnion*, *Leptophytum*), the colder waters of the North Atlantic (biogeographical regions Arctic, Subarctic, and Boreal) provide the only geographically extensive coralline flora to be fully analyzed for linkage between morphology, physiology, ecology, and biogeography supported by DNA sequence analyses. Similar analyses of *Lithophyllum* (*Pseudolithophyllum*) *orbiculatum*, an additional important species of the Boreal fringe, are presently being undertaken by two of the current authors (WHA, PWG).

Plates

NOTES FOR SPECIMEN DESIGNATIONS IN PLATES

Specimen designations may include the following data: type of specimen, sample number, DNA analysis sample number, herbarium abbreviation, official specimen number, and origin of specimen. See Adey and Lebednik (1967) for details on origin data. Examples defined as follows:

Foslie Isotype, no. 234	Sample extracted from Holotype, numbered and deposited in Foslie Collection of Coralline Collection, Herbarium US
DNA S186	DNA extracted from this sample and numbered for analysis
US 171025	Official specimen number, Herbarium US (U.S. National Herbarium)
61-14; 61-43	Specimen numbers in Coralline Collection, Herbarium US (see Table 1 for details).

Plates 1–8 are by W. H. Adey; plates 9–11 are by M. C. Nash. The SEM images showing sections in plates 1–8 are of vertical fractures made with a razor blade or fine wire cutters; sections were then mounted and coated with carbon. The procedures for plates 9–11 are described in “Materials and Methods.”

PLATE 1. (*Opposite page*) *Phymatolithon laevigatum*: scanning electron microscopy (SEM) images.

A. Hypothallium (mid image) and lower perithallium (above); plant tightly attached to granite (crystals below hypothallium). Interfilament “stripe” (arrows in transition zone in lower perithallium). Foslie Isotype, no. 234; DNA S186; US 171025; Helgoland, Germany.

B. Perithallium with wound tissue (right) in broken-out conceptacle. Much of the vertical fracture in this specimen occurs along the perithallium interfilament and presents as numerous vertical stripes. The wound tissue typically consists of large, thin-walled cells, superficially similar to hypothallium and possessing high Mg content, as does the hypothallium. 64-14; Pictou, Nova Scotia, Canada.

C. Surface view of epithallium. Roofs of most epithallial cells have sloughed; lateral walls remain, with scattered epithallial cell roof fragments (arrows). 61-43; DNA S179; US 171009; Woods Hole, Massachusetts, USA.

D. Vertical fracture with perithallial cell walls (mostly inner wall, IW) having many fusions. Arrows indicate fusions perpendicular to the plane of the fracture. Above the leftmost fusion, IW has reformed and is perpendicular to the fusion axis. Numbering and locality as in A.

E. Surface view of crust with several of the bowl-shaped bi-tetrasporangial conceptacles diagnostic for this species; each conceptacle has a strongly raised rim. Numbering and locality as in A.

F. Mature bi-tetrasporangial conceptacle in section, showing bowl shape of both cavity and roof, as well as the raised rim. Numbering and locality as in A.

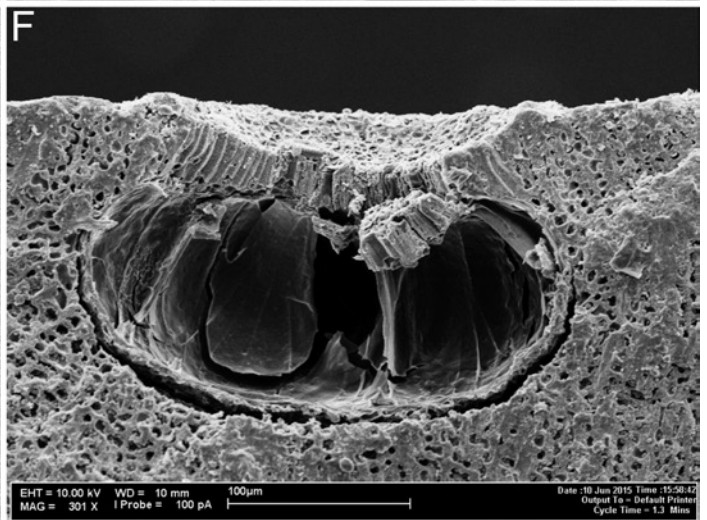
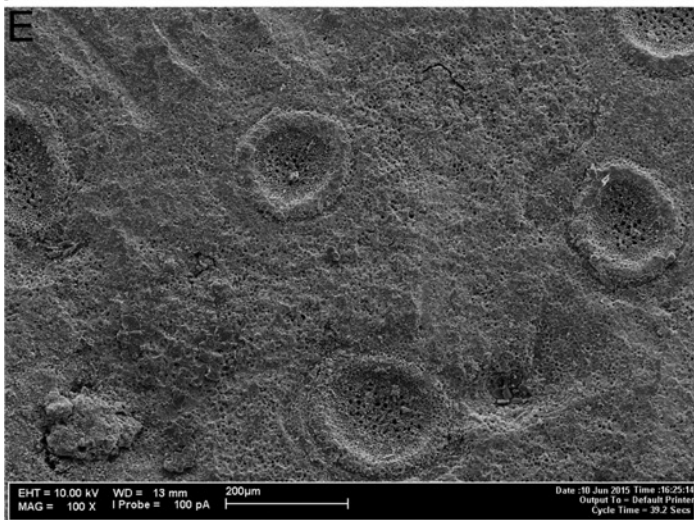
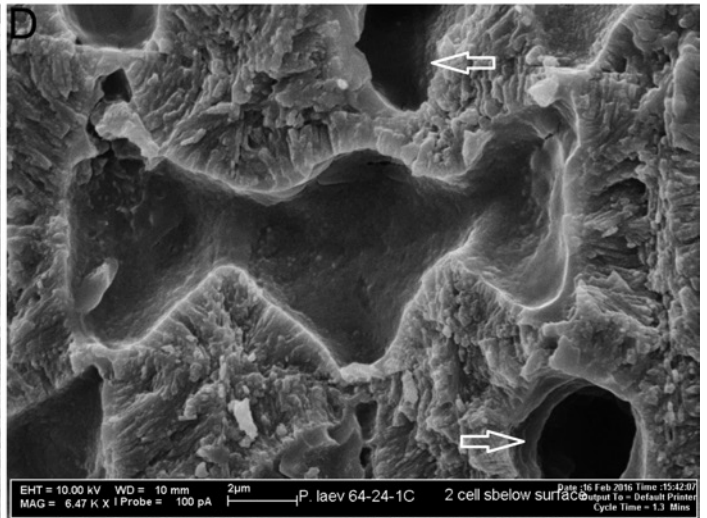
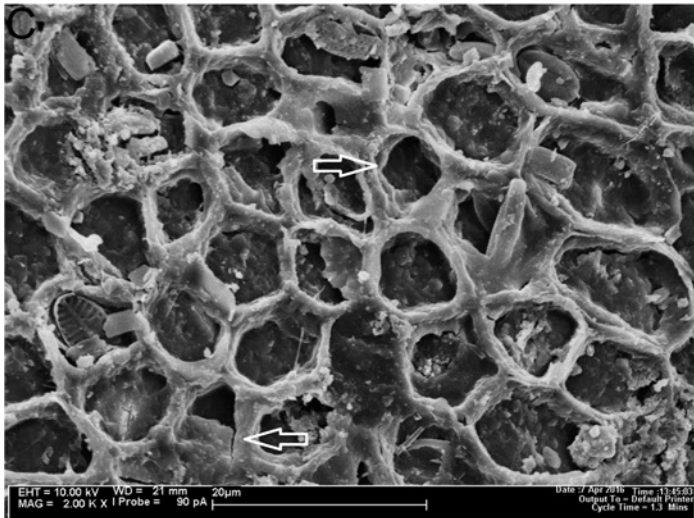
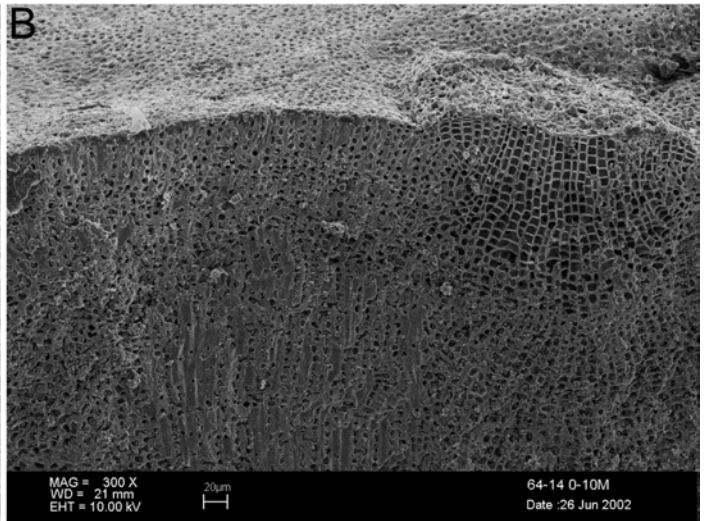
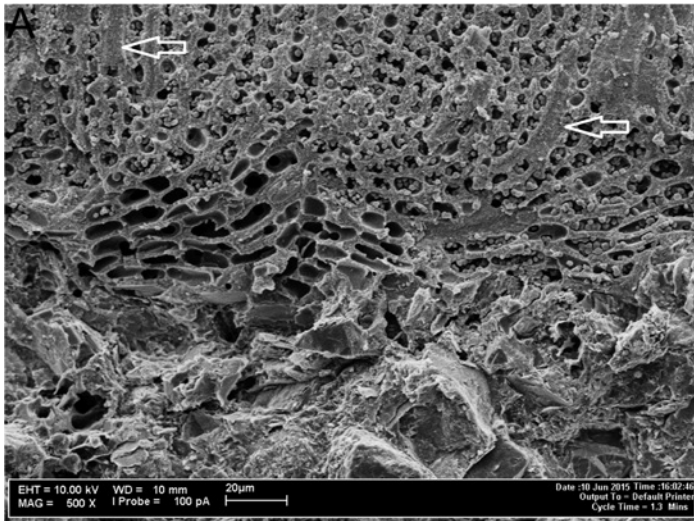


PLATE 2. (*Opposite page*) *Phymatolithon rugulosum*: SEM images.

A. Perithallium with vertical fractures both axially, along filaments, and along interfilament (IF) carbonate band, creating “stripes.” Holotype; 61-41A-3; DNA S163; US 171023; Maine, USA.

B. Surface view at conceptacle margin with pores from broken-out sporangial plugs (right arrow) and epithallial cells with partially intact calcified roofs and interfilament ring (left arrow). 61-35; DNA S170; US 171012; Maine, USA.

C. Immature conceptacle with lateral shelf being built by conceptacle wall tissue with the characteristic of “wound” tissue, typical of rapid growth areas in perithallium. The lower part of this tissue will later be crushed by sporangial lateral expansion (see E). Numbering and locale as in B.

D. Abundant mature, sunken bi-tetrasporangial conceptacles with the distinctive partly sunken lateral “shelves” characteristic of this species. Numbering and locale as in A.

E. Mature bi-tetrasporangial conceptacles with lateral crushing by sporangia removing lower shelf wound tissue as well as lateral and basal vegetative tissue. These crushed cells likely serve as nurse tissue. Numbering and locale as in A.

F. Surface view of conceptacle at higher magnification showing distinctive shelf and sporangial pores. Numbering and locale as in A.

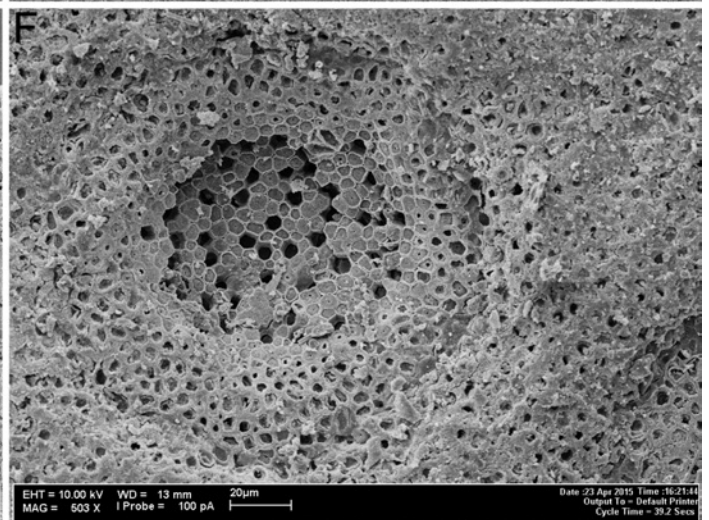
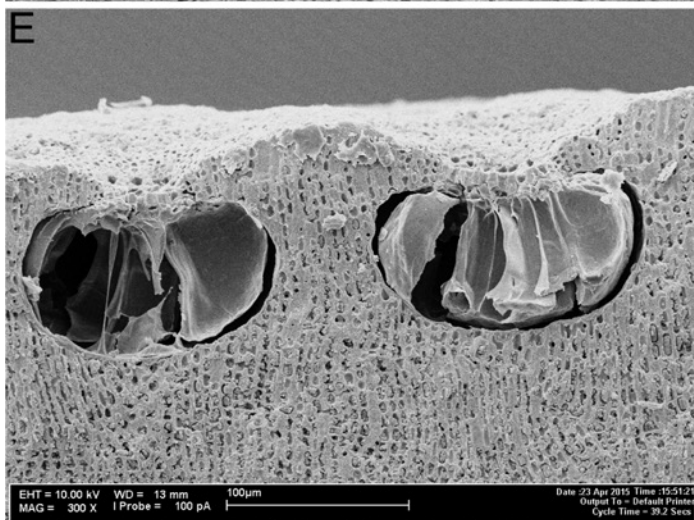
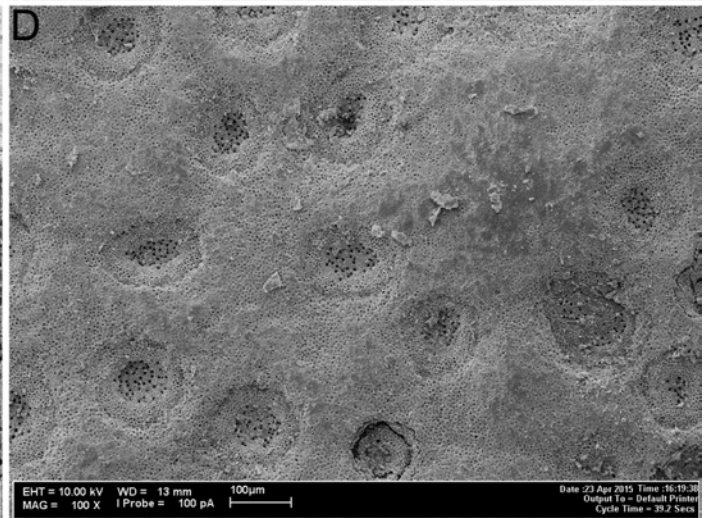
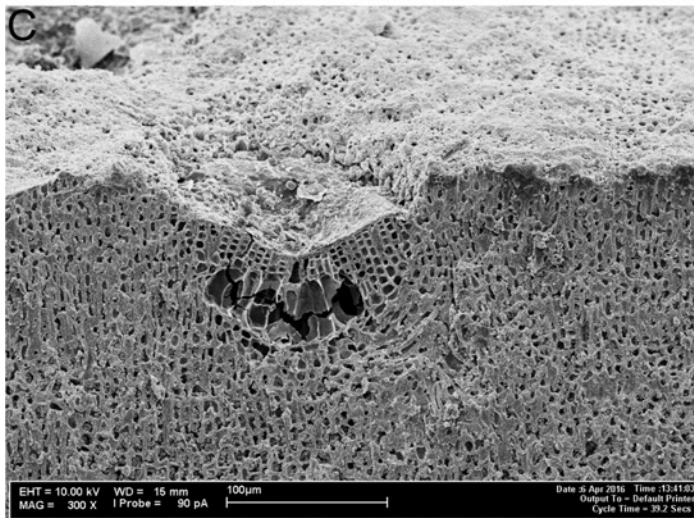
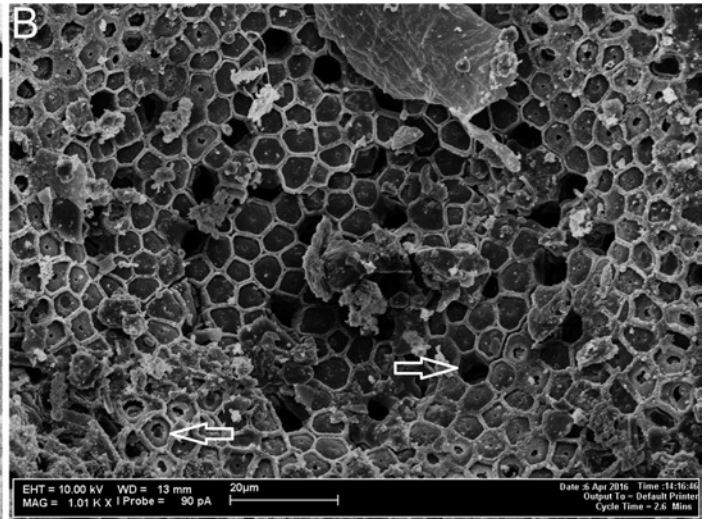
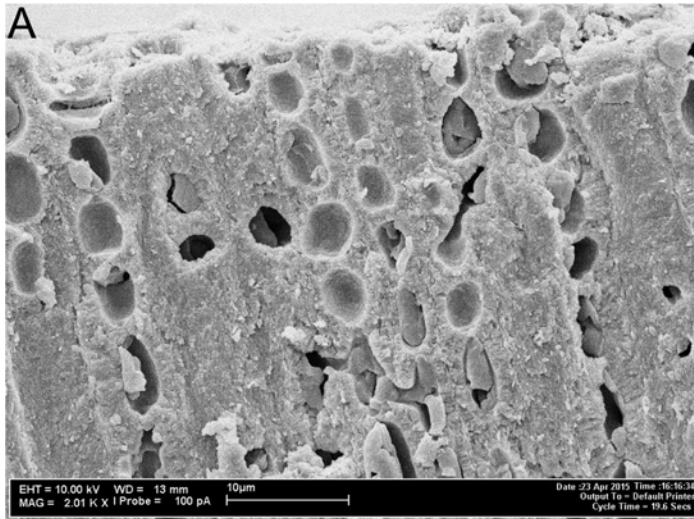


PLATE 3. (*Opposite page*) *Phymatolithon nantuckensis*: stained microtome sections.

A. Young crust with thin hypothallium (bottom arrow), perithallium (middle arrow), and epithallium (top arrow). In contrast to most *Phymatolithon* species, in which epithallial cells are present on less than 30% of filaments, $\frac{3}{4}$ of the measured filaments in this species bore epithallial cells. 61-12; DNA S283; US 171021; Nantucket, Massachusetts, USA.

B. Multiple, thin, overgrowing crusts, partly filling broken-out conceptacles, creating the complex morphology characteristic of this species. Typical lightly raised tetrasporangial conceptacles. Numbering and locale as in A.

C. Mature bi-tetrasporangial conceptacle with tetrasporangia, an undivided sporangium, and sporangial plugs. Numbering and locale as in A.

D. Mature fertilized carpogonial conceptacle. Single carposporangium forming in the center of conceptacle and dendritic fusion cells (below). Numbering and locale as in A.

E. Mature carposporangial conceptacle with carposporangia (horizontal arrow) and single gonimoblast cells (vertical arrow). Numbering and locale as in A.

F. Base of carposporangial conceptacle showing developing carposporangium (horizontal arrow), single gonimoblast cell (right vertical arrow), and fusion cell (left vertical arrow). Numbering and locale as in A.

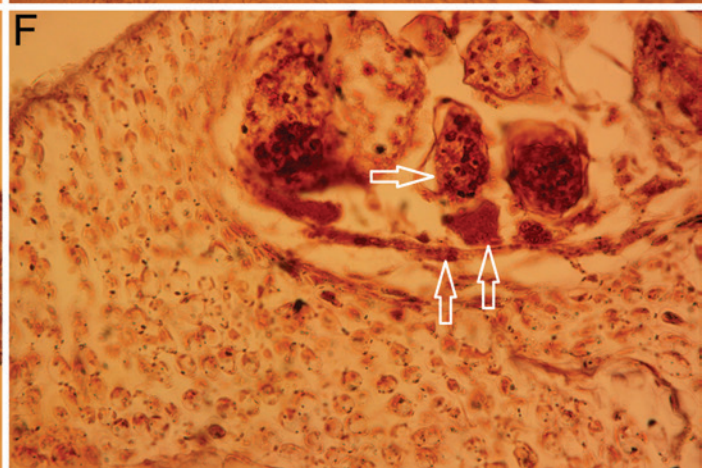
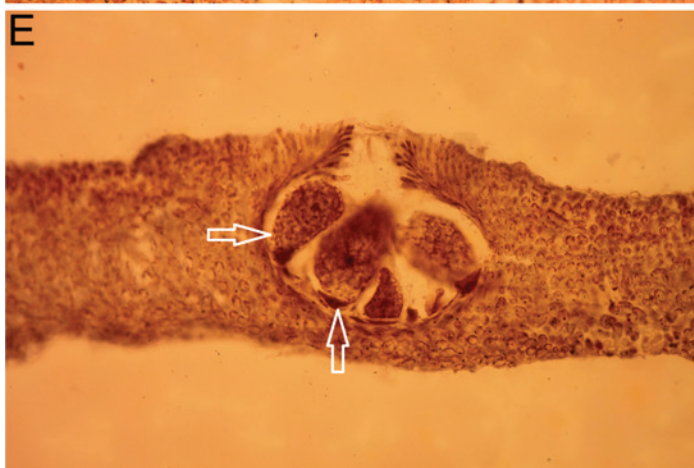
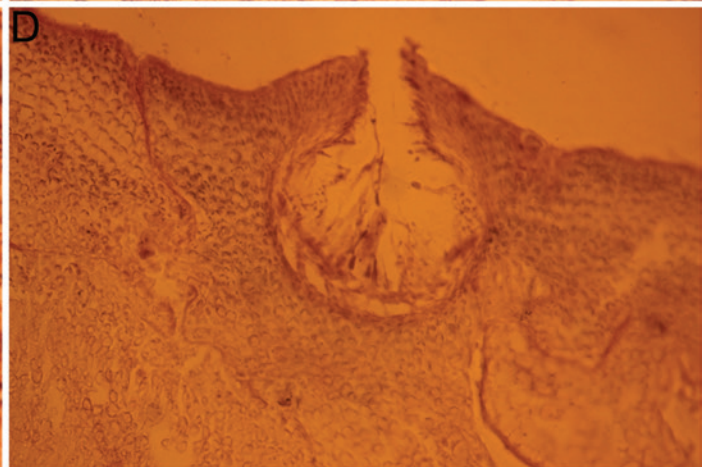
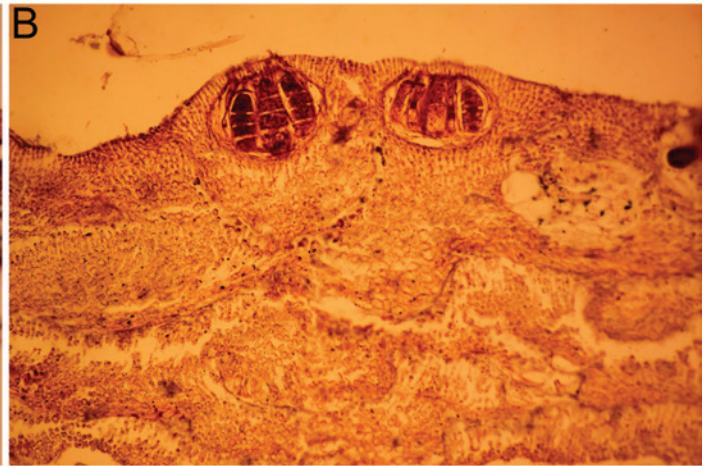
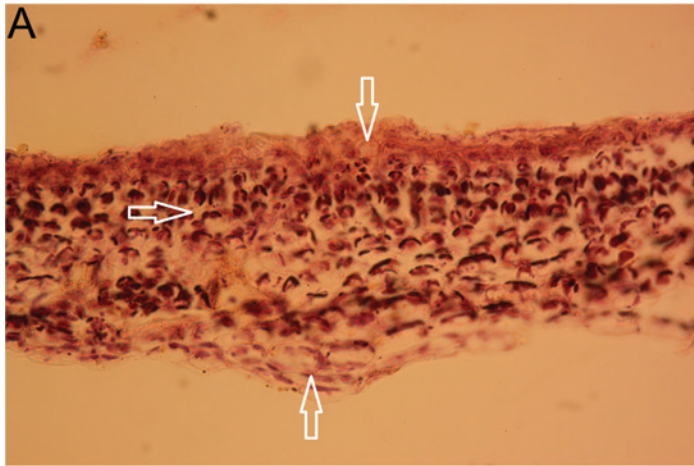


PLATE 4. (*Opposite page*) *Phymatolithon squamulosum*: SEM images.

A. Perithallium and hypothallium in crust growing over fragment of barnacle shell. 67-2, 0-10F, DNA S212. US170995. Trondheimsfjord, Norway.

B. Two *P. squamulosum* crusts meeting. Left: crust developing fast-growing perithallium with large thin-walled cells characteristic of wound tissue, likely precedent to overgrowing crust on right (see Figure 3). 66-14; DNA S227; US171020; Kolgrafafjord, Iceland.

C. Crust overgrowing itself and developing a bi-tetrasporangial conceptacle. Note fast-growing (thin-walled) cells that form conceptacle sides; these fast-growing perithallial tissues resemble hypothallial cells, with their thin walls and high magnesium (Mg) levels, but unlike most hypothallium consist mostly of IW wall (see text and F). Numbering and locale as in B.

D. Typical dense aggregation of raised bi-tetrasporangial conceptacles with detritus collecting between the conceptacles (see E). Numbering and locale as in B.

E. Typical raised flat-topped bi-tetrasporangial conceptacle without a raised rim. Striations are caused by mollusk grazers. Numbering and locale as in A.

F. Mature bi-tetrasporangial conceptacle showing fast-growing, thin-walled cells that form the sides; crushing by developing sporangia initiated. Numbering and locale as in B.

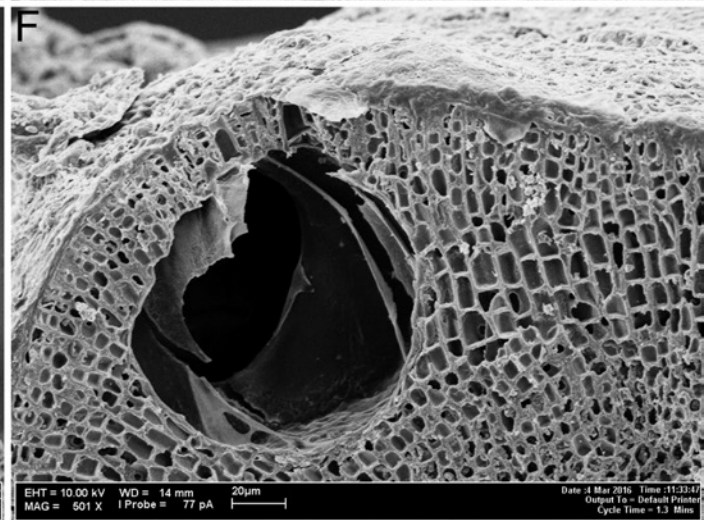
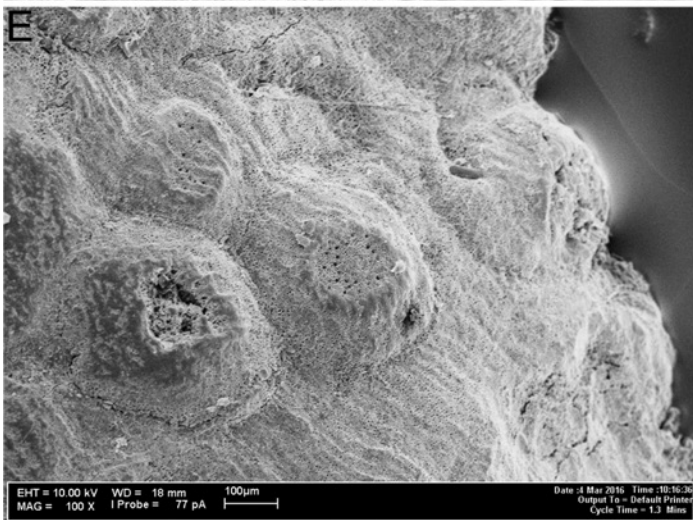
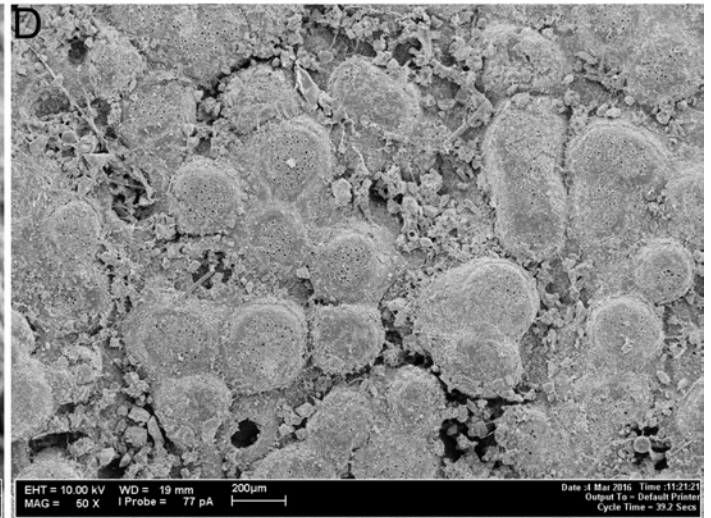
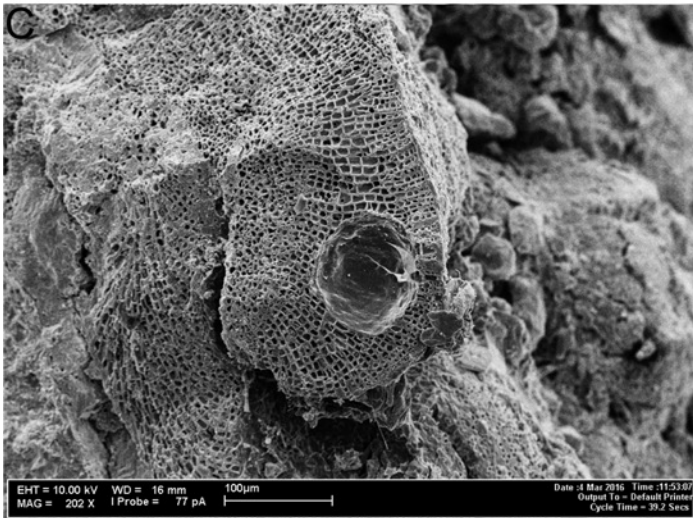
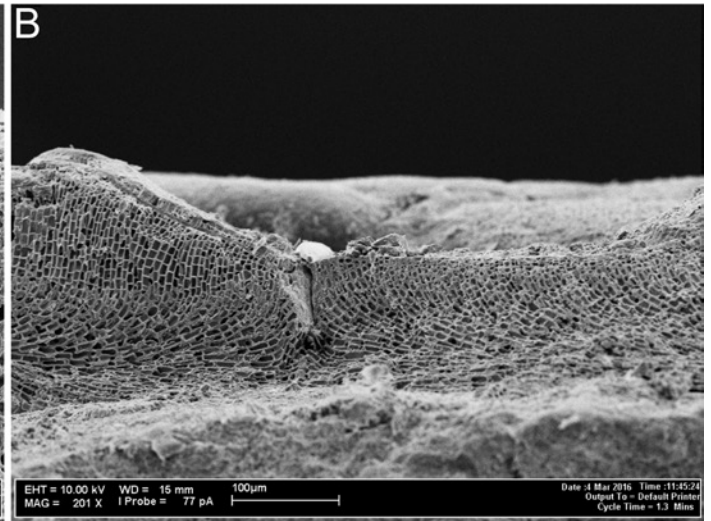
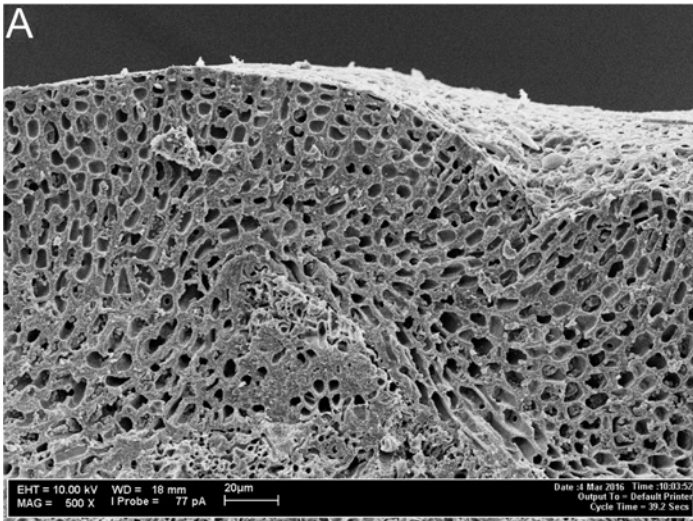


PLATE 5. (*Opposite page*) *Phymatolithon borealis*: stained microtome images.

A. Moderately thick crust, likely several years old (note banding), with single basal hypothallium and without overgrowing hypothallium. 66-43, 0-10C; DNA S223; US 170999; Trondheimsfjord, Norway.

B. Thick crust with several years of buried bi-tetrasporangial conceptacles typical of the species. 66-26-4; DNA S136; US 170980; Grindavik, S. Iceland.

C. Young crust with mature tetrasporic conceptacle. Conceptacle fully sunken with a raised rim. Numbering and locale as in A.

D. Mature male conceptacle. Walls clothed with dense dendroid branches bearing spermatangial mother cells. 66-42-1; DNA S224; US 171000; Trondheimsfjord, Norway.

E. Fully sunken, mature carpogonial conceptacle with numerous trichogynes. Roof formed from lateral in-growing. 67-1; Trondheimsfjord, Norway.

F. Sunken carposporangial conceptacle with one-celled gonimoblasts (small arrows) and carposporangia (large arrows). Left pair rotated by sectioning. 67-1; Trondheimsfjord, Norway.

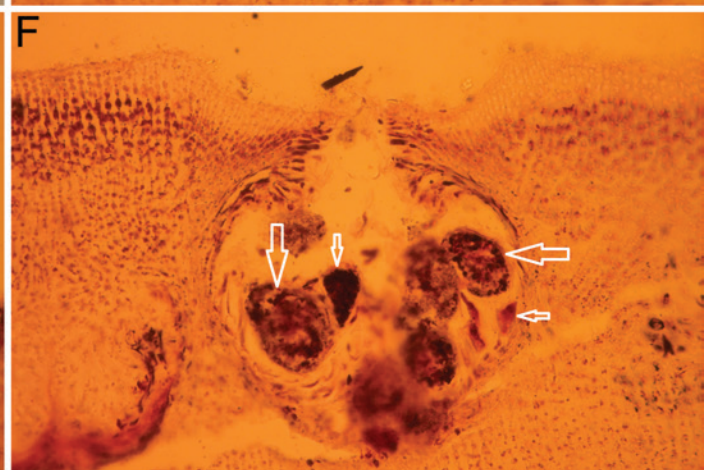
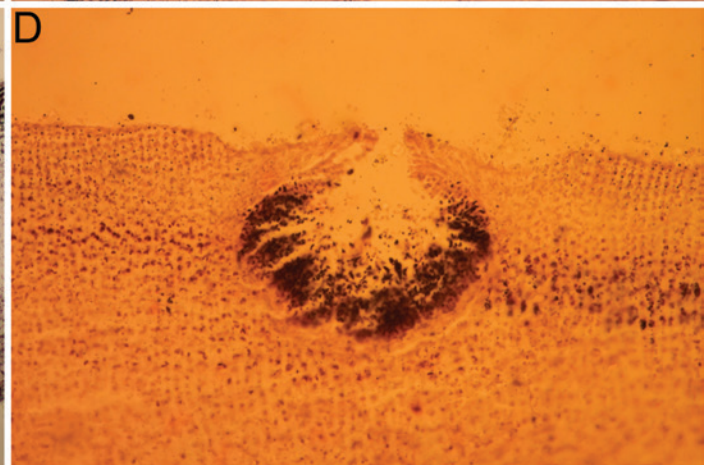
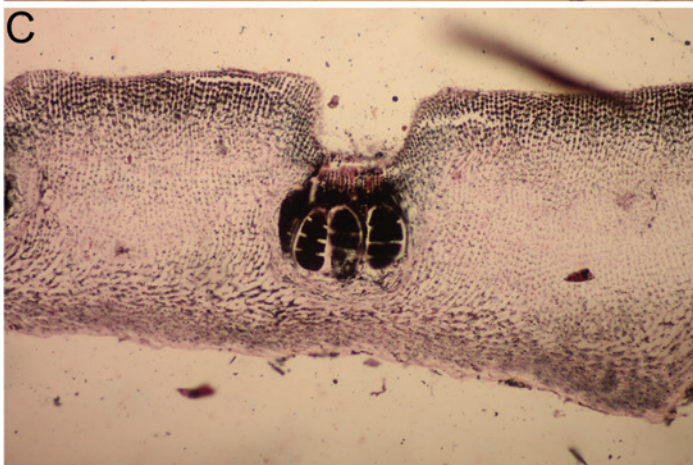
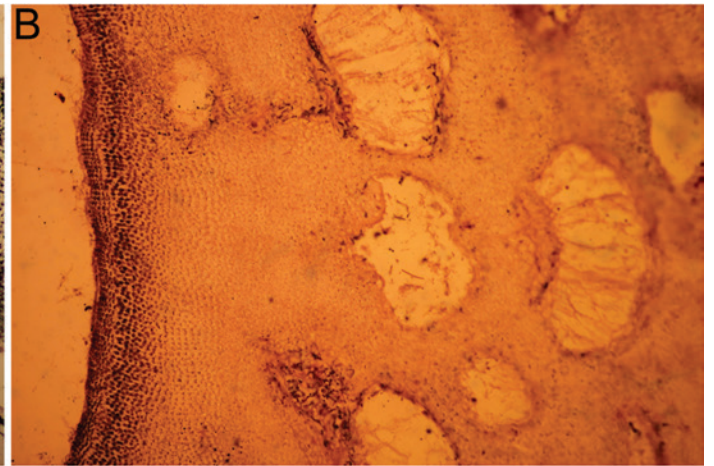
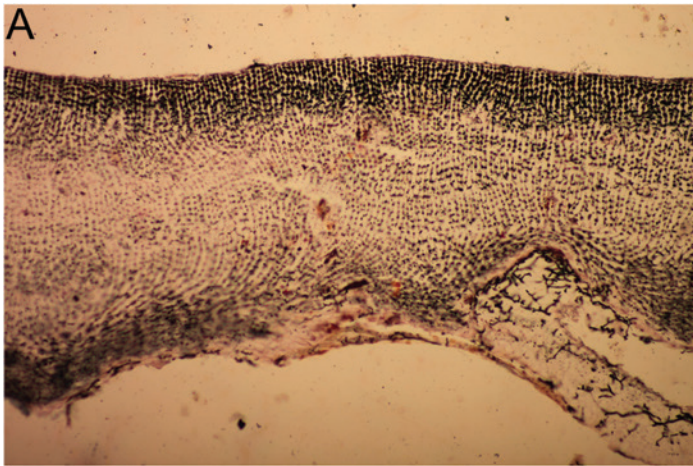


PLATE 6. (*Opposite page*) *Phymatolithon borealis*: SEM images.

A. Two-year-old crust growing over older crust (below). Center conceptacle buried; a year older with overlying wound repair. 66-17-13; 90-120A; DNA S139; US 171018; Kollafjord, W. Iceland.

B. Perithallium with overlying halite crystals (caused by specimen drying from seawater). Meristem (upper right arrow), interfilament, as stripe (mid-right arrow). Fusions (left and bottom right arrows). 66-26-40-10; DNA S136; US 170980; Grindavik, S. Iceland.

C. Surface extension of upper cell walls (IW) and interfilament (IF) around meristem cells (top arrow). Epithallial cell with partial calcite upper wall roof (lower arrow). Numbering and locale as in B.

D. Perithallial cells with 1–2 μm thick calcitic walls (IW) and very thin layer of interfilament (IF) calcite granules between the cells. Abundant fusions. Numbering and locale as in A.

E. Crust with small bi-tetrasporangial conceptacles bearing a slightly raised rim (not an inner shelf); also not bowl shaped (see A). Numbering and locale as in A.

F. Thick crust with layers of buried conceptacle cavities. Conceptacle grown out with wound tissue (mid right). 66-27 0-10K; DNA S116; US 171979; Heimey, Westmanneyjar, S. Iceland.

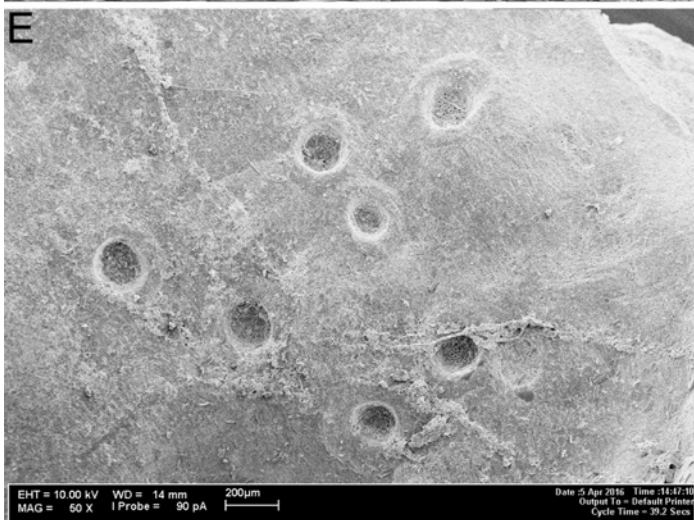
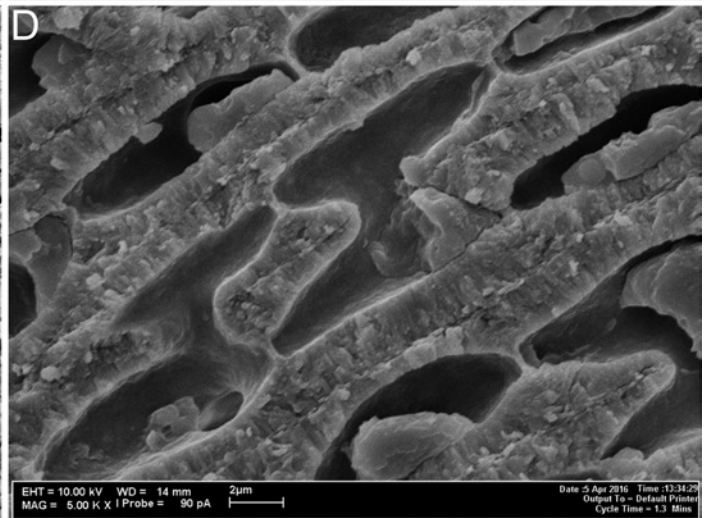
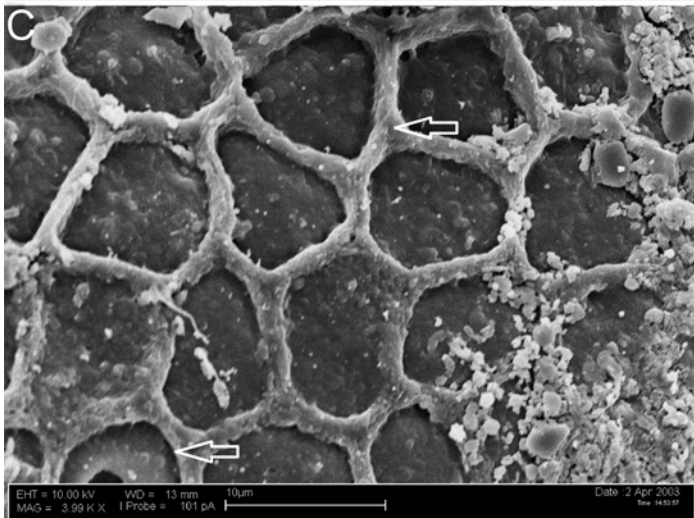
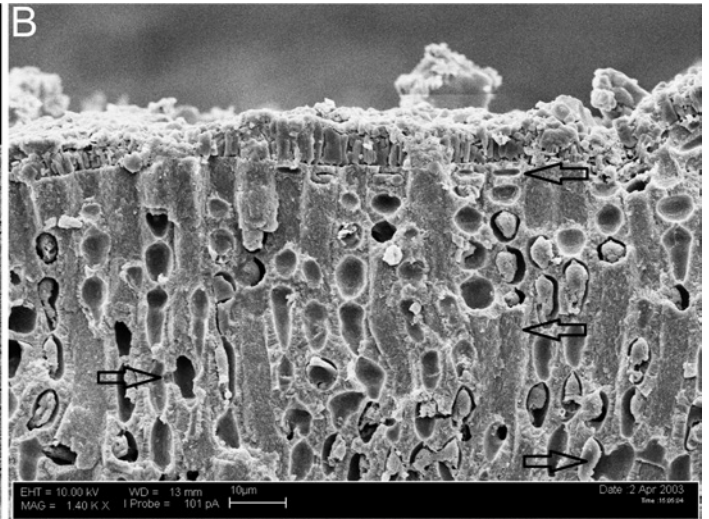


PLATE 7. (Opposite page) *Phymatolithon investiens*: stained microtome sections.

A. Developing bi-tetrasporangial conceptacle formed deep in perithallium, with overlying plug being shed. Sporangial mother cells bearing thick cap walls. 66-42-5B; Trondheimsfjord, Norway.

B. Young bi-tetrasporangial conceptacle with sporangial mother cells having fully developed cap walls (pore plugs). Numbering and locale as in A.

C. Young female conceptacle with overlying plug of perithallial tissue being shed; roof being formed from overgrowing perithallium (roof tissue). 68-29-1; Leirviken, Ranfjorden, north-western Norway.

D. As in C. Numbering and locale as in C.

E. Young female conceptacle with carpogonial filaments maturing and initiating trichogynes. Roof overgrowing. 68-34-11; Tromsøy, off Biological Station, northern Norway.

F. Raised female conceptacles with mature and partially fertilized carpogonia. Roof overgrowth nearly complete. Numbering and locale as in E.

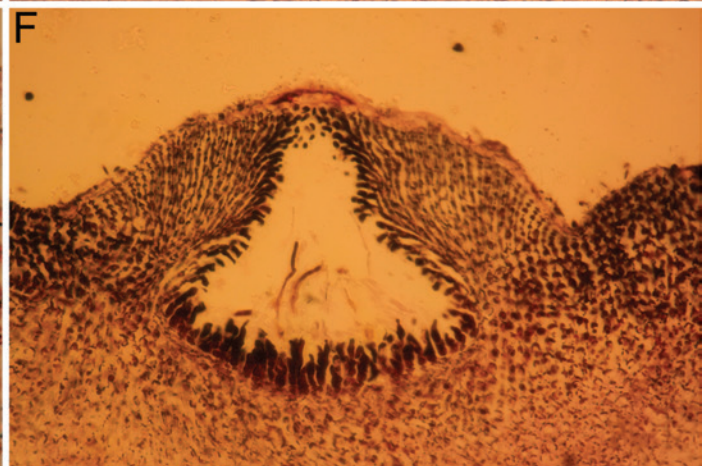
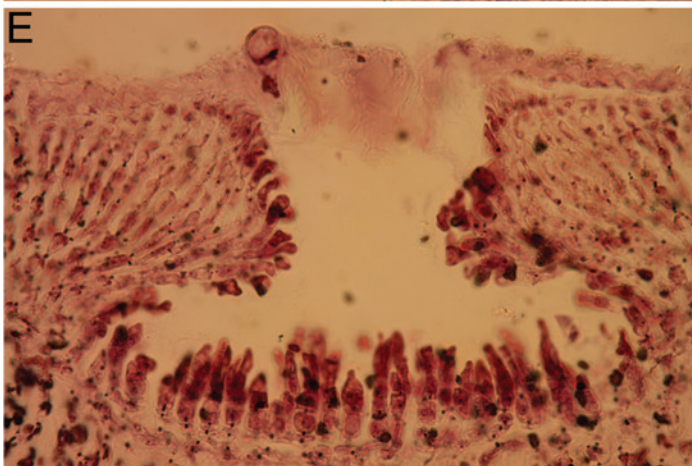
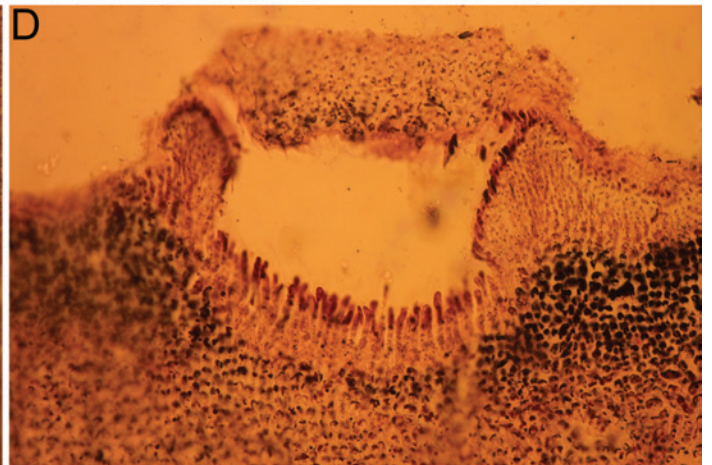
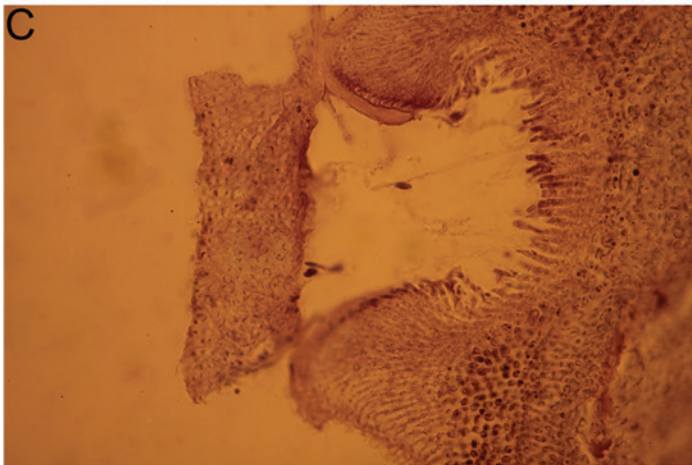
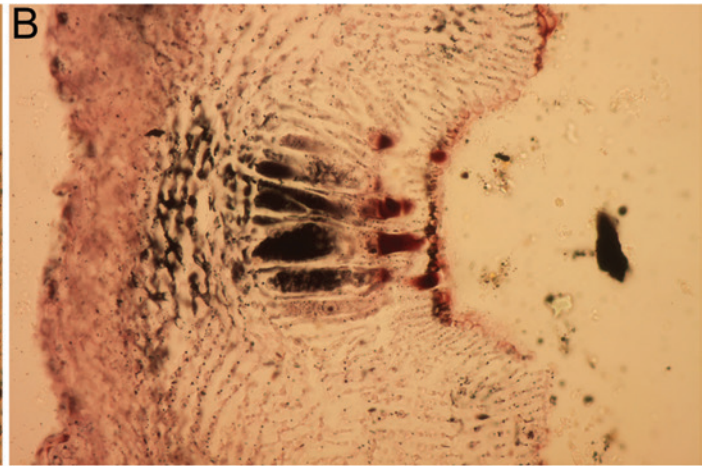
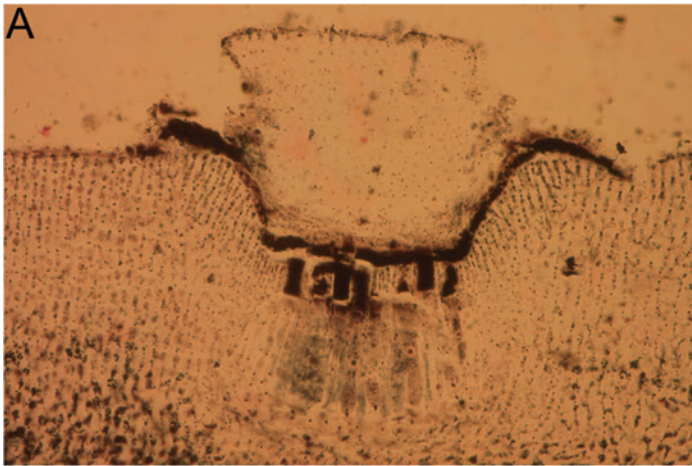


PLATE 8. (*Opposite page*) *Phymatolithon investiens*: SEM images.

A. Crust of thick hypothallium and perithallium. Arrows show fractures along interfilament as frequent vertical stripes. The large-lumen, thin-walled hypothallial cells are indicative of minimum IW wall with high magnesium content (see text). 68-30-3; Lofoten Islands, northern Norway.

B. Surface of mostly meristem cells with projecting interfilament margins. Arrows indicate scattered epithallial cells with partially calcified roofs partially broken out. Numbering and locale as in A.

C. Vertical fracture in upper perithallium. Upper arrow, meristem cell. Middle arrow, interfilament in section. Lower arrow, fracture along interfilament surface. Numbering and locale as in A.

D. Sunken pore plate of mature bi-tetrasporangial conceptacle. Arrow indicates raised rim. 69-2-6; DNA S222; US 171006; Tromsøy, northern Norway.

E. Double crust formed by upper overgrowing older crust, with mature carposporangial conceptacle (left) and unfertilized, degenerating female conceptacle with wound repair tissue filling cavity below (arrows). Numbering and locale as in D.

F. Raised mature carposporangial conceptacle. Some of the underside of the roof, as well as laterally and below conceptacle cavity, shows crushing of vegetative cells (nurse tissue) to form space for developing carposporangia (blot over left side of roof is mounting cement). Numbering and locale as in D.

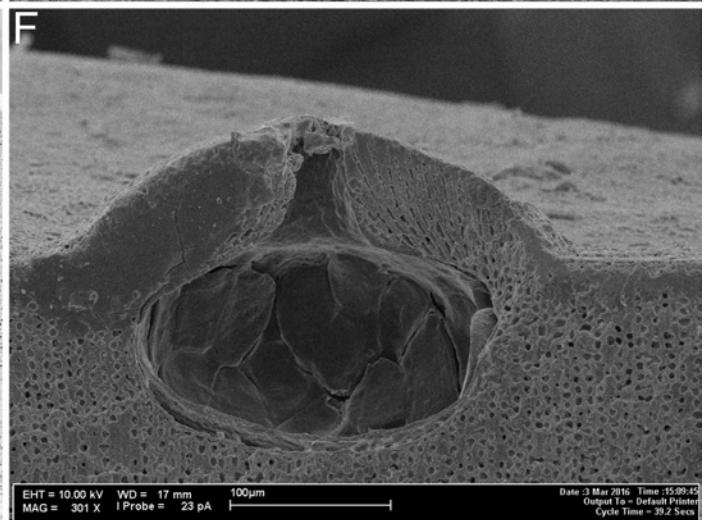
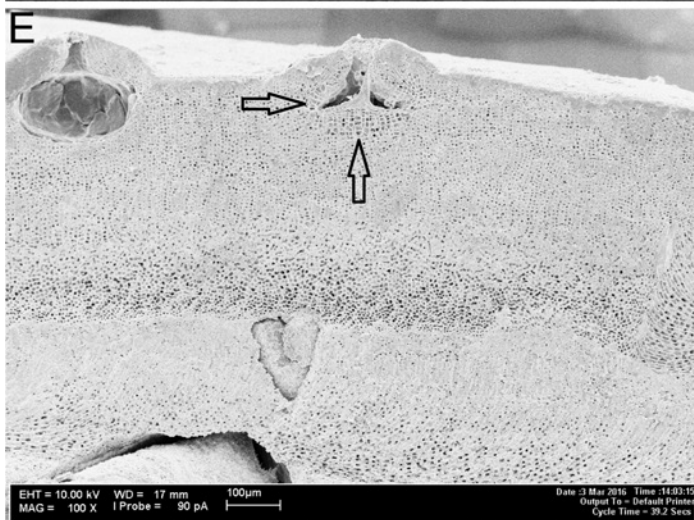
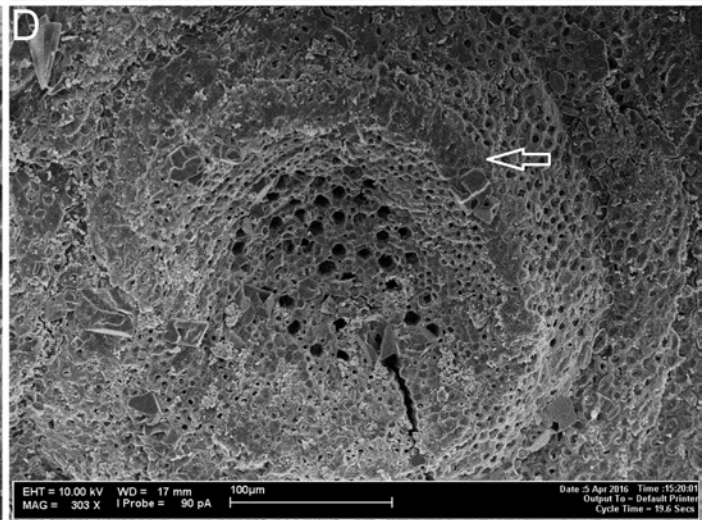
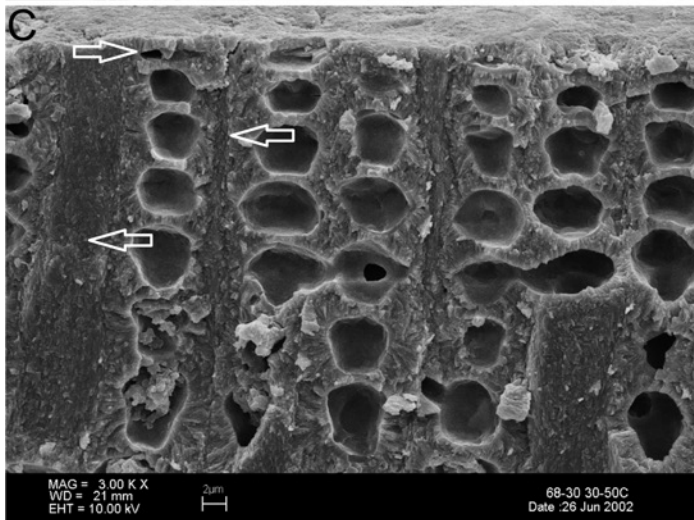
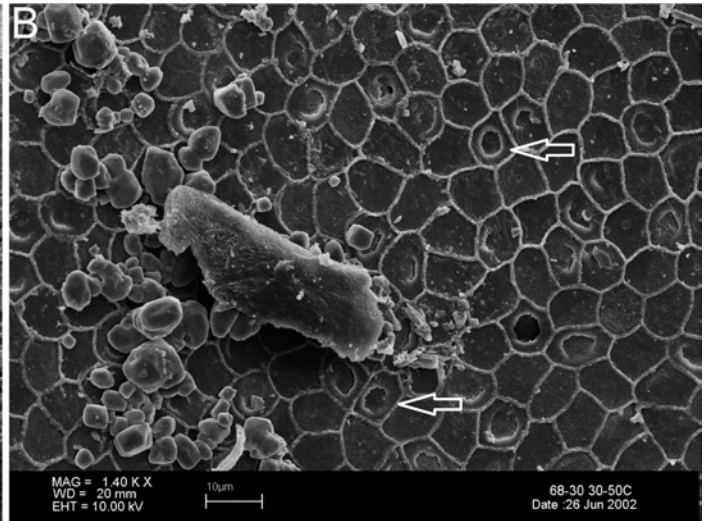
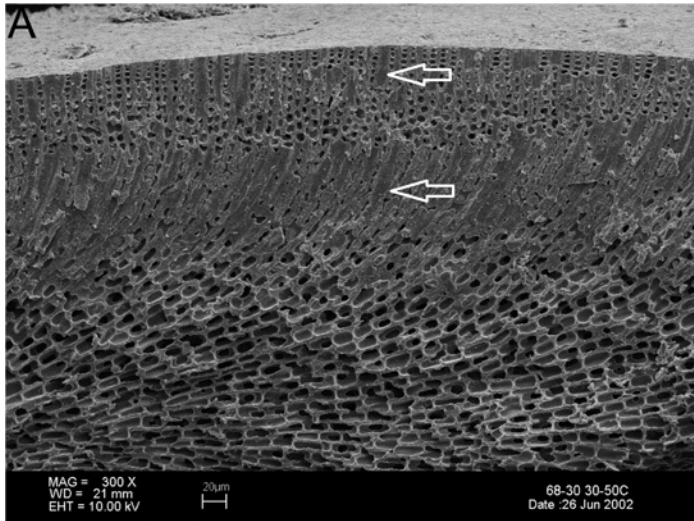


PLATE 9. (*Opposite page*) *Phymatolithon* spp.: magnesium calcite cell walls.

A, B. *P. borealis*.

C. *P. laevigatum*.

D. *P. investiens*. (See white box in E; black box in Plate 10E.) In all three species above, radial magnesium calcite grains of the inner cell walls (IW) provide most of the carbonate structure, as well as tops and bottoms of the cell walls which are filled to the corners. Interfilament (IF) is 1–2 grains thick.

E. *P. investiens*. Radial grains are composed of multiple short shorter grains (black arrows) with radial alignment.

F. *P. rugulosum*. Inner cell walls are radial as in other species, but interfilament is thicker (to 1 μm ; see Plate 11.)

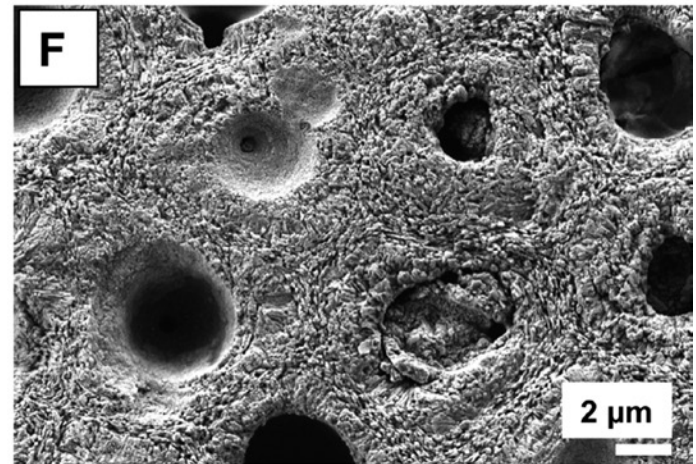
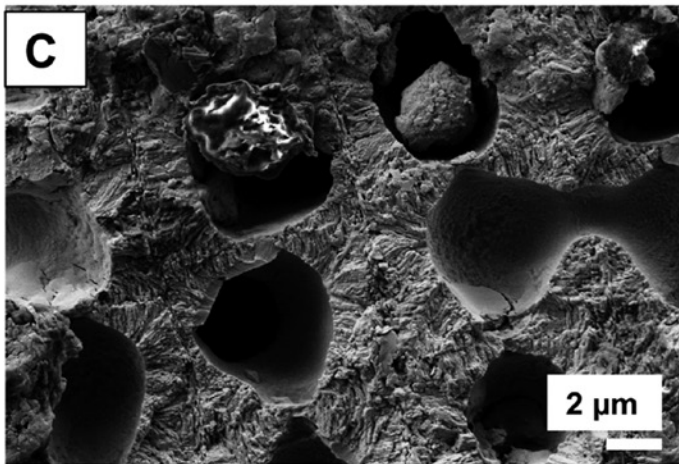
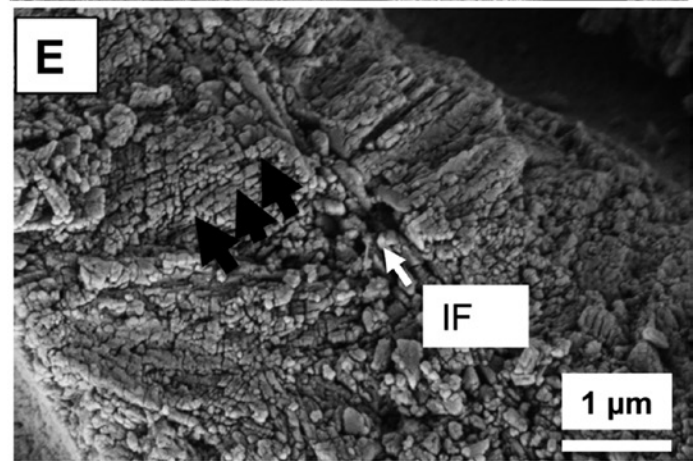
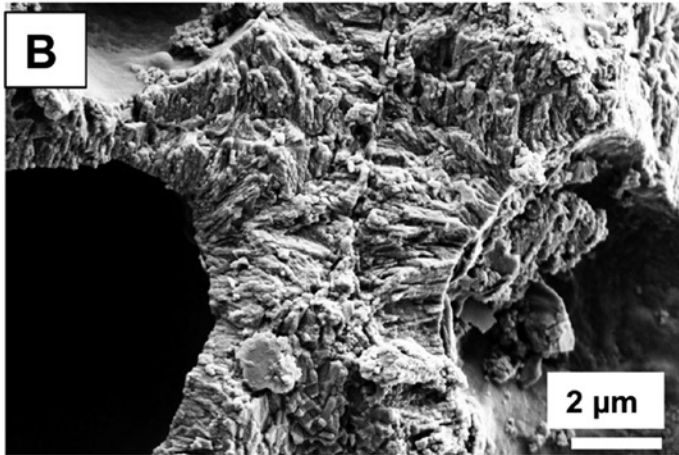
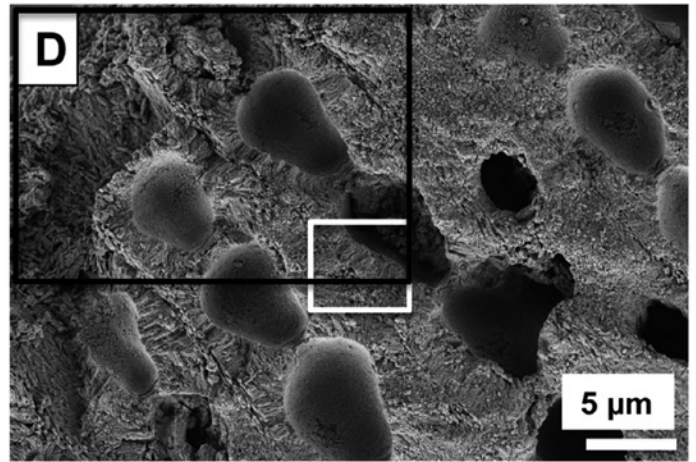
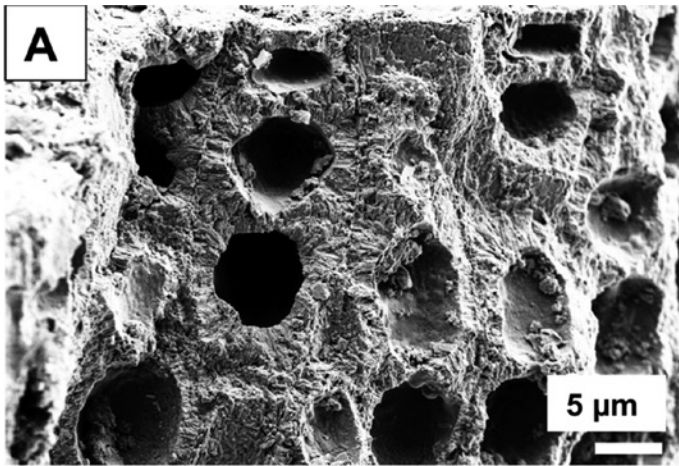


PLATE 10. (*Opposite page*) *Phymatolithon* spp.: magnesium calcite wall details, inner wall (CW), and interfilament (IF).

A. *P. borealis* with interfilament grains (IF) approximately 200–400 nm in length coating the external wall of the adjacent cell. Grains are aligned vertically (against cell wall, CW) and roughly parallel to filament axis.

B. *P. investiens* with interfilament (IF) grains aligned similarly to those in *P. borealis*.

C, D. *P. laevigatum* sample has fractured along the interfilament planes, exposing intact cell walls coated in interfilament grains. Interfilament grains are comparable to those in both *P. borealis* and *P. investiens*. Cell fusions (CF).

E. Plan view: *P. rugulosum* differs with a wider thickness of interfilament; grains do not exhibit any particular orientation.

F. *P. rugulosum* interfilament has secondary mineralization to blocky magnesium calcite (white arrows); original grains are elongate (black arrows).

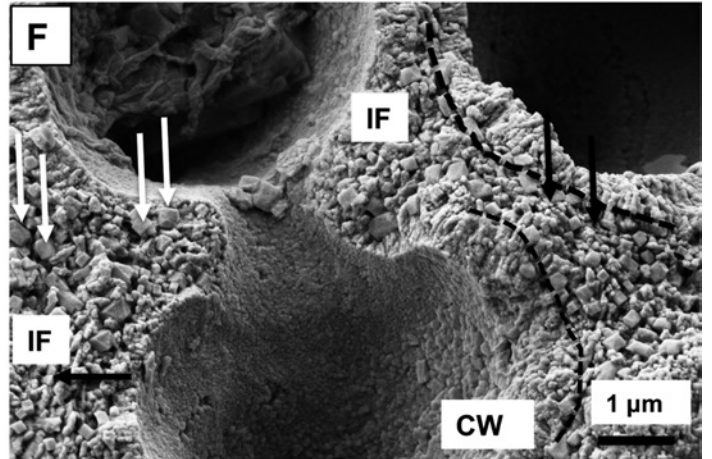
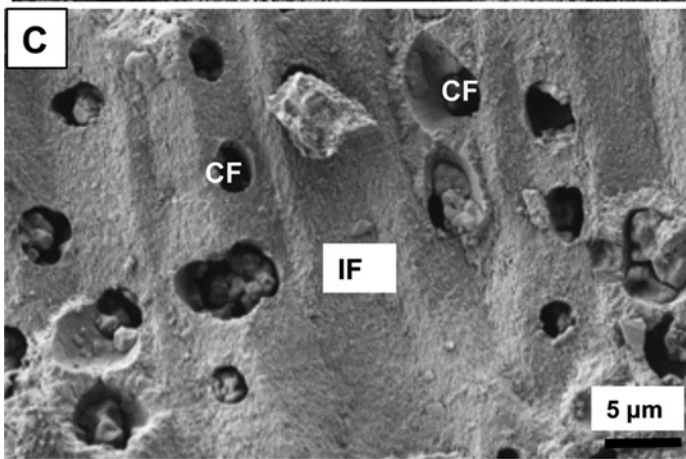
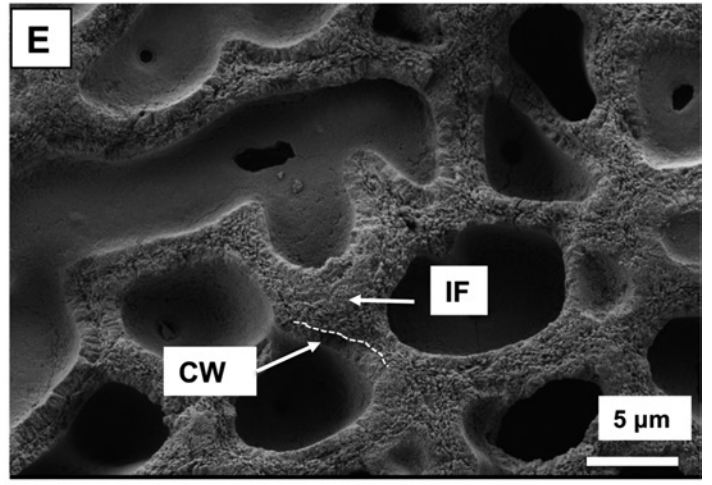
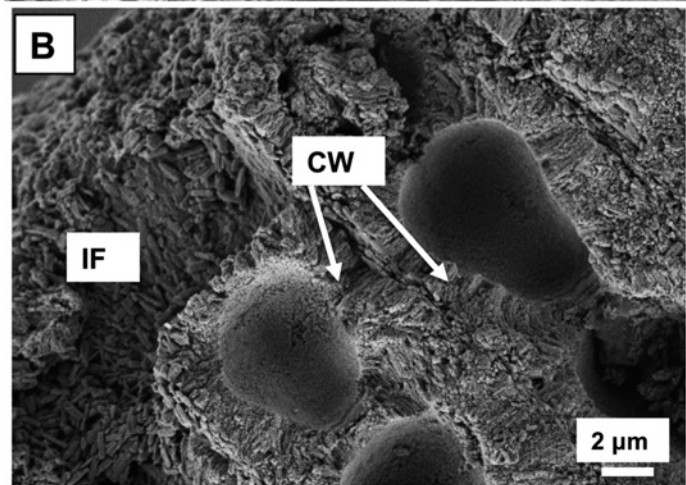
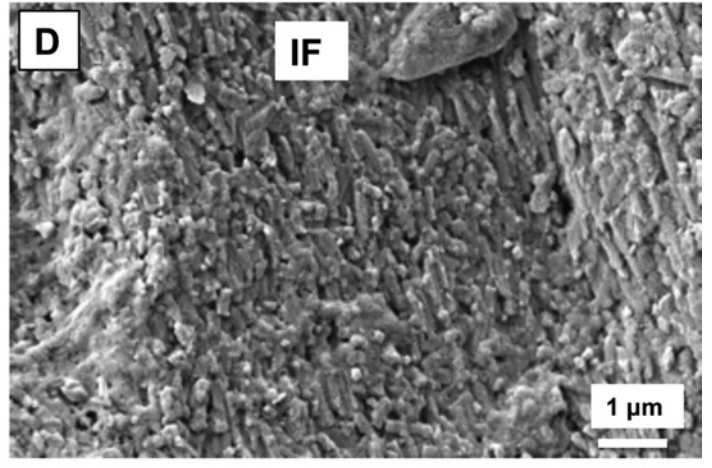
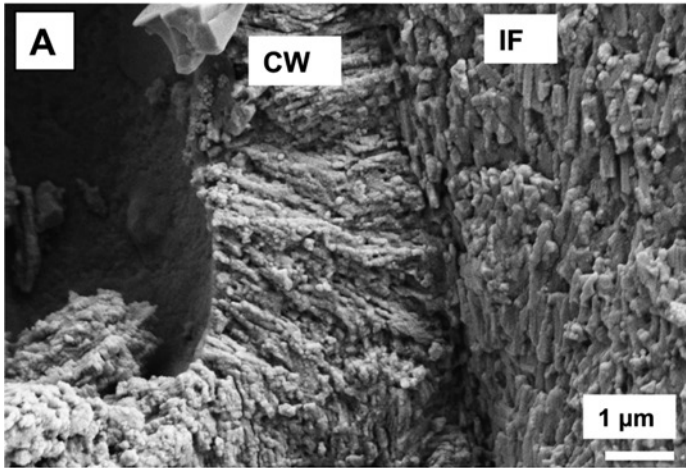


PLATE 11. (*Opposite page*) *Phymatolithon rugulosum*: magnesium calcite walls.

A. Surface of *P. rugulosum*. Epithallus is not present, exposing the meristem cells in plan view cross section.

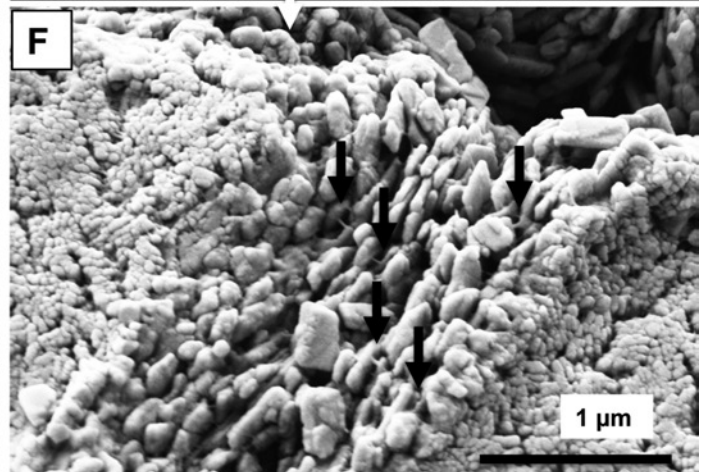
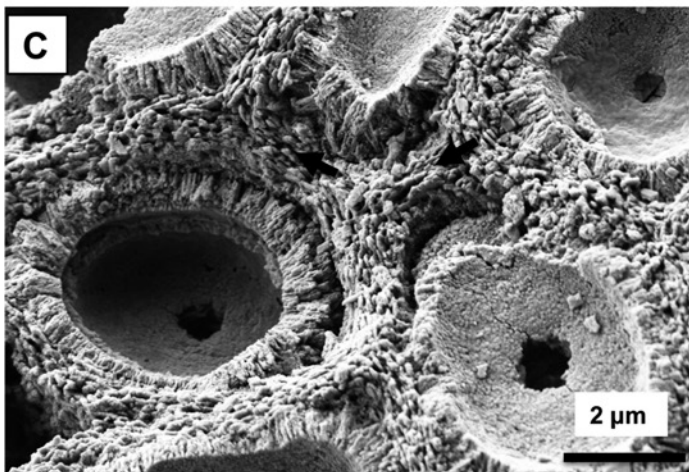
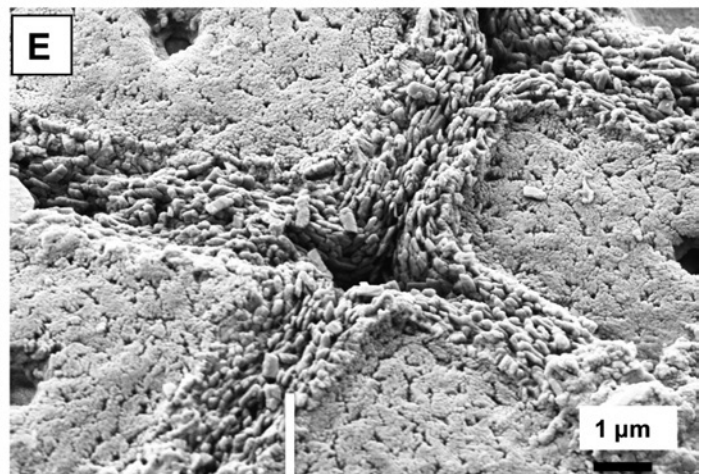
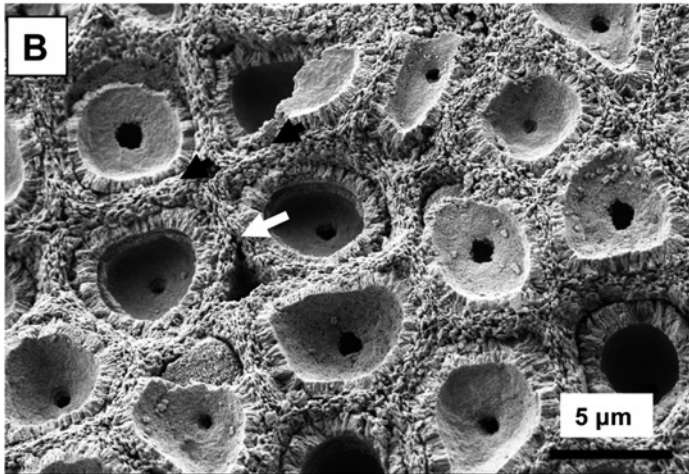
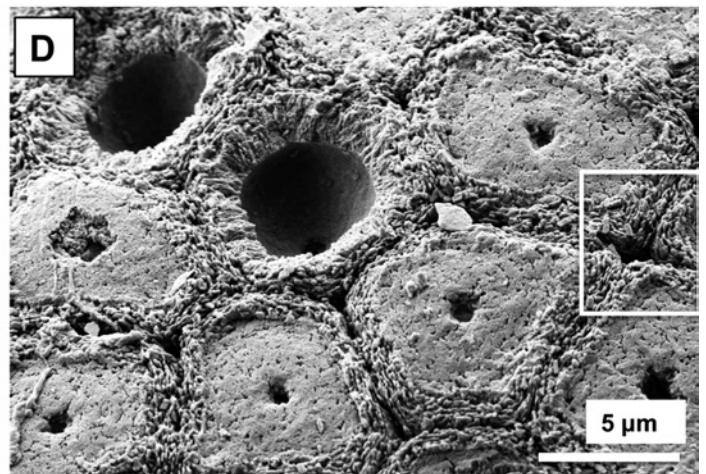
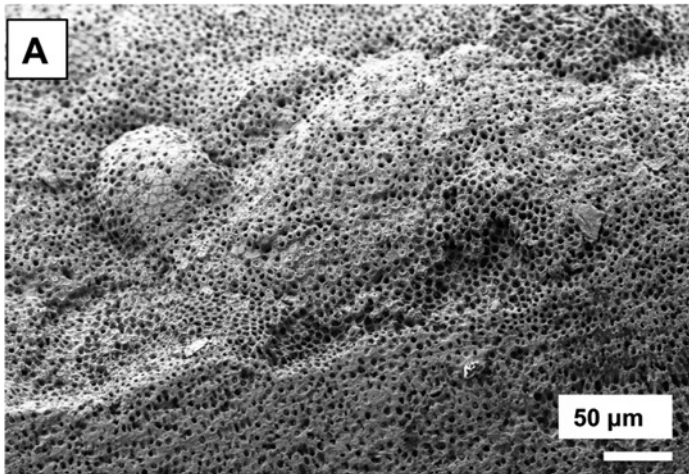
B. Perithallial cells below broken-out meristem in plan view. Cell walls with radial magnesium calcite (black arrows); gaps in interfilament (white arrow).

C. Interfilament grains aligned to plane of nearest cell wall (black arrows).

D. Meristem cells in surface view without epithallium; interfilament grains reach to surface. Gaps in interfilament at cell corner junctions. White box magnified in E.

E. Interfilament bends through corners, and clearly there must have been organic material constraining growth to this shape.

F. Interfilament of E at greater magnification (black arrows).



Appendix: Supplementary Materials

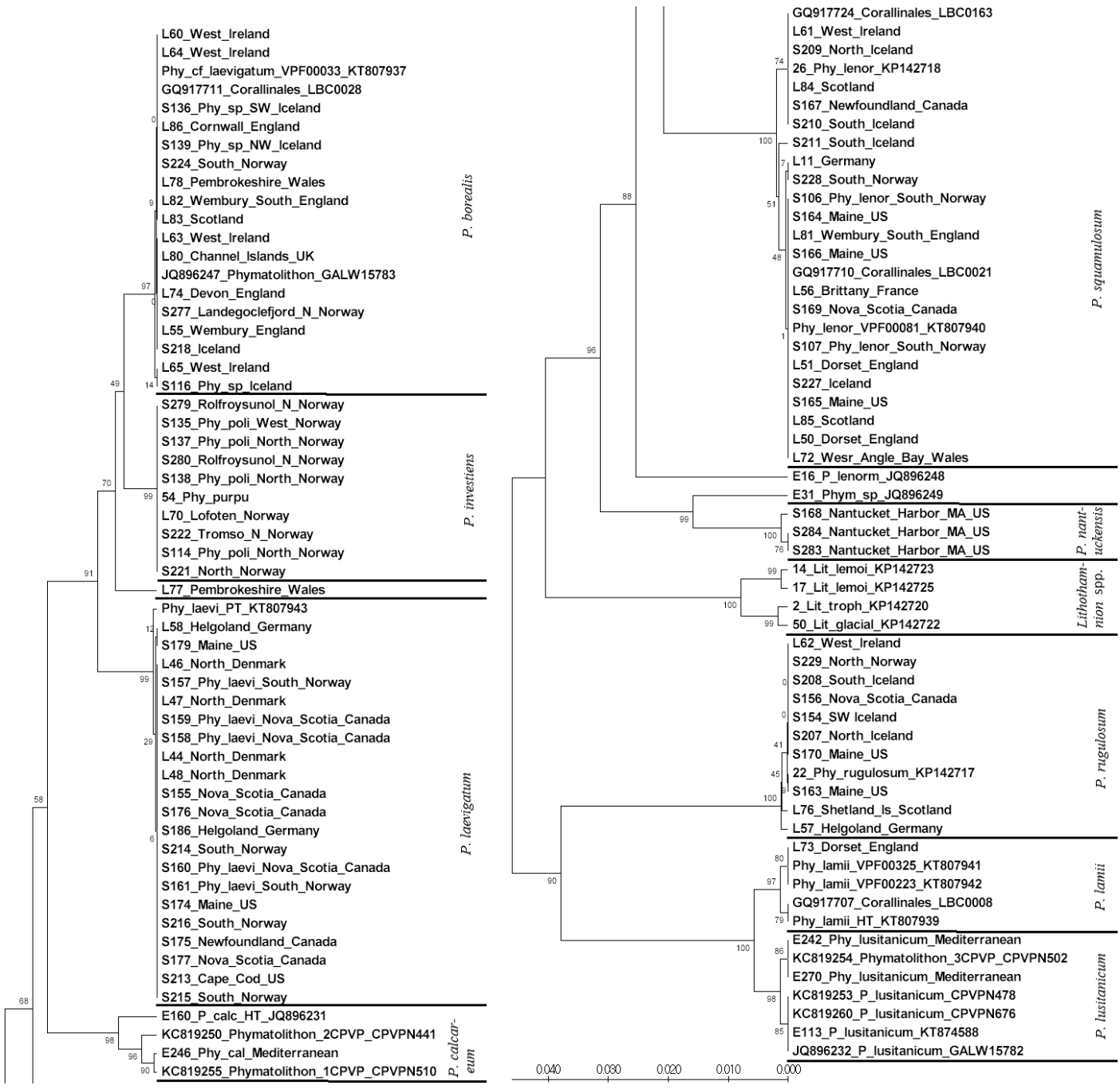


FIGURE A1. *Phymatolithon* (*P.*) tree of all utilized samples: combined rbcL and psbA data sets with identical sequences by using unpaired group method with arithmetic mean (UPGMA) with uncorrected p-distances (proportion [p] of nucleotide sites at which two sequences being compared are different) and 1,000 resamplings for statistical support (see text). Tree was split to fit on the page; upper portion is on left and bottom extension is to the right. Basic locality information is included. Expanded subsets allowing locality and station identification are given in Appendix Figures A2a, A2b, and A2c. See Table 1 in main text for station latitude and longitude as well as site ecological data. Figure by J. Hernandez-Kantun.

Phymatolithon laevigatum

Phy_laevi_PT_KT807943
 L58_Helgoland_Germany, **Holotype**
 S179_Maine_US, Massachusetts, 61-43-1, 06m, Woods Hole, Cape Cod
 L46_North_Denmark
 S157_Phy_laevi_South_Norway, 66-39, 0-10 C, Trondhiemsfjord
 L47_North_Denmark
 S159_Phy_laevi_Nova_Scotia_Canada, 64-2, 0-10B, Shannon Is.
 S158_Phy_laevi_Nova_Scotia_Canada, 64-5, 0-30D, Bras D'Or Lakes
 L44_North_Denmark
 L48_North_Denmark
 S155_Nova_Scotia_Canada
 S176_Nova_Scotia_Canada, 64-5, 0-6m, Bras D'Or Lakes
 S186_Helgoland_Germany, FT-234, Foslie **Isotype**
 S214_South_Norway, 66-42, 0-10 A, Trondheimsfjord
 S160_Phy_laevi_Nova_Scotia_Canada, 64-12, 30-50C, Cape Breton
 S161_Phy_laevi_South_Norway, 67-10, 10-30C, Hardangerfjord
 S174_Maine_US, 62-19-7, 1-2m, Eagle Is., Penobscot Bay
 S216_South_Norway, 67-9-1, Intertidal, Logoyfjord
 S175_Newfoundland_Canada, 64-26-1, Humber Arm
 S177_Nova_Scotia_Canada, 64-1-1, Intertidal, Port Hebert
 S213_Cape_Cod_US, 61-10-1, 20-25, Vineyard Sound
 S215_South_Norway, 67-2, 0-10 R, Trondheimsfjord

FIGURE A2a. Station locality information for *Phymatolithon laevigatum* keyed to tree of Figure A1. Figure by J. Hernandez-Kantun.

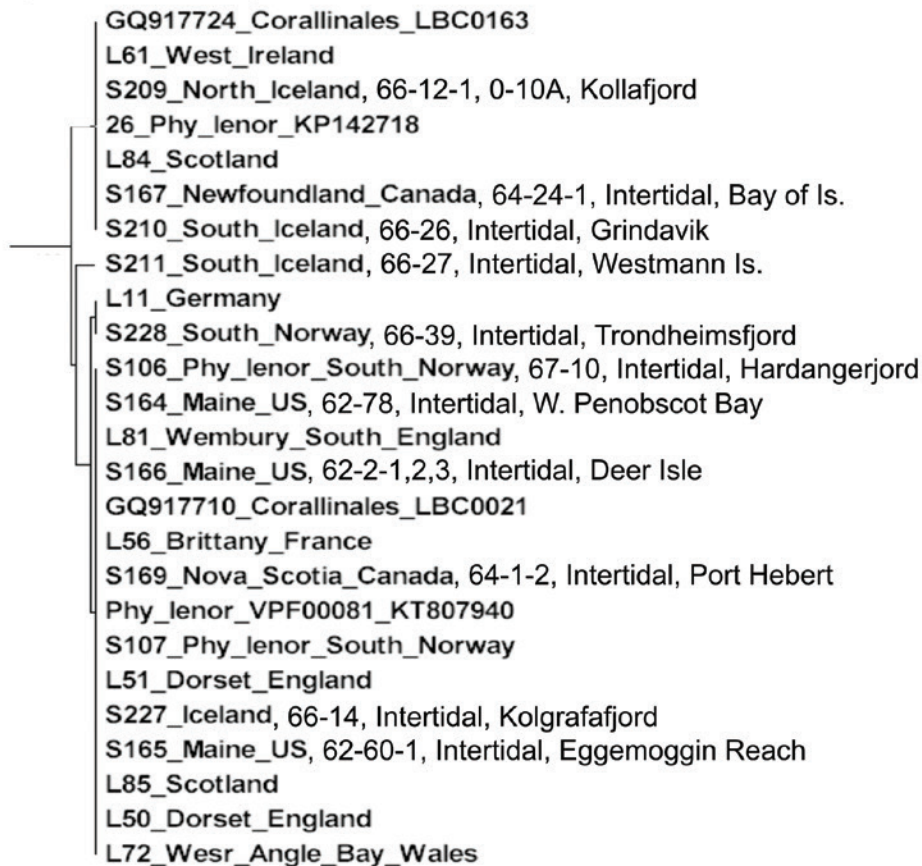
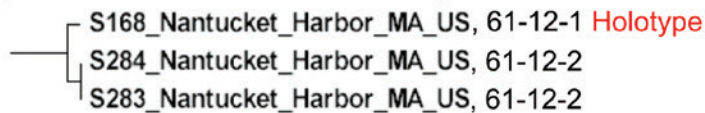
Phymatolithon rugulosum***Phymatolithon squamulosum******Phymatolithon nantuckensis* sp nov**

FIGURE A2b. Station locality information for *Phymatolithon rugulosum*, *P. squamulosum*, and *P. nantuckensis* keyed to tree of Figure A1. Figure by J. Hernandez-Kantun.

***Phymatolithon borealis* sp nov**

L60_West_Ireland
 L64_West_Ireland
 Phy_cf_laevigatum_VPF00033_KT807937
 GQ917711_Corallinales_LBC0028
 S136_Phy_sp_SW_Iceland, 66-26-4, 0-10, Grindavik
 L86_Cornwall_England
 S139_Phy_sp_NW_Iceland, 66-17-13, 90-120A, Hunafloi
 S224_South_Norway, 66-42-1, 0-10, Trondheimsfjord
 L78_Pembrokeshire_Wales
 L82_Wembury_South_England
 L83_Scotland
 L63_West_Ireland
 L80_Channel_Islands_UK
 JQ896247_Phymatolithon_GALW15783
 L74_Devon_England
 S277_Landegoclefjord_N_Norway, 66-36-3, 0-10, North Norway
 L55_Wembury_England
 S218_Iceland, 66-6, 30-50F, Grindavik
 L65_West_Ireland
 S116_Phy_sp_Iceland, 66-27, 0-10 K, Westmann Is. **Holotype**

***Phymatolithon investiens* (zonatum)**

S279_Rolfroysunol_N_Norway, 69-8(2), 40-45m, Revbotn
 S135_Phy_poli_West_Norway, 67-10, Intertidal, Hardangerfjord
 S137_Phy_poli_North_Norway, 69-10, 35-45m, Gjesvaer
 S280_Rolfroysunol_N_Norway, 69-8(2), 40-45m, Revbotn
 S138_Phy_poli_North_Norway, 66-28-3, Intertidal, Kvaloy, Hammerfest
 54_Phy_purpu
 L70_Lofoten_Norway
 S222_Tromso_N_Norway, 69-2-6, 70-90, Tromso, North Norway
 S114_Phy_poli_North_Norway, 69-9, 10-30C, Akkenfjord
 S221_North_Norway, 69-8, 40-45m, Rolfroysund

FIGURE A2c. Station locality information for *Phymatolithon borealis* and *P. investiens* keyed to tree of Figure A1. Figure by J. Hernandez-Kantun.

TABLE A1. Information on DNA specimens with station locality data and museum/herbarium acquisition code numbers. Abbreviations: PCR, polymerase chain reaction; USNH, United States National Herbarium (US). Collection data presented are as follows: collection locality; collection date; site information if known; authority. A dash (–) indicates data are not available/not known. Samples in bold are type specimens. See Table 1 in main text for station latitude and longitude information as well as site ecological data.

Name of sample	PCR code	Herbarium code; collection code	Collection data	USNH Algal Collection number
<i>Phymatolithon borealis</i> sp. nov.	S116	US 170979; 66-27, 0-10 K	Westmanneyjar, Iceland; 17 Aug 1966; <i>leg.</i> W. H. Adey	170979
<i>Phymatolithon borealis</i>	S136	US 170980; 66-26-4, 0-10	West Grindavik, southwest Iceland; 11 Aug 1966; <i>leg.</i> W. H. Adey	170980
	S139	US 171017; 66-17-13, 90-120 A	Hunafloi, northwest Iceland; 28 Jun 1966; <i>leg.</i> W. H. Adey	171017
	S218	US 170981; 66-26, 30-50 F	West Grindavik, southwest Iceland; 11 Aug 1966; <i>leg.</i> W. H. Adey	170981
	S223	US 170999; 66-43-1, 0-10 C	Digertmulen, Trondheimsfjord, Norway; 27 Dec 1966; <i>leg.</i> W. H. Adey	170999
	S224	US 171000; 66-42-1, 0-10 F	Digertmulen, Trondheimsfjord, Norway; 23 Nov 1966; <i>leg.</i> W. H. Adey	171000
	S277	US 171001; 66-36-3, 0–3 m	Landegodefjord, north Norway; 17 Sep 1966; <i>leg.</i> W. H. Adey	171001
	L55	BM000657777; Sample 83/497; Box 1933	Wembury, south Hams District, England; 5 Dec 1983; on rock; <i>leg.</i> Y. M. Chamberlain	–
	L60	BM000657702; Sample 83/180; Box 1896	Fanore, County Clare, Ireland; 1 Mar 1983; on rock, low intertidal; <i>leg.</i> Y. M. Chamberlain	–
	L63	BM000712102; Sample LI760825/1; Box 2545	Fanore, south of Black Head, Ireland; 25 Aug 1976; on pebbles used to cover <i>Paracentrotus</i> ; <i>leg.</i> L. M. Irvine	–
	L64	BM000657730; Sample 83/307; Box 1910	Fanore, County Clare, Ireland; 12 Jul 1983; <i>leg.</i> P. J. Cooke	–
	L65	BM000530600; Box 1110	Bellacragher Bay, Connacht, Ireland; May 1911; <i>leg.</i> A. D. Cotton	–
	L74	BM000657996; Sample 88/121; Box 2058	South Devon, Wembury, England; 24 Nov 1988; mid- and low-tide rocks; <i>leg.</i> Y. M. Chamberlain	–
	L78	BM000712357; Box 2637	South Haven, Pembrokeshire, Wales; Aug 1983; pool in cave; <i>leg.</i> S. Hescoock	–
	L80	BM000712417; Box 2660	Kimmeridge, Dorset; England; 25 May 1982; lagoons and reef	–
	L82	BM000712507; Box 2688	Wembury, south Hams District, England; 28 Mar 1987; mud and silt cover after storm; <i>leg.</i> unknown	–
	L83	BM000711754; Sample LI100207/1; Box 2879	Plockton, Scotland; 7 Feb 1970; <i>leg.</i> L. Irvine	–
	L86	BM001032134; Box 3861	East Cornwall, Hannafore Point, Looe, England; 50°20'42"N, 4°27'6"W; 2 Feb 2010; <i>leg.</i> J. Wilbraham	–
	E22.6IX12all	–	–	–
<i>Phymatolithon calcareum</i>	E246	–	–	–

TABLE A1. (Continued)

Name of sample	PCR code	Herbarium code; collection code	Collection data	USNH Algal Collection number
<i>Phymatolithon investiens</i> (type)	S273	US 171024; F.T. 233	As <i>Lithothamnion investiens</i> , Lyngo, north Tromso, Norway; 15 Jun 1892; isotype from the Foslie Collection	171024
<i>Phymatolithon investiens</i>	L70	BM000530363; Box 904	As <i>Phymatolithon polymorphum</i> f. <i>intermedia</i> ; locality and leg. unknown	–
	S114	US 170997; 69-9, 10-30 C	Hjelmsøy, Akkarfjord, north Norway; 25 Jun 1969; leg. W. H. Adey	170997
	S135	US 171002; 69-10, 35–45 m	Gjesvaer, north Norway; 25 Jun 1969; leg. W. H. Adey	171002
	S137	US 171004; 69-10	Gjesvaer, north Norway; 25 Jun 1969; intertidal; leg. W. H. Adey	171004
	S138	US 171003; 66-28-3, intertidal	Northwest corner of Kvaløy, north Norway; 29 Aug 1966; leg. W. H. Adey	171003
	S221	US 171006; 69-8 (2), 40–45 m	Rolfroysund, north Norway; 24 Jun 1969; leg. W. H. Adey	171006
	S222	US 171005; 69-2-6, 70-90	Off Biological Station, Tromsø, north Norway; 14 Apr 1969; leg. W. H. Adey	171005
	S279	US 171026; 69-8 (2), 40–45 m	Revabotn, Rolfroysund, north Norway; 24 Jun 1969; leg. W. H. Adey	171026
	S280	US 171007; 69-8 (2), 40–45 m	Revabotn, Rolfroysund, north Norway; 24 Jun 1969; 40–45 m; leg. W. H. Adey	171007
	<i>Phymatolithon laevigatum</i> (type)	S186	US 171025; F.T. 234	Helgoland, Germany; isotype from Foslie Collection
<i>Phymatolithon laevigatum</i>	S155	US168008; 64-1, 0-10 D	Harding Point, Port Hebert, Nova Scotia, Canada, 6 Jun, 1964; leg. W. H. Adey	168008
	S157	US 170984; 66-39, 0-10 C	Beitstadfjord, Trondheimsfjord, south Norway; 13 Oct 1966; leg. W. H. Adey	170984
	S158	US 168113; 64-5, 0-30 D	Bras D'Or Lakes, Nova Scotia, Canada; 11 Jul 1964; leg. W. H. Adey	168113
	S159	US 168045; 64-2, 0-10 B	Southeast side of Shannon Island, Nova Scotia, Canada; 8 Jun 1964; leg. W. H. Adey	168045
	S160	US 168447; 64-12, 30-50 C	Beaton Point, Mabou, Cape Breton, Nova Scotia, Canada; 25 Jun 1964; leg. W. H. Adey	168447
	S161	US 170985; 67-11, 10-30 C	Hardangerfjord, south Norway; 31 Jul 1967; leg. W. H. Adey	170985
	S174	US 171008; 62-19-7, 1–2 m	Eagle Island, Penobscot Bay, Maine, USA; 28 Apr 1962; leg. W. H. Adey	171008
	S175	US 170986; 64-26-1C, 0–3 m	Humber Arm, west coast of Newfoundland, Canada; 21 Jul 1964; leg. W. H. Adey	170986
	S176	US 170987; 64-5, 0–6 m	Bras D'Or Lakes, Nova Scotia, Canada; 11 Jul 1964; leg. W. H. Adey	170987
	S177	US 168001; 64-1-1, intertidal	Port Hebert, Nova Scotia, Canada; 6 Jun 1964; leg. W. H. Adey	168001
	S179	US 171009; 61-43-1, 0–6 m	Woods Hole, south of Cape Cod, Massachusetts, USA; 17 Nov 1961; leg. W. H. Adey	171009

TABLE A1. (Continued)

Name of sample	PCR code	Herbarium code; collection code	Collection data	USNH Algal Collection number
<i>Phymatolithon laevigatum</i> (continued)	S213	US 171010; 61-10-1, 20-25	Martha's Vineyard, Vineyard Sound, south of Cape Cod, Massachusetts, USA; 27 Jul 1961; <i>leg.</i> W. H. Adey	171010
	S214	US 170988; 66-42, 0-10A	Digertmulen, Trondheimsfjord, Norway; 23 Nov 1966; <i>leg.</i> W. H. Adey	170988
	S215	US 170989; 67-2, 0-10 R	Prestvaagen, Vaerra Botnen, Trondheimsfjord, Norway; 3 Feb 1967; <i>leg.</i> W. H. Adey	170989
	S216	US 170990; 67-9-1, intertidal	Tobehl, Indre Solen, Lagoyfjord, south Norway; 26 Jul 1967; <i>leg.</i> W. H. Adey	170990
	L44	BM000569182; Sample 1401; Box 1660b	Helligsø, north Denmark; 13 Aug 1985; sublittoral 1–2 m; scattered stones on sandy seashore; <i>leg.</i> Ian Tittley	–
	L46	BM000569181; Sample 1401; Box 1660a	Helligsø, north Denmark; 13 Aug 1985; sublittoral 1–2 m; scattered stones on sandy seashore; <i>leg.</i> Ian Tittley	–
	L47	BM000569300; Sample 1400; Box 1659	Jylland, Oddeund, north Denmark; 13 Aug 1985; inner sheltered areas, scattered stones on sandy seafloor; sublittoral 1–2 m; <i>leg.</i> Ian Tittley	–
	L48	BM000569299; Sample 1400; Box 1659	Jylland, Oddeund, north Denmark; 13 Aug 1985; inner sheltered areas, scattered stones on sandy seafloor; sublittoral 1–2 m; <i>leg.</i> Ian Tittley	–
	L58	BM000659096; Box 729	Foslie Herbario, Helgoland, Germany; 29 Jan 1894; <i>leg.</i> Dr. Kuckuck	–
	E242	–	–	–
E270	–	–	–	
36	–	–	–	
<i>Phymatolithon nantuckensis</i> sp. nov.	S168	US 171011; 61-12-1, 5 m	Nantucket Harbor, Massachusetts, USA; 1 Aug 1961; <i>leg.</i> W. H. Adey	171011
<i>Phymatolithon nantuckensis</i>	S283	US 171021; 61-12, 5 m	Nantucket Harbor, Massachusetts, USA; 1 Aug 1961; <i>leg.</i> W. H. Adey	171021
	S284	US 171022; 61-12, 5 m	Nantucket Harbor, Massachusetts, USA; 1 Aug 1961; <i>leg.</i> W. H. Adey	171022
<i>Phymatolithon rugulosum</i> (type)	S163	US 171023; 61-41, A-3	Merchant Island, Maine, USA; 2 Nov. 1961; <i>leg.</i> W. H. Adey	171023
<i>Phymatolithon rugulosum</i>	S154	US 170991; 66-26, 50-70 H	Stadhur, Grindavík, southwest Iceland; 11 Aug 1966; <i>leg.</i> W. H. Adey	170991
	S156	US 168021; 64-1, 10-30 B	Port Hebert, Nova Scotia, Canada; 6 Jun 1964; <i>leg.</i> W. H. Adey	168021
	S170	US 171012; 61-35-5A, 5 m	Merchant Island, Maine, USA; 30 Sep 1961; <i>leg.</i> W. H. Adey	171012
	S207	US 170992; 66-12, 30-50 G	Hofsvik, Kollafjord, north Iceland; 10 Jun 1966; <i>leg.</i> W. H. Adey	170992
	S208	US 170993; 66-27, 30-50 C	Heimaey, Westmanneyjar, south Iceland; 17 Aug 1966; <i>leg.</i> W. H. Adey	170993

TABLE A1. (Continued)

Name of sample	PCR code	Herbarium code; collection code	Collection data	USNH Algal Collection number
<i>Phymatolithon rugulosum</i> (continued)	S229	US 170994; 69-14, 50-70 V	Veidnesodden, Syltefjord, north Norway; 2 Jul 1969; <i>leg.</i> W. H. Adey	170994
	L57	BM000659095; Sample 21, p. 139; Box 430	Foslie Herbarium, Helgoland, Germany; 1893; <i>leg.</i> Dr. Kuckuck	–
	L62	BM000657696; Sample 83/170; Box 1892	Carrickadda, County Clare, Ireland; 28 Feb 1983; <i>leg.</i> Y. M. Chamberlain	–
	L76	BM000711982; Box 2496	Shetland Islands, Marki Ness, Sullom Voe, Scotland; Aug 1973; depth 4.5 m, overgrowing on a mussel shell; <i>leg.</i> D. Irvine and divers	–
<i>Phymatolithon squamulosum</i> (type)	L68	BM000044670; Box 434	As <i>Lithothamnion squamulosum</i> isotype; Stensund [now Steinsund], Sulen [now Sula], indre [= inner], Sogn, Norway (Woelkerling et al., 2005:267). Jul 1894; ‘nederst lit. reg, beskyttet [= lowest littoral region, protected].’ (Woelkerling et al., 2005: 265); <i>leg.</i> Boye	–
<i>Phymatolithon squamulosum</i>	S106	US 171013; 67-10, intertidal	Kvindherredsfjord, Hardangerfjord, south Norway; 30 Jul 1967; <i>leg.</i> W. H. Adey	171013
	S107	US 170995; 67-2, 0-10 F	Prestvaagen, Trondheimsfjord, south Norway; 3 Feb 1967; <i>leg.</i> W. H. Adey	170995
	S164	US 171014; 62-78, intertidal	North of Rockland Breakwater, west Penobscot Bay, Gulf of Maine, USA; 24 Aug 1962; <i>leg.</i> W. H. Adey	171014
	S165	US 171015; 62-60-1, intertidal	Eggemoggin Reach, Maine, USA; 31 Jul 1962; <i>leg.</i> W. H. Adey	171015
	S166	US 171016; 62-1, intertidal	Dunham Point, Deer Isle, Maine, USA; 3 Jan 1962; <i>leg.</i> W. H. Adey	171016
	S167	US 170996; 64-24-1, intertidal	Guernsey Island, Bay of Islands, Newfoundland, Canada; 15 Jul 1964; <i>leg.</i> W. H. Adey	170996
	S169	US 168002; 64-1-2, intertidal	Port Hebert, Nova Scotia, Canada; 6 Jun 1964; <i>leg.</i> W. H. Adey	168002
	S209	US 170964; 66-12-1, 0-10A	Hofsvik, Kollafjord, north Iceland; 10 Jun 1966; <i>leg.</i> W. H. Adey	170964
	S210	US 171018; 66-26, intertidal	Stadhur, Grindavik, south Iceland; 11 Aug 1966; <i>leg.</i> W. H. Adey	171018
	S211	US 171019; 66-27, intertidal	Heimey, Westmanneyjar, south Iceland; 17 Aug 1966; <i>leg.</i> W. H. Adey	171019
	S227	US 171020; 66-14, intertidal	Kolgrafafjord, Iceland; 19 Jun 1966; <i>leg.</i> W. H. Adey	171020
	S228	US 170998; 66-39, intertidal	Inderoen, Beitstadfjord, Trondheimsfjord, Norway; 13 Oct 1966; <i>leg.</i> W. H. Adey	170998
	L11	BM000044805; Box 565	As <i>Lithothamnion sonderi</i> , Helgoland, Germany; 1893; <i>leg.</i> Hauck	–
	L50	BM000044392; Specimen 87/22; Box 1779	As <i>Phymatolithon brunneum</i> holotype, Lulworth, Dorset, England; 17 Feb 1987; on rocks together with <i>Phymatolithon lenormandii</i> and occurring immediately above the <i>P. purpureum</i> zone; <i>leg.</i> Y. M. Chamberlain	–

TABLE A1. (Continued)

Name of sample	PCR code	Herbarium code; collection code	Collection data	USNH Algal Collection number
<i>Phymatolithon squa- mulosum</i> (continued)	L51	BM000044392; Specimen 87/22; Box 1779	As <i>Phymatolithon lenormandii</i> , Lulworth, Dorset, England; 17 Feb 1987; on rocks and occurring immediately above the <i>P. purpureum</i> zone; <i>leg.</i> Y. M. Chamberlain	–
	L56	BM000657936; Specimen 86/60; Box 2010	Trévignon, Trégunc, France; 24 Apr 1986; common from tide line downward; <i>leg.</i> Y. M. Chamberlain	–
	L61	BM000657694; Sample 83/186; Box 1890	Carrickadda, County Clare, Ireland; 28 Feb 1983; sandy channel near laboratory; <i>leg.</i> Y. Chamberlain	–
	L72	BM000657787; Sample 84/39; Box 1940	West Angle, Pembrokeshire, England; 18 Feb 1984; on exposed rock at extreme low water spring tides; <i>leg.</i> Y. M. Chamberlain	–
	L81	BM000712504; Box 2687	Peacehaven, East Sussex, England; 26 Jan 2003; chalk platform; <i>leg.</i> K. Sheppard	–
	L84	BM001032132; Box 3849	Applecross, Scotland; 57°26'02"N, 05°48'50"W; 16 Oct 2009; <i>leg.</i> J. Brodie and J. Wilbraham	–
	L85	BM001032117; Box 3851	Badnaban, northwest Scotland; 58°08'13"N, 05°16'16"W; 18 Oct 2009; <i>leg.</i> J. Brodie and J. Wilbraham	–

References

- Adey, W. 1964. The Genus *Phymatolithon* in the Gulf of Maine. *Hydrobiologia*, 24:377–420. <https://doi.org/10.1007/BF00170412>.
- Adey, W. 1965. The Genus *Clathromorphum* in the Gulf of Maine. *Hydrobiologia*, 26:539–573. <https://doi.org/10.1007/BF00045545>.
- Adey, W. 1966a. The Genera *Lithothamnion*, *Leptophytum* (nov. gen.) and *Phymatolithon* in the Gulf of Maine. *Hydrobiologia*, 28:321–370. <https://doi.org/10.1007/BF00130389>.
- Adey, W. 1966b. Distribution of Saxicolous Crustose Corallines in the Northwestern North Atlantic. *Journal of Phycology*, 2:49–54. <https://doi.org/10.1111/j.1529-8817.1966.tb04593.x>.
- Adey, W. 1968. The Distribution of Crustose Corallines on the Icelandic Coast. *Scientia Islandica Reykjavik*, 1:16–25.
- Adey, W. 1970a. The Crustose Corallines of the Northwestern North Atlantic, Including *Lithothamnium lemoinii* n. sp. *Journal of Phycology*, 6:225–229.
- Adey, W. 1970b. Some Relationships Between Crustose Corallines and Their Substrate. *Scientia Islandica Reykjavik*, 2:21–25.
- Adey, W. 1970c. A Revision of the Foslie Crustose Coralline Herbarium, Including a Preliminary World Phytogeographic Survey. *Det Kongelige Norske Videnskabers Selskabs Skrifter*, 1:1–46.
- Adey, W. 1971. The Sublittoral Distribution of Crustose Corallines on the Norwegian Coast. *Sarsia*, 46:41–58. <https://doi.org/10.1080/00364827.1971.10411187>.
- Adey, W. 1973. Temperature Control of Reproduction and Productivity in a Subarctic Coralline Alga. *Phycologia*, 12:111–118. <https://doi.org/10.2216/i0031-8884-12-3-111.1>.
- Adey, W. 1998. Coral Reefs: Algal Structured and Mediated Ecosystems in Shallow, Turbulent Alkaline Seas. *Journal of Phycology*, 34:393–406. <https://doi.org/10.1046/j.1529-8817.1998.340393.x>.
- Adey, W., and P. Adey, 1973. Studies on the Biosystematics and Ecology of the Epilithic Crustose Corallinales of the British Isles. *British Phycological Journal*, 8:1–60. <https://doi.org/10.1080/00071617300650381>.
- Adey, W., A. Athanasiadis, and P. Lebednik. 2001. Re-instatement of *Leptophytum* and Its Type *Leptophytum leave*: Taxonomy and Biogeography of the Genera *Leptophytum* and *Phymatolithon* (Corallinales, Rhodophyta). *European Journal of Phycology*, 36:191–203. <https://doi.org/10.1080/09670260110001735338>.
- Adey, W., Y. Chamberlain, and L. Irvine. 2005. Morphology, Reproduction and Ecology of *Lithothamnion tophi-forme* Unger (Corallinales, Rhodophyta), an Arctic Coralline. *Journal of Phycology*, 41:1010–1024. <https://doi.org/10.1111/j.1529-8817.2005.00123.x>.
- Adey, W., J. Halfar, and B. Williams. 2013. Biological, Physiological and Ecological Factors Controlling High Magnesium Carbonate Formation and a Precision Arctic/Subarctic Marine Climate Archive: The Coralline Genus *Clathromorphum* Foslie emend Adey. *Smithsonian Contributions to Marine Science*, 40:1–41. <https://doi.org/10.5479/si.1943667X.40.1>.
- Adey, W., and L.-A. Hayek. 2011. Elucidating Marine Biogeography with Macrophytes: Quantitative Analysis of the North Atlantic Supports the Thermogeographic Model and Demonstrates a Distinct Subarctic region in the Northwestern Atlantic. *Northeastern Naturalist*, 18:1–125. <https://doi.org/10.1656/045.018.m801>.
- Adey, W., J. Halfar, A. Humphreys, D. Belanger, P. Gagnon, and M. Fox. 2015a. Subarctic Rhodolith Beds Promote Longevity of Crustose Coralline Algal Buildups and Their Climate Archiving Potential. *Palaeos*, 30:281–293. <https://doi.org/10.2110/palo.2014.075>.
- Adey, W., J. J. Hernandez-Kantun, G. Johnson, and P. Gabrielson. 2015b. DNA Sequencing, Anatomy and Calcification Patterns Support a Monophyletic, Subarctic, Carbonate Reef-forming *Clathromorphum* (Hapalidiales, Corallinales, Rhodophyta). *Journal of Phycology*, 51:189. <https://doi.org/10.1111/jpy.12266>.
- Adey, W., and P. Lebednik. 1967. *Catalog of the Foslie Herbarium*. Kongelige Norske Videnskabers Selskab Museet, Trondheim, Norway.

- Adey, W., T. Masaki, and H. Akioka. 1974. *Ezo epiyessoense*, a New Parasitic Genus and Species of Corallinaceae. *Phycologia*, 13:329–344. <https://doi.org/10.2216/i0031-8884-13-4-329.1>.
- Adey, W., and D. McKibbin. 1970. Studies of the Maerl Species *Phymatolithon calcareum* nov. comb. and *Lithothamnium corallioides* in the Ria de Vigo. *Botanica Marina*, 13:100–106. <https://doi.org/10.1515/botm.1970.13.2.100>.
- Adey, W., and C. Sperapani. 1971. The Biology of *Kvaleya epilaeve*, a New Parasitic Genus and Species of Corallinaceae. *Phycologia*, 10:29–42. <https://doi.org/10.2216/i0031-8884-10-1-29.1>.
- Adey, W., and R. Steneck. 2001. Thermogeography over Time Creates Biogeographic Regions: A Temperature/Space/Time-Integrated Model and an Abundance-Weighted Test for Benthic Marine Algae. *Journal of Phycology*, 37:677–698. <https://doi.org/10.1046/j.1529-8817.2001.00176.x>.
- Babbini, L., and G. Bressan. 1997. Recensement de Corallinacées de la Mer Méditerranée et considérations phytogéographiques. *Bibliotheca Phycologica*, 103:1–421.
- Basso, D., A. Caragnano, L. Le Gall, and G. Rodondi. 2015. The Genus *Lithophyllum* in the North-western Indian Ocean, with Description of *L. yemenense* sp. nov., *L. socotraense* sp. nov., *L. subplicatum* comb. et stat. nov., and the Resumed *L. affine*, *L. kaiseri*, and *L. subreduncum* (Rhodophyta, Corallinales). *Phytotaxa*, 208:183–200. <https://doi.org/10.11646/phytotaxa.208.3.1>.
- Broom, J., D. Hart, T. Farr, W. Nelson, K. Neill, A. Harvey, and W. Woelkerling. 2008. Utility of psbA and nSSU for Phylogenetic Reconstruction in the Corallinales Based on New Zealand Taxa. *Molecular Phylogenetics and Evolution*, 46:958–973. <https://doi.org/10.1016/j.ympev.2007.12.016>.
- Chamberlain, Y. 1991. Observations on *Phymatolithon lamii* (Lemoine) Chamberlain comb. nov. (Rhodophyta, Corallinales) in the British Isles with an Assessment of Its Relationship to *P. rugulosum*, *Lithophyllum lamii* and *L. melobesioides*. *British Phycological Journal*, 26:219–233. <https://doi.org/10.1080/00071619100650201>.
- Chan, P., J. Halfar, C. J. D. Norley, S. I. Pollmann, Walter H. Adey, and D. W. Holdsworth. 2017. Micro-Computed Tomography: Applications for High-Resolution Skeletal Density Determinations: An Example using Annually Banded Crustose Coralline Algae. *Geochemistry, Geophysics, Geosystems*, 18(9):3542–3553. <https://doi.org/10.1002/2017GC006966>.
- Darwin, C. 1859. *The Origin of Species, by means of natural selection*. London: John Murray. Facs. Ed. Cambridge, Mass.: Harvard University Press. 1964.
- Foslie, M. 1895. The Norwegian Forms of *Lithothamnion*. *Kongelige Norske Videnskabers Selskabs Skrifter*, 1894:29–208. 22 Pl.
- Foslie, M. 1898. Systematical Survey of the *Lithothamnium*. *Kongelige Norske Videnskabers Selskabs Skrifter*, 1898:1–7.
- Foslie, M. 1900. Revised Systematical Survey of the Melobesieae. *Kongelige Norske Videnskabers Selskabs Skrifter*, 1900:1–22.
- Freshwater, D. W., and J. Rueness. 1994. Phylogenetic Relationships of Some European *Gelidium* (Gelidiales, Rhodophyta) Species Based upon *rbcL* Sequence Analysis. *Phycologia*, 33:187–194. <https://doi.org/10.2216/i0031-8884-33-3-187.1>.
- Gabrielson, P. W., K. A. Miller, and P. Martone. 2011. Morphometric and Molecular Analyses Confirm Two Distinct Species of *Calliarthron* (Corallinales, Rhodophyta), a Genus Endemic to the Northeast Pacific. *Phycologia*, 50:298–316. <https://doi.org/10.2216/10-42.1>.
- Guiry, M. D., and G. M. Guiry. 2017. *AlgaeBase*. World-wide electronic publication, National University of Ireland, Galway. <http://www.algaebase.com>.
- Halfar, J., W. Adey, A. Kronz, E. Edinger, and W. Fitzhugh. 2013. Unprecedented Sea-Ice Decline Archived by Novel Multi-Century Annual-Resolution Algal Proxy. *Proceedings of the National Academy of Sciences of the United States of America*, 110:197837–197841. <https://doi.org/10.1073/pnas.1313775110>.
- Hernandez-Kantun, J. J., R. Riosmena-Rodriguez, W. Adey, and F. Rindi. 2014. Analysis of the *cox2-3* Spacer Region for Population Diversity and Taxonomic Implications in Rhodolith-forming Species (Rhodophyta: Corallinales). *Phytotaxa*, 190:331–354. <https://doi.org/10.11646/phytotaxa.190.1.20>.
- Hernandez-Kantun, J. J., F. Rindi, W. Adey, S. Heesch, V. Peña, L. Le Gall, and P. W. Gabrielson. 2015. Sequencing Type Material Resolves the Identity and Distribution of the Generitype *Lithophyllum incrustans*, and Related European Species *L. hibernicum* and *L. bathyporum* (Corallinales, Rhodophyta). *Journal of Phycology*, 51:791–807. <https://doi.org/10.1111/jpy.12319>.
- Hernandez-Kantun, J. J., P. Gabrielson, J. R. Hughey, L. Pezzolesi, F. Rindi, N. M. Robinson, V. Peña, R. Riosmena-Rodriguez, L. LeGall, and W. Adey. 2016. Reassessment of Branched *Lithophyllum* spp. (Corallinales, Rhodophyta) in the Caribbean Sea with Global Implications. *Phycologia*, 55:619–639. <https://doi.org/10.2216/16-7.1>.
- Heydrich, F. 1897a. Corallinaceae, insbesondere Melobesieae. *Berichte der Deutsche Botanischen Gesellschaft*, 15:34–71.
- Heydrich, F. 1897b. Melobesieae. *Berichte der Deutsch Botanischen Gesellschaft*, 15:403–420.
- Heydrich, F. 1900. Die Lithothamnien von Helgoland. *Wissenschaftliche Meeresuntersuchungen, N.F. (Abteilung Helgoland)*, 4:63–82.
- Hind, K. R., P. W. Gabrielson, S. C. Lindstrom, and P. T. Martone. 2014a. Misleading Morphologies and the Importance of Sequencing Type Specimens for Resolving Coralline Taxonomy (Corallinales, Rhodophyta): *Pachyarthron cretaceum* Is *Corallina officinalis*. *Journal of Phycology*, 50:760–764. <https://doi.org/10.1111/jpy.12205>.
- Hind, K. R., P. W. Gabrielson, and G. W. Saunders. 2014b. Molecular-assisted Alpha Taxonomy Reveals Pseudocryptic Diversity among Species of *Bossia* (Corallinales, Rhodophyta) in the Eastern Pacific Ocean. *Phycologia*, 53:443–456. <https://doi.org/10.2216/13-239.1>.
- Hind, K. R., P. W. Gabrielson, C. Jensen, and P. Martone. 2016. *Crusticorallina* gen. nov., a Non-geniculate Genus in the Subfamily Corallinoideae (Corallinales, Rhodophyta). *Journal of Phycology*, 52:929–941. <https://doi.org/10.1111/jpy.12449>.
- Hind, K. R., K. A. Miller, M. Young, C. Jensen, P. W. Gabrielson, and P. T. Martone. 2015. Resolving Cryptic Species of *Bossia* (Corallinales, Rhodophyta) Using Contemporary and Historical DNA. *American Journal of Botany*, 102:1–19. <https://doi.org/10.3732/ajb.1500308>.
- Hind, K., and G. Saunders. 2013. A Molecular Phylogenetic Study of the Tribe Corallineae (Corallinales, Rhodophyta) with an Assessment of Genus-level Taxonomic Features and Descriptions of Novel Genera. *Journal of Phycology*, 49:103–114. <https://doi.org/10.1111/jpy.12019>.
- Huelsensbeck, J. P., and F. Ronquist. 2001. MRBAYES: Bayesian Inference of Phylogeny. *Bioinformatics*, 17:754–755. <https://doi.org/10.1093/bioinformatics/17.8.754>.
- Hughey, J. R., and P. W. Gabrielson. 2012. Comment on “Acquiring DNA from Dried Archival Red Algae (Florideophyceae) for the Purpose of Applying Available Names to Contemporary Genetic Species: A Critical Assessment.” *Botany*, 90:1191–1194. <https://doi.org/10.1139/b2012-102>.
- Irvine, L., and Y. Chamberlain. 1994. *Seaweeds of the British Isles: Vol. 1, Rhodophyta, Part 2B. Corallinales, Hildenbrandiales*. London: The Natural History Museum.
- Johnson, L., S. Brawley, and W. Adey. 2012. Secondary Spread of Invasive Species: Historic Patterns and Underlying Mechanisms of the Continuing Invasion of the European Rockweed *Fucus serratus* in Eastern North America. *Biological Invasions*, 14:79–97. <https://doi.org/10.1007/s10530-011-9976-z>.
- Lebednik, P. 1977 ('1976'). The Corallinaceae of Northwestern North America. I. *Clathromorphum* Foslie emend. Adey. *Syesis*, 9:59–112.
- Nash, M., and W. Adey. 2017a. Anatomical Structure Over-rides Temperature Controls on Magnesium Uptake: Calcification in the Arctic/Subarctic Coralline Algae *Leptophytum leave* and *Kvaleya epilaeve* (Rhodophyta; Corallinales). *Biogeosciences, Discussions* 1–40. <https://doi.org/10.5194/bg-2017-180>.
- Nash, M., and W. Adey. 2017b. Multiple Phases of Mg-Calcite in Crustose Coralline Suggest Caution for Temperature Proxy and Ocean Acidification Assessment: Lessons from the Ultrastructure and Biomineralization in the Genus *Phymatolithon* (Rhodophyta; Corallinales) in the Boreal North Atlantic Ocean. *Journal of Phycology*, 53:970–984. <https://doi.org/10.1111/jpy.12559>.
- Nash, M., B. Opdyke, U. Troitzsch, B. Russell, W. Adey, A. Kato, G. Diaz-Pulido, C. Brent, M. Gardner, J. Prichard, and D. Kline. 2012. Dolomite-rich Coral Reef Coralline Algae Resist Dissolution in Acidified Conditions. *Nature Climate Change*, 3:263–272. <https://doi.org/10.1038/nclimate17609>.
- Peña, V., O. De Clerck, J. Afonso-Carillo, E. Ballesteros, I. Bárbara, R. Barreiro, and L. Le Gall. 2015a. An Integrative Systematic Approach to Species Diversity and Distribution in the genus *Mesophyllum* (Corallinales, Rhodophyta) in Atlantic and Mediterranean Europe. *European Journal of Phycology*, 50:20–36. <https://doi.org/10.1080/09670262.2014.981294>.
- Peña, V., C. Pardo, L. López, B. Carro, J. Hernandez-Kantun, W. H. Adey, I. Bárbara, R. Barreiro, and L. Le Gall. 2015b. *Phymatolithon lusitanicum* sp. nov. (Hapalidiales, Rhodophyta): The Third Most Abundant Maerl-forming Species in the Atlantic Iberian Peninsula. *Cryptogamie Algologie*, 36:429–459. <https://doi.org/10.7872/crya/v36.iss4.2015.429>.
- Ragazzola, F., L. Foster, C. Jones, T. Scott, J. Fietzke, M. Kilburn, and D. Schmidt. 2016. Impact of High CO₂ on the Geochemistry of the Coralline Algae *Lithothamnion glaciale*. *Scientific Reports*, 6:20572. <https://doi.org/10.1038/srep20572>.

- Rambaut, A., and A. J. Drummond. 2007. Tracer v1.4. Available at <http://beast.bio.ed.ac.uk/Tracer>.
- Rosler, A., F. Perfectti, V. Peña, and J. C. Braga. 2016. Phylogenetic Relationship of Corallinaceae (Corallinales, Rhodophyta): Taxonomic Implications for Reef-building Corallines. *Journal of Phycology*, 52:412–431. <https://doi.org/10.1111/jpy.12404>.
- Saunders, G.W., and D. C. McDevit. 2012. Acquiring DNA from Dried Archival Red Algae (Floridophyceae) for the Purpose of Applying Available Names to Contemporary Genetic Species: A Critical Appraisal. *Botany*, 90:191–203. <https://doi.org/10.1139/b11-079>.
- Silvestro, D., and I. Michalak. 2011. RAXMLGUI: A Graphical Front-end for RAXML. Available at <https://sites.google.com/site/raxmlgui/>.
- Sissini, M. N., M. C. Oliveira, P. W. Gabrielson, N. M. Robinson, Y. B. Ololodkov, R. Riosmena-Rodriguez, and P. A. Horta. 2014. *Mesophyllum erubescens* (Corallinales, Rhodophyta)—So Many Species in One Epithet. *Phytotaxa*, 190:299–319. <https://doi.org/10.11646/phytotaxa.190.1.18>.
- Steneck, R. 1982. A Limpet–Coralline Alga Association: Adaptations and Defenses Between a Selective Herbivore and Its Prey. *Ecology*, 63:507–522. <https://doi.org/10.2307/1938967>.
- Steneck, R. 1992. “Plant–Herbivore Co-evolution. A Reappraisal from the Marine Realm and Its Fossil Record.” In *Plant–Animal Interactions in the Marine Benthos*, ed. D. M. John, S. J. Hawkins, and J. H. Price, pp. 447–491. Oxford: Clarendon Press.
- Suneson, S. 1943. The Structure, Life-History, and Taxonomy of the Swedish Corallinaceae. *Lunds Universitets Arsskrift* (2), 39:1–66, 9 pl.
- Tamura, K., D. Peterson, N. Peterson, G. Stecher, M. Nei, and S. Kumar. 2011. MEGA5: Molecular evolutionary genetics analysis using maximum likelihood, evolutionary distance, and maximum parsimony methods. *Molecular Biology and Evolution*, 28:2731–2739. <https://doi.org/10.1093/molbev/msr121>.
- Thiers, B. 2017. (continuously updated) Index Herbariorum: A Global Directory of Public Herbaria and Associated Staff. New York Botanical Garden’s Virtual Herbarium. <http://sweetgum.nybg.org/ih/>.
- van der Merwe, E., K. Miklasz, A. Channing, G.W. Maneveldt, and P. W. Gabrielson. 2015. DNA Sequencing Resolves Species of *Spongites* (Corallinales, Rhodophyta) in the Northeast Pacific and South Africa, including *S. agulhensis* sp. nov. *Phycologia* 54(5):471–490. <https://doi.org/10.2216/15-38.1>.
- Woelkerling, W. J. 1988. *The Coralline Red Algae: An Analysis of the Genera and Subfamilies of Nongeniculate Corallinaceae*. London and Oxford: British Museum (Natural History) and Oxford University Press. 767 pp.
- Woelkerling, W. J., G. Gustavsen, H. Mikaelbost, T. Presto, and S. Sostad. 2005. The Coralline Red Algal Herbarium of Mikael Foslie: Revised Catalog with Analysis. *Gunneria*, 77:1–625.
- Woelkerling, W. J., and L. Irvine. 1986. The Neotypification and Status of *Phymatolithon* (Corallinaceae, Rhodophyta). *British Phycological Journal*, 21:55–80.
- Yoon, H. S., J. D. Hackett, and D. Bhattacharya. 2002. A Single Origin of the Peridinin and Fucoxanthin Containing Plastids in Dinoflagellates Through Tertiary Endosymbiosis. *Proceedings of the National Academy of Sciences of the United States of America*, 99:11724–11729. <https://doi.org/10.1073/pnas.172234799>.

Index

Letters following page references: t refers to tables, f refers to figures, p refers to plates.

- Ascophyllum*, 40, 42
- bi-tetrasporangial conceptacle, 3, 18, 27–32, 44–47; in *P. borealis*, 42, 60, 62; in *P. investiens*, 43, 64, 66; in *P. laevigatum*, 40–41, 52; in *P. nantuckensis*, 41, 56; in *P. rugulosum*, 41, 54; in *P. squamulosum*, 41–42, 58
- Boreal–Subarctic transition zone, 2, 4t, 18, 19f, 26, 29t, 31, 32t, 33t, 40–48
- calcification, 18, 23, 27, 44, 45, 49
- carbonate wall: dissolved, 32, 45, 46; structure of, 3, 18, 50
- carpogonium, 18, 31, 32, 34f, 45, 47; in *P. borealis*, 60, 66; in *P. investiens*, 64; in *P. nantuckensis*, 56
- carposporangium, 18, 30–32, 34f, 45, 47, 56
- Clathromorphum*, 1–2, 26, 44, 45, 47–50
- Clathromorphum circumscriptum*, 42, 47, 48
- Clathromorphum compactum*, 45, 47, 49
- conceptacle, 33t. *See also* bi-tetrasporangial conceptacle; asexual, 29t; development of, 50; gametangial, 27, 31–32, 44–47
- Corallinophycidae, 49
- DNA, 2, 3, 18, 80–84t
- epithallium, 18, 44, 45, 49; in *P. borealis*, 42, 62; in *P. investiens*, 43, 66; in *P. laevigatum*, 52; in *P. nantuckensis*, 41, 56; in *P. rugulosum*, 41, 54; in *P. squamulosum*, 42
- hypothallium, 18, 23, 26, 27, 49–50; in *P. borealis*, 42, 60; in *P. investiens*, 43, 66; in *P. laevigatum*, 40, 52; in *P. nantuckensis*, 41, 56; in *P. rugulosum*, 41; in *P. squamulosum*, 42, 58; thickness of, 20f, 21, 22f–24f, 26f, 29, 30f, 40, 43–44
- Kvaleya*, 26, 49
- Kvaleya epilaeve*, 50
- Leptophytum*, 26, 48, 50
- Leptophytum laeve*, 30, 47, 50
- Lithophylloideae, 49
- Lithophyllum*, 48
- Lithophyllum bibernicum*, 43
- Lithophyllum orbiculatum*, 2
- Lithophyllum zonatum*, 43
- Lithothamnion*, 1–3, 26, 45, 48–50
- Lithothamnion glaciale*, 50
- Lithothamnion investiens*, 43
- Lithothamnion polymorphum*, 34f
- Lithothamnion sonderi*, 2, 45
- Lithothamnion squamulosum*, 42
- Lithothamnion tophiforme*, 45
- magnesium, 3; level of, 18, 26, 27, 45, 49–50
- magnesium calcite, 3, 68, 69p, 70, 71p, 72, 73p; level of, 26, 45, 50
- Mastophoroideae, 49
- Melobesia lenormandii*, 42
- nurse tissue, 27, 45, 54, 66
- perithallium, 18, 25, 26, 44–47, 49, 50; and cell size, 21, 22f, 23, 40; in *P. borealis*, 42, 62; in *P. investiens*, 43, 64, 66; in *P. laevigatum*, 40–41, 52; in *P. nantuckensis*, 41, 56; in *P. rugulosum*, 41, 54, 72; in *P. squamulosum*, 42, 58
- Phymatolithon*, 3; distribution of, 4–17t, 18; magnesium calcite cell wall of, 68, 69p, 70, 71p; phylogram of, 19f, 76f; taxonomy of, 1–2

- Phymatolithon borealis*, 3, 18, 42; asexual conceptacle of, 29t; bi-tetrasporangial conceptacle of, 29–30, 30f, 46, 47; and calcification, 49; carpogonium of, 34f; and cell fusion, 27f; cell size of, 23f–26f; as climate archivist, 50; conceptacle of, 31, 32t, 33t; confused with *P. investiens*, 43; distribution of, 38f, 40, 48; DNA information on, 80t; hypothallium of, 20f, 21, 43; perithallium of, 21, 22f, 25, 44; and reproduction, 28, 32; SEM images of, 62, 63p; stained microtome images of, 60, 61p; staining bodies of, 28f, 45; station locality information for, 79f
- Phymatolithon calcareum*, 18, 80t
- Phymatolithon investiens*, 3, 18, 42–43; asexual conceptacle of, 29t; bi-tetrasporangial conceptacle of, 29, 30, 46, 47; and calcification, 49; carpogonium of, 34f; and cell fusion, 27f; cell size of, 23f–26f; conceptacle of, 31, 32, 32t; confused with *P. borealis*, 42; distribution of, 33, 39f, 40, 43–44, 48; DNA information on, 81t; hypothallium of, 18, 20f, 21, 43; perithallium of, 21, 22f, 25, 44; and reproduction, 28, 32; SEM images of, 66, 67p; stained microtome sections of, 64, 65p; staining bodies of, 28f, 45; station locality information for, 79f
- Phymatolithon laevigatum*, 2, 3, 18, 40–41; asexual conceptacle of, 29t; bi-tetrasporangial conceptacle of, 29–30, 30f, 46, 47; and calcification, 49; and cell fusion, 27f; cell size of, 24f–26f; conceptacle of, 31f, 32t, 33t; confused with *P. rugulosum*, 41; distribution of, 36f, 40, 48; DNA information on, 81–82t; hypothallium of, 18, 20f, 21, 44; perithallium of, 21, 22f, 23, 25, 44; SEM images of, 52, 53p; staining bodies of, 28f, 45; station locality information for, 77f; thallus, 18
- Phymatolithon lamii*, 18, 41
- Phymatolithon lenormandii*, 18, 32, 42, 43
- Phymatolithon lusitanicum*, 18, 41, 82t
- Phymatolithon nantuckensis*, 3, 18, 41; bi-tetrasporangial conceptacle of, 30f, 46–47; carpogonium of, 34f; cell size of, 24f–26f; conceptacle of, 31, 32, 32t, 33t; distribution of, 33, 39f, 48; DNA information on, 82t; hypothallium of, 18, 20f, 21, 44; perithallium of, 21, 22f, 44; and reproduction, 28, 32; stained microtome sections of, 56, 57p; station locality information for, 78f; thallus of, 18
- Phymatolithon polymorphum*, 28, 32
- Phymatolithon purpureum*, 34f, 42
- Phymatolithon rugulosum*, 2, 3, 18, 41; asexual conceptacle of, 29t; bi-tetrasporangial conceptacle of, 29, 30, 30f, 46, 47; and calcification, 49; and cell fusion, 27f; cell size of, 24f–26f; conceptacle of, 31, 32t; confused with *P. laevigatum*, 40; distribution of, 33, 35f, 40, 48; DNA information on, 82–83t; hypothallium of, 18, 20f, 21, 44; magnesium calcite wall of, 72, 73p; perithallium of, 21, 22f, 44; and reproduction, 32; SEM images of, 54, 55p; station locality information for, 78f; thallus of, 18
- Phymatolithon squamulosum*, 3, 18, 41–42; asexual conceptacle of, 29t; bi-tetrasporangial conceptacle of, 30f, 46–47; and cell fusion, 27f; cell size of, 24f–26f; conceptacle of, 32, 32t, 33t; distribution of, 33, 37f, 40, 48; DNA information on, 83–84t; hypothallium of, 18, 20f, 43, 44; perithallium of, 21, 22f, 23, 44; and reproduction, 28, 32; SEM images of, 58, 59p; station locality information for, 78f; thallus of, 18
- reproduction, 28–30, 32
- Sporolithon tenue*, 3
staining bodies, 28, 45
- thallus, 18
tissue variation, 26–27
- wall mineralogy, 26–27
wall structure, 49, 50
wound tissue, 26–27, 45, 49–50; *P. borealis*, 62; *P. investiens*, 31, 66; *P. laevigatum*, 52; *P. rugulosum*, 54; *P. squamulosum*, 58

SUMMARY OF REQUIREMENTS FOR SMITHSONIAN CONTRIBUTIONS SERIES

For comprehensive guidelines and specifications, visit <https://scholarlypress.si.edu>.

ABSTRACTS must not exceed 300 words.

TEXT must be prepared in a recent version of Microsoft Word; use a Times font in 12 point for regular text; be double spaced; and have 1" margins.

REQUIRED ELEMENTS are title page, abstract, table of contents, main text, and references.

FIGURES must be numbered sequentially (1, 2, 3, etc.) in the order called out; have components lettered consistently (in size, font, and style) and described in captions; include a scale bar or scale description, if appropriate; include any legends in or on figures rather than in captions. Figures must be original and must be submitted as individual TIF or EPS files.

FIGURE FILES must meet all required specifications in the Digital Art Preparation Guide. Color images should be requested only if required.

TAXONOMIC KEYS in natural history manuscripts should use the aligned-couplet form for zoology. If cross referencing is required between key and text, do not include page references within the key, but number the keyed-out taxa, using the same numbers with their corresponding heads in the text.

SYNONYMY IN ZOOLOGY must use the short form (taxon, author, year:page), with full reference at the end of the manuscript under "References."

REFERENCES should be in alphabetical order, and in chronological order for same-author entries. Each reference should be cited at least once in main text. Complete bibliographic information must be included in all citations. Examples of the most common types of citations can be found at SISP's website under Resources/Guidelines.